Contraction Analysis of Nonlinear Systems

by

Winfried Stefan Lohmiller

Submitted to the Department of Mechanical Engineering
in partial fulfillment of the requirements for the degree of

Doctor of Philosophy in Mechanical Engineering

at the

MASSACHUSETTS INSTITUTE OF TECHNOLOGY

February 1999

Author .....
Department of Mechanical Engineering
October 31, 1998

Certified by .....
Jean-Jacques E. Slotine
Professor of Mechanical Engineering and Information Sciences;
Professor of Brain and Cognitive Sciences
Thesis Supervisor

Certified by .....
Kai-Yeung Siu
Assistant Professor of Mechanical Engineering
Thesis Committee

Certified by .....
Dana Yoerger
Associate Scientist, Woods Hole Oceanographic Institution; Lecturer,
Department of Mechanical Engineering at MIT
Thesis Committee

Accepted by .....
Ain A. Sonin
Chairman, Department Committee on Graduate Students

Contraction Analysis of Nonlinear Systems

by

Winfried Stefan Lohmiller

Submitted to the Department of Mechanical Engineering
on October 31, 1998, in partial fulfillment of the
requirements for the degree of
Doctor of Philosophy in Mechanical Engineering

Abstract

This thesis derives new results in nonlinear system analysis using methods inspired from fluid mechanics and differential geometry. Based on a differential analysis of convergence, these results may be viewed as generalizing the classical Krasovskii theorem, as well as linear eigenvalue analysis. A central feature is that convergence and limit behavior are in a sense treated separately, leading to significant conceptual simplifications.

We establish new combination properties of nonlinear dynamic systems and use them to derive simple controller and observer designs for mechanical systems such as aircraft, underwater vehicles, and robots. The method is also applied to chemical chain reactions and mixture processes. The relative simplicity of these designs stems from their effective exploitation of the systems' structural specificities.

Next, we analyze and quantify the global stability properties of physical partial differential equations such as the heat equation, or the Schroedinger equation.

Lyapunov exponents are not coordinate-invariant, and thus their exact physical meaning is somewhat questionable. As an alternative, we suggest an extension of linear eigenvalue analysis to nonlinear dynamic systems.

Finally, the thesis derives new controller and observer designs for general nonlinear dynamic systems. In particular, an extension of feedback linearization is proposed when the corresponding integrability conditions are violated.

Thesis Supervisor: Jean-Jacques E. Slotine
Title: Professor of Mechanical Engineering and Information Sciences; Professor of Brain and Cognitive Sciences

Thesis Committee: Kai-Yeung Siu
Title: Assistant Professor of Mechanical Engineering

Thesis Committee: Dana Yoerger
Title: Associate Scientist, Woods Hole Oceanographic Institution; Lecturer, Department of Mechanical Engineering at MIT

Acknowledgments

I wish to express my deepest gratitude to my advisor, Professor Jean-Jacques Slotine. He was a constant source of support, ideas, and excellent guidance.

Special thanks go to Prof. Siu, Dr. Yoerger, Dr. Niemeyer, Christophe Bernard, Jesse Hong, and Jacob Feder for their great professional help and stimulating discussions.

I furthermore deeply appreciate the many friendships I have found here: Paolo Narvaez, Craig Barrack, Markus Hogberg, Anthony Chatelain, Carol Lee, Markus Mueller, Thorsten Hornung, Stefan Gumhold, Lutz Klinkner, and Martin Grepl. They all provided numerous pieces of helpful advice and comments and made this time thoroughly enjoyable.

Finally, I am most grateful to my family and all my friends in Germany, who supported and encouraged my work.

Support for this work was provided in part by grants from Fujitsu, Furukawa Electric, and the National Aeronautics and Space Administration.

Contents

List of Figures

Chapter 1

Introduction

Nonlinear system analysis has been very successfully applied to particular classes of systems and problems, but it still lacks generality, as e.g. in the case of feedback linearization, or explicitness, as e.g. in the case of Lyapunov theory (Isidori, 1995; Marino and Tomei, 1995; Khalil, 1995; Vidyasagar, 1992; Slotine and Li, 1991; Nijmeyer and Van der Schaft, 1990). In this thesis, a body of new results is derived using elementary tools from continuum mechanics and differential geometry, leading to what we shall call *contraction analysis*.

Intuitively, contraction analysis is based on a slightly different view of what stability is, inspired by fluid mechanics. Regardless of the exact technical form in which it is defined, stability is generally viewed relative to some nominal motion or equilibrium point. Contraction analysis is motivated by the elementary remark that talking about stability does not require one to known what the nominal motion is: intuitively, a system is stable in some region if initial conditions or temporary disturbances are somehow "forgotten," i.e., if the final behavior of the system is independent of the initial conditions. All trajectories then converge to the nominal motion. In turn, this shows that stability can be analyzed *differentially* – do nearby trajectories converge to one another? – rather than through finding some implicit motion integral as in Lyapunov theory, or through some global state transformation as in feedback linearization. Not surprisingly such differential analysis turns out to be significantly simpler than its integral counterpart. To avoid any ambiguity, we shall call "convergence" this form of stability.

We consider general deterministic systems of the form

$$\dot{\mathbf{x}} = \mathbf{f}(\mathbf{x}, t) \tag{1.1}$$

where $\mathbf{f}$ is an $n \times 1$ nonlinear vector function and $\mathbf{x}$ is the $n \times 1$ state vector. The above equation may also represent the closed-loop dynamics of a controlled system with state feedback $\mathbf{u}(\mathbf{x}, t)$. In this thesis, all quantities are assumed to be real and smooth, by which is meant that any required derivative or partial derivative exists and is continuous.

In Chapter 2, we first recast elementary analysis tools from continuum mechanics in a general dynamic system context, leading to a simple sufficient condition for

system convergence. Chapter 3 generalizes this result to a necessary and sufficient convergence condition.

System combination properties are derived in Chapter 4, that are applied to mechanical controller and observer designs in Chapter 5. Chapter 6 discusses corresponding nonlinear chemical observer and controller designs in the context of chain reactions and constrained mixture processes.

While existence, uniqueness, and smoothness of solutions of large classes of partial differential equations have been extensively studied (Evans, 1998), comparatively little seems to be known on the physically central question of stability – are initial conditions or temporary disturbances eventually "forgotten," and if so, how fast? Chapter 7 applies the derived convergence principles to classes of physical systems described by nonlinear partial differential equations, providing in turn a new perspective on the qualitative properties of these systems.

The Lyapunov exponents of a chaotic system, while independent of the choice of norm (Ruelle, 1982), are not *coordinate-invariant*, and thus they may not be viewed as intrinsic physical quantities. As a trivial example, consider the plant $\dot{x} = x$ and define the invertible coordinate transformation $z = \sinh x$. The dynamics between two neighboring trajectories in x and z coordinates are

$$\delta\dot{x} = \delta x \qquad\qquad \delta\dot{z} = (1 + x\tanh x)\delta z \tag{1.2}$$

While the divergence rate in both coordinate systems is indeed the same at the equilibrium point $z_e = x_e = 0$, it obviously differs in the rest of the state space. The Lyapunov exponents, which measure this divergence rate, are thus not coordinate invariant.

Chapter 8 attempts to offer an alternative view, by suggesting a simple coordinate-invariant generalization of linear eigenvalue analysis to nonlinear dynamic systems, based on an exact differential analysis of convergence. The discussion is illustrated with two simple nonlinear eigenvector fields.

Finally, we derive in Chapter 9 general controller and observer designs for nonlinear continuous systems before Chapter 10 generalizes the original contraction mapping theorem of discrete systems. Chapter 11 discusses the corresponding discrete-time controller and observer designs. Brief concluding remarks are offered in Chapter 12.

Chapter 2

A basic convergence result

This chapter derives the basic convergence principle of this thesis, which we first introduced in (Lohmiller and Slotine, 1996 - 1998). Considering the local flow at a given point $\mathbf{x}$ leads to a convergence analysis between two neighboring trajectories. If all neighboring trajectories converge to each other (contraction behavior) global exponential convergence to a single trajectory can then be concluded.

The plant equation (1.1) can be thought of as an n-dimensional fluid flow, where $\dot{\mathbf{x}}$ is the n-dimensional "velocity" vector at the n-dimensional position $\mathbf{x}$ and time t. Assuming as we do that $\mathbf{f}(\mathbf{x},t)$ is continuously differentiable, (1.1) yields the exact differential relation

$$\delta\dot{\mathbf{x}} = \frac{\partial \mathbf{f}}{\partial \mathbf{x}}(\mathbf{x},t)\ \delta\mathbf{x} \tag{2.1}$$

where $\delta\mathbf{x}$ is a virtual displacement – recall that a virtual displacement is an infinitesimal displacement *at fixed time.* Note that virtual displacements, pervasive in physics and in the calculus of variations, and extensively used in this thesis, are also well-defined mathematical objects. Formally, $\delta\mathbf{x}$ defines a linear tangent differential form, and $\delta\mathbf{x}^T\delta\mathbf{x}$ the associated quadratic tangent form (Arnold, 1978; Schwartz, 1993), both of which are differentiable with respect to time.

Consider now two neighboring trajectories in the flow field $\dot{\mathbf{x}} = \mathbf{f}(\mathbf{x},t)$, and the virtual displacement $\delta\mathbf{x}$ between them (Figure 2-1). The squared distance between these two trajectories can be defined as $\delta\mathbf{x}^T\delta\mathbf{x}$, leading from (2.1) to the rate of change of length

$$\frac{d}{dt}(\delta\mathbf{x}^T\delta\mathbf{x}) = 2\ \delta\mathbf{x}^T\delta\dot{\mathbf{x}} = 2\ \delta\mathbf{x}^T\frac{\partial \mathbf{f}}{\partial \mathbf{x}}\ \delta\mathbf{x}$$

Denoting by $\lambda_{max}(\mathbf{x},t)$ the largest eigenvalue of the *symmetric part* of the Jacobian $\frac{\partial \mathbf{f}}{\partial \mathbf{x}}$ (i.e., the largest eigenvalue of $\frac{1}{2}(\frac{\partial \mathbf{f}}{\partial \mathbf{x}} + \frac{\partial \mathbf{f}}{\partial \mathbf{x}}^T)$), we thus have

$$\frac{d}{dt}(\delta\mathbf{x}^T\delta\mathbf{x}) \leq 2\ \lambda_{max}\ \delta\mathbf{x}^T\delta\mathbf{x}$$

and hence,

$$\|\delta\mathbf{x}\| \leq \|\delta\mathbf{x}_o\|\ e^{\int_o^t \lambda_{max}(\mathbf{x},t)dt} \tag{2.2}$$

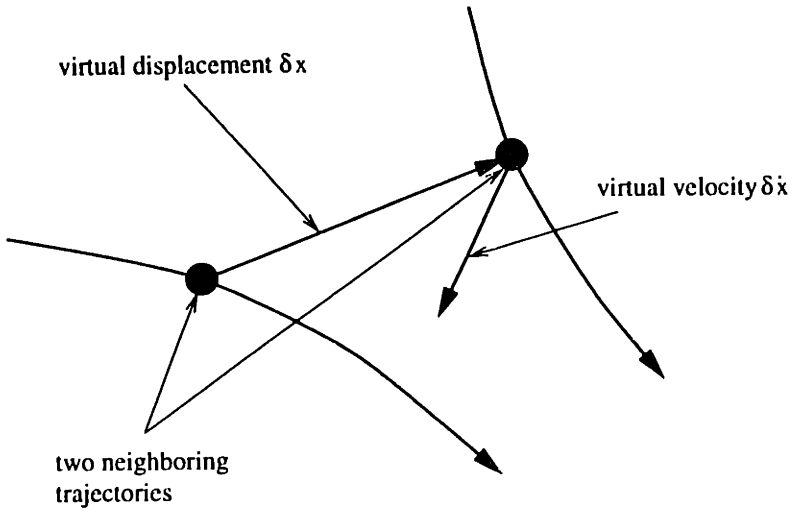

Figure 2-1: Virtual dynamics of two neighboring trajectories

Assume now that $\lambda_{max}(\mathbf{x}, t)$ is uniformly strictly negative (i.e., $\exists\, \beta > 0,\ \forall \mathbf{x},\ \forall t \geq 0,\ \lambda_{max}(\mathbf{x}, t) \leq -\beta < 0.$). Then, from (2.2) any infinitesimal length $\|\delta \mathbf{x}\|$ converges exponentially to zero. By path integration, this immediately implies that the length of any finite path converges exponentially to zero. This motivates the following definition.

Definition 1 *Given the system equations* $\dot{\mathbf{x}} = \mathbf{f}(\mathbf{x}, t)$, *a region of the state space is called a contraction region if the Jacobian* $\frac{\partial \mathbf{f}}{\partial \mathbf{x}}$ *is uniformly negative definite in that region.*

By $\frac{\partial \mathbf{f}}{\partial \mathbf{x}}$ uniformly negative definite we mean that

$$\exists\, \beta > 0,\ \forall \mathbf{x},\ \forall t \geq 0,\ \frac{1}{2}\left(\frac{\partial \mathbf{f}}{\partial \mathbf{x}} + \frac{\partial \mathbf{f}}{\partial \mathbf{x}}^T\right) \leq -\beta\, \mathbf{I} < 0$$

More generally, by convention all matrix inequalities will refer to the *symmetric parts* of the square matrices involved – for instance, we shall write the above as $\frac{\partial \mathbf{f}}{\partial \mathbf{x}} \leq -\beta\ \mathbf{I} < 0$. By a region we mean an open connected set. Extending the above definition, a *semi-contraction* region corresponds to $\frac{\partial \mathbf{f}}{\partial \mathbf{x}}$ being negative semi-definite, and an *indifferent* region to $\frac{\partial \mathbf{f}}{\partial \mathbf{x}}$ being skew-symmetric.

Consider now a ball of constant radius centered about a given trajectory, such that given this trajectory the ball remains within a contraction region at all times (i.e., $\forall t \geq 0$). Because any length within the ball decreases exponentially, any trajectory starting in the ball remains in the ball (since by definition the center of the ball is a particular system trajectory) and converges exponentially to the given trajectory (Figure 2-2). Thus, as in stable linear time-invariant (LTI) systems, the initial conditions are exponentially "forgotten." This leads to the following theorem:

Theorem 1 *Given the system equations* $\dot{\mathbf{x}} = \mathbf{f}(\mathbf{x}, t)$, *any trajectory, which starts in a*

ball of constant radius centered about a given trajectory and contained at all times in a contraction region, remains in that ball and converges exponentially to this trajectory.

Furthermore, global exponential convergence to the given trajectory is guaranteed if the whole state space is a contraction region.

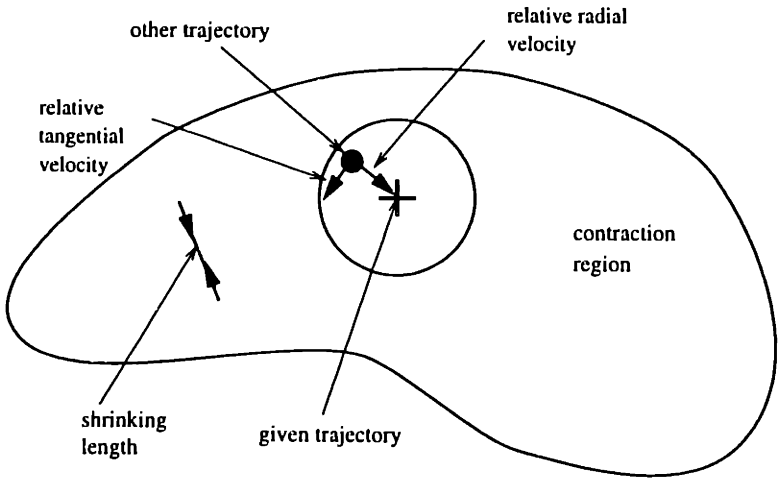

Figure 2-2: Convergence of two trajectories

This sufficient exponential convergence result may be viewed as a strengthened version of Krasovskii's classical theorem on global asymptotic convergence (Krasovskii, 1959, page 92; Hahn, 1967, page 270), an analogy we shall generalize further in the next chapter. Note that its proof is very straightforward, even in the non-autonomous case, and even in the non-global case, where it guarantees explicit regions of convergence. Also, note that the ball in the above theorem may not be replaced by an arbitrary convex region – while radial distances would still decrease, tangential velocities could let trajectories escape the region.

Note that Theorem 1 could have also been derived from the error dynamics

$$\dot{\tilde{\mathbf{x}}} = \mathbf{f}(\tilde{\mathbf{x}}, t) = \int_o^1 \frac{\partial \mathbf{f}}{\partial \mathbf{x}}(\mathbf{x}_d + \lambda \tilde{\mathbf{x}}) d\lambda$$

with $\tilde{\mathbf{x}} = \mathbf{x} - \mathbf{x}_d$, where $\mathbf{x}$ represents a general trajectory and $\mathbf{x}_d$ a given trajectory. The following Lyapunov analysis

$$\dot{V} = \frac{d}{dt}\left(\tilde{\mathbf{x}}^T \tilde{\mathbf{x}}\right) = 2\, \tilde{\mathbf{x}}^T \int_o^1 \frac{\partial \mathbf{f}}{\partial \mathbf{x}}(\mathbf{x}_d + \lambda \tilde{\mathbf{x}}) d\lambda\, \tilde{\mathbf{x}}$$

then shows for uniformly negative definite $\frac{\partial \mathbf{f}}{\partial \mathbf{x}}$ exponential convergence of $\tilde{\mathbf{x}}$ to zero.

Example 2.1: In the system

$$\dot{x} = -x + e^t$$

the Jacobian is uniformly negative definite and exponential convergence to a single trajectory is guaranteed. This result is of course obvious from linear control theory. □

Example 2.2: Consider the system

$$\dot{x} = -t(x^3 + x)$$

For $t \geq t_o > 0$, the Jacobian is again uniformly negative definite and exponential convergence to the unique equilibrium point $x = 0$ is guaranteed. □

Chapter 3

Generalization of the convergence analysis

Theorem 1 can be vastly extended simply by using a more general definition of differential length. The result may be viewed as a generalization of linear eigenvalue analysis and of the Lyapunov matrix equation. Furthermore, it leads to a necessary and sufficient characterization of exponential convergence.

3.1 General definition of length

The line vector $\delta\mathbf{x}$ between two neighboring trajectories in Figure 2-1 can also be expressed using the differential coordinate transformation

$$\delta\mathbf{z} = \Theta\delta\mathbf{x} \tag{3.1}$$

where $\Theta(\mathbf{x}, t)$ is a square matrix. Note that formally $\delta\mathbf{z}$ represents a normal coordinate system (Lovelock and Rund, 1989). This leads to a generalization of our earlier definition of squared length

$$\delta\mathbf{z}^T\delta\mathbf{z} = \delta\mathbf{x}^T\mathbf{M}\ \delta\mathbf{x} \tag{3.2}$$

where $\mathbf{M}(\mathbf{x}, t) = \Theta^T\Theta$ represents a symmetric and continuously differentiable *metric* – formally, equation (3.2) defines a Riemann space (Lovelock and Rund, 1989, page 243). Since (3.1) is in general not integrable, we cannot expect to find explicit new coordinates $\mathbf{z}(\mathbf{x}, t)$, but $\delta\mathbf{z}$ and $\delta\mathbf{z}^T\delta\mathbf{z}$ can always be defined, which is all we need. We shall assume $\mathbf{M}$ to be uniformly positive definite, so that exponential convergence of $\delta\mathbf{z}$ to $\mathbf{0}$ also implies exponential convergence of $\delta\mathbf{x}$ to $\mathbf{0}$. In addition we assume $\mathbf{M}$ to be initially bounded, so that an initially bounded virtual displacement $\delta\mathbf{x}$ leads to an initially bounded squared infinitesimal length $\delta\mathbf{x}^T\mathbf{M}\ \delta\mathbf{x}$.

A distance vector between two points P_1 and P_2 with respect to the metric $\mathbf{M}$ can be defined as the path integral $\int_{P_1}^{P_2}\delta\mathbf{z}$. This path integral is path dependent if $\mathbf{z}$ does not exist. In this case we have to compute $\int_{P_1}^{P_2}\delta\mathbf{z}$ along the forward image of an initial connecting path between P_1 and P_2.

Distance between two points P_1 and P_2 with respect to the metric $\mathbf{M}$ is defined

as the smallest path integral $\int_{P_1}^{P_2} \|\delta \mathbf{z}\|$ between these two points, with the 2-norm $\|\delta \mathbf{z}\| = \sqrt{\delta \mathbf{z}^T \delta \mathbf{z}}$. Accordingly, a ball of center $\mathbf{c}$ and radius R is defined as the set of all points whose distance to $\mathbf{c}$ with respect to $\mathbf{M}$ is strictly less than R.

The two equivalent definitions of length in (3.2) lead to two formulations of the rate of change of length: using local coordinates $\delta \mathbf{z}$ leads to a generalization of linear eigenvalue analysis (Section 3.2), while using the original system coordinates $\mathbf{x}$ leads to a generalized Lyapunov equation (Section 3.3).

3.2 Nonlinear eigenvalue analysis

Using (3.1), the time derivative of $\delta \mathbf{z} = \Theta \delta \mathbf{x}$ can be computed as

$$\frac{d}{dt}\,\delta \mathbf{z} \;=\; \dot{\Theta}\delta \mathbf{x} + \Theta \delta \dot{\mathbf{x}} \;=\; \left(\dot{\Theta} + \Theta \frac{\partial \mathbf{f}}{\partial \mathbf{x}}\right) \Theta^{-1} \delta \mathbf{z} \;=\; \mathbf{F}\;\delta \mathbf{z} \tag{3.3}$$

Formally, the *generalized Jacobian*

$$\mathbf{F} = \left(\dot{\Theta} + \Theta \frac{\partial \mathbf{f}}{\partial \mathbf{x}}\right) \Theta^{-1} \tag{3.4}$$

represents the covariant derivative of $\mathbf{f}$ in $\delta \mathbf{z}$ coordinates (Lovelock and Rund, 1989, page 76). The rate of change of squared length can be written

$$\frac{d}{dt}(\delta \mathbf{z}^T \delta \mathbf{z}) \;=\; 2\;\delta \mathbf{z}^T\;\frac{d}{dt}\;\delta \mathbf{z} \;=\; 2\;\delta \mathbf{z}^T\;\mathbf{F}\;\delta \mathbf{z}$$

Similarly to the reasoning in Theorem 1, exponential convergence of $\delta \mathbf{z}$ (and thus of $\delta \mathbf{x}$) to $\mathbf{0}$ can be determined in regions with uniformly negative definite $\mathbf{F}$. The following example illustrates that this coordinate transformation indeed allows to generalize Theorem 1 and can be regarded as an extension of eigenvalue analysis in LTI systems.

Example 3.1: Consider a stable LTI system

$$\dot{\mathbf{x}} = \mathbf{A}\mathbf{x}$$

whose Jacobian $\mathbf{A}$ is not necessarily uniformly negative definite. Let us transform this system with $\mathbf{z} = \Theta \mathbf{x}$ (where Θ is constant) into a real Jordan form

$$\dot{\mathbf{z}} = \Theta \mathbf{A} \Theta^{-1}\,\mathbf{z} = \Lambda\,\mathbf{z}$$

For instance, one may have

$$\Lambda = \begin{pmatrix} \lambda_1 & \rho & 0 & 0 & 0 \\ 0 & \lambda_1 & 0 & 0 & 0 \\ 0 & 0 & \lambda_3 & 0 & 0 \\ 0 & 0 & 0 & \lambda_{4real} & \lambda_{4im} \\ 0 & 0 & 0 & -\lambda_{4im} & \lambda_{4real} \end{pmatrix}$$

where the λ_i's are the eigenvalues of the system, and $\rho < 2\lambda_1$ is the normalization factor of the Jordan form. The generalized Jacobian $\mathbf{F} = \mathbf{\Lambda}$ is uniformly negative definite if and only if the system is strictly stable, a result which obviously extends to the general n-dimensional case.

This result also allows one to compute an explicit region of exponential convergence for a controller design based on linearization about an equilibrium point, by using the corresponding constant $\mathbf{\Theta}$ in the generalized Jacobian $\mathbf{F} = \left(\dot{\mathbf{\Theta}} + \mathbf{\Theta}\frac{\partial \mathbf{f}}{\partial \mathbf{x}}\right)\mathbf{\Theta}^{-1}$. Note that this robustness computation even applies to systems that depend on unknown constant parameters or state dependent functions as long as $\mathbf{F}$ can be shown to be uniformly negative definite.

Now, consider instead a gain-scheduled system (see (Lawrence and Rugh, 1995) for a recent reference). Let $\mathbf{A}(\mathbf{x}, t) = \frac{\partial \mathbf{f}}{\partial \mathbf{x}}$ be the Jacobian of the corresponding nonlinear, non-autonomous closed-loop system $\dot{\mathbf{x}} = \mathbf{f}(\mathbf{x}, t)$, and define at each point a coordinate transformation $\mathbf{\Theta}(\mathbf{x}, t)$ as above. Uniform negative definiteness of $\mathbf{F} = \mathbf{\Lambda} + \dot{\mathbf{\Theta}}\mathbf{\Theta}^{-1}$ (a condition on the "logarithmic" derivative of $\mathbf{\Theta}$) then implies exponential convergence of this design. □

Note that the analysis above can be extended to complex coordinate transformations $\mathbf{\Theta}(\mathbf{x}, t)$ by replacing the squared length $\delta\mathbf{z}^T\delta\mathbf{z}$ with $\delta\mathbf{z}^T\delta\mathbf{z}^*$, where $*$ indicates complex conjugation.

3.3 Metric analysis

Equation (3.3) can equivalently be written in $\delta\mathbf{x}$ coordinates

$$\mathbf{\Theta}^T \frac{d}{dt}\delta\mathbf{z} \;=\; \mathbf{M}\delta\dot{\mathbf{x}} + \mathbf{\Theta}^T\dot{\mathbf{\Theta}}\delta\mathbf{x} \;=\; \left(\mathbf{M}\frac{\partial \mathbf{f}}{\partial \mathbf{x}} + \mathbf{\Theta}^T\dot{\mathbf{\Theta}}\right)\delta\mathbf{x} \tag{3.5}$$

using the covariant velocity differential $\mathbf{M}\delta\dot{\mathbf{x}} + \mathbf{\Theta}^T\dot{\mathbf{\Theta}}\delta\mathbf{x}$ (Lovelock and Rund, 1989). The rate of change of length is

$$\frac{d}{dt}\left(\delta\mathbf{x}^T\mathbf{M}\,\delta\mathbf{x}\right) = \delta\mathbf{x}^T\left(\frac{\partial \mathbf{f}}{\partial \mathbf{x}}^T\mathbf{M} + \dot{\mathbf{M}} + \mathbf{M}\frac{\partial \mathbf{f}}{\partial \mathbf{x}}\right)\delta\mathbf{x} \tag{3.6}$$

so that exponential convergence to a single trajectory can be concluded in regions of $\left(\frac{\partial \mathbf{f}}{\partial \mathbf{x}}^T\mathbf{M} + \mathbf{M}\frac{\partial \mathbf{f}}{\partial \mathbf{x}} + \dot{\mathbf{M}}\right) \leq -\beta_M\mathbf{M}$ (where β_M is a strictly positive constant). It is immediate to verify that these are of course exactly the regions of uniformly negative definite $\mathbf{F}$ in (3.4). If we restrict the metric $\mathbf{M}$ to be constant, this exponential convergence result represents a generalization and strengthening of Krasovskii's generalized asymptotic global convergence theorem. It may also be regarded as an extension of the Lyapunov matrix equation in LTI systems.

3.4 Generalized contraction analysis

The above leads to the following generalized definition, superseding Definition 1 (which corresponds to $\Theta = \mathbf{I}$ and $\mathbf{M} = \mathbf{I}$).

Definition 2 *Given the system equations* $\dot{\mathbf{x}} = \mathbf{f}(\mathbf{x}, t)$, *a region of the state space is called a contraction region with respect to a uniformly positive definite and initially bounded metric* $\mathbf{M}(\mathbf{x}, t) = \Theta^T\Theta$, *if* $\mathbf{F}$ *in* (3.4) *or equivalently* $\frac{\partial \mathbf{f}}{\partial \mathbf{x}}^T\mathbf{M} + \mathbf{M}\frac{\partial \mathbf{f}}{\partial \mathbf{x}} + \dot{\mathbf{M}}$ *are uniformly negative definite in that region.*

Note that if the metric is defined in a compact set then the regularity of Θ implies a uniformly positive definite metric $\mathbf{M}$. Regions of uniformly negative $\int_t^{t+T} \lambda_{max} d\tau, \forall\, T > 0$, where λ_{max} corresponds to the largest eigenvalue of the symmetric part of $\mathbf{F}$, are called weakly contraction regions. As earlier, regions where $\mathbf{F}$ or equivalently $\frac{\partial \mathbf{f}}{\partial \mathbf{x}}^T\mathbf{M} + \mathbf{M}\frac{\partial \mathbf{f}}{\partial \mathbf{x}} + \dot{\mathbf{M}}$ are negative semi-definite (skew-symmetric) are called semi-contracting (indifferent). The generalized convergence result can be stated as:

Theorem 2 *Given the system equations* $\dot{\mathbf{x}} = \mathbf{f}(\mathbf{x}, t)$, *any trajectory, which starts in a ball of constant radius with respect to the metric* $\mathbf{M}(\mathbf{x},t)$, *centered at a given trajectory and contained at all times in a (weakly)-contraction region with respect to* $\mathbf{M}(\mathbf{x},t)$, *remains in that ball and converges exponentially to this trajectory.*

Furthermore global exponential convergence to the given trajectory is guaranteed if the whole state space is a contraction region with respect to the metric $\mathbf{M}(\mathbf{x},t)$.

In the remainder of this thesis we always assume this generalized form when we discuss contraction behavior.

3.5 A converse theorem

Conversely, consider now an exponentially convergent system, which implies that $\exists \beta > 0$, $\exists k \geq 1$, such that along any system trajectory $\mathbf{x}(t)$ and $\forall t \geq 0$,

$$\delta\mathbf{x}^T\delta\mathbf{x} \leq k\ \delta\mathbf{x}_o^T\delta\mathbf{x}_o\ e^{-\beta t} \tag{3.7}$$

Defining a metric $\mathbf{M}(\mathbf{x}(t), t)$ by the ordinary differential equation (Lyapunov equation)

$$\dot{\mathbf{M}} = -\beta\mathbf{M} - \mathbf{M}\,\frac{\partial \mathbf{f}}{\partial \mathbf{x}} - \frac{\partial \mathbf{f}}{\partial \mathbf{x}}^T\mathbf{M} \qquad \mathbf{M}(t=0) = k\mathbf{I} \tag{3.8}$$

and using (3.6), we can write (3.7) as

$$\delta\mathbf{x}^T\delta\mathbf{x}\ \leq\ \delta\mathbf{x}^T\mathbf{M}\,\delta\mathbf{x}\ =\ k\,\delta\mathbf{x}_o^T\delta\mathbf{x}_o\,e^{-\beta t} \tag{3.9}$$

Since this holds for any $\delta\mathbf{x}$, the above shows $\mathbf{M} \geq \mathbf{I}$ or $\mathbf{M}$ is uniformly positive definite. Thus, any exponentially convergent system is contracting with respect to a suitable metric. Note from the linearity of (3.8) that $\mathbf{M}$ is always bounded for bounded t. Furthermore, while $\mathbf{M}$ may become unbounded as $t \to +\infty$, this does

not create a technical difficulty, since the boundedness of $\delta\mathbf{x}^T\mathbf{M}\delta\mathbf{x}$ (from (3.9)) still implies that $\delta\mathbf{x}$ tends to zero exponentially. Thus, Theorem 2 actually corresponds to a *necessary and sufficient* condition for exponential convergence of a system. In this sense it generalizes and simplifies a number of previous results in dynamic system theory.

3.6 A note to Krasovskii's theorem and Lyapunov theory

It should be clear to the reader familiar with the many versions of Krasovskii's theorem that by now we have ventured quite far from this classical result. Indeed, Krasovskii's theorem provides a sufficient, asymptotic convergence result, corresponding to a constant metric $\mathbf{M}$. Also, it does not exploit the possibility of a pure differential coordinate change as in (3.1). Note that the type of proof used here is very significantly simpler than that used, say, for the global non-autonomous version of Krasovskii's theorem. This in turn allows many further extensions, as the next sections demonstrate.

It is interesting to note that contraction theory analyzes an *infinitesimal* distance $\delta\mathbf{z}^T\delta\mathbf{z}$ between two neighboring trajectories. In contrast Lyapunov theory (see e.g., Slotine and Li, 1991) regards a *finite* distance $V(\mathbf{x},t)$ between two non-neighboring trajectories. One key advantage of such an exact local analysis is the inherent linear behavior that allows to extend many results from linear system theory as illustrated in the following sections. Also note that the finite distance $\int_{P_1}^{P_2}||\delta\mathbf{z}||$ between two trajectories P_1 and P_2 cannot be expressed with a Lyapunov function candidate $V(\mathbf{x},t)$ since $\int_{P_1}^{P_2}||\delta\mathbf{z}||$ not only depends on $\mathbf{x}$ and t, but also on the connecting path between P_1 and P_2. We will use $\int_{P_1}^{P_2}||\delta\mathbf{z}||$ at several occasions later on.

3.7 Weak contraction systems

In this Section we derive a simple convergence condition for semi-contracting systems. The idea is simple: Whereas we have used in Section 2 only first time-derivatives on a virtual displacement to characterize a flow field, we now perform a complete Taylor series expansion to analyze a semi-contracting virtual dynamics.

We first consider a semi-contracting, analytic virtual dynamics in $\delta\mathbf{z}$

$$\frac{d}{dt}\delta\mathbf{z} = \mathbf{F}\delta\mathbf{z}$$

before we go to the corresponding metric dynamics. The corresponding virtual length dynamics is

$$\frac{d}{dt}\left(\delta\mathbf{z}^T\delta\mathbf{z}\right) = -2\delta\mathbf{z}^T\mathbf{F}_s\delta\mathbf{z}$$

with positive semi-definite $\mathbf{F}_s = -\frac{1}{2}\left(\mathbf{F}+\mathbf{F}^T\right)$. Factorizing $\mathbf{F}_s$ as $\sqrt{\mathbf{F}}_s^T\sqrt{\mathbf{F}}_s$, say with

a Cholesky factorization, allows to compute the time-derivatives of $\delta\mathbf{z}^T\delta\mathbf{z}$ as

$$\begin{aligned}
\frac{d}{dt}\left(\delta\mathbf{z}^T\delta\mathbf{z}\right) &= -2\,\delta\mathbf{z}^T\left(L^o\sqrt{\mathbf{F}}_s^T\,L^o\sqrt{\mathbf{F}}_s\right)\delta\mathbf{z} \\
\frac{d^2}{dt^2}\left(\delta\mathbf{z}^T\delta\mathbf{z}\right) &= -2\,\delta\mathbf{z}^T\left(L^1\sqrt{\mathbf{F}}_s^T\,L^o\sqrt{\mathbf{F}}_s + L^o\sqrt{\mathbf{F}}_s^T\,L^1\sqrt{\mathbf{F}}_s\right)\delta\mathbf{z} \\
\frac{d^3}{dt^3}\left(\delta\mathbf{z}^T\delta\mathbf{z}\right) &= -2\,\delta\mathbf{z}^T\left(L^2\sqrt{\mathbf{F}}_s^T\,L^o\sqrt{\mathbf{F}}_s + 2L^1\sqrt{\mathbf{F}}_s^T\,L^1\sqrt{\mathbf{F}}_s + L^o\sqrt{\mathbf{F}}_s^T\,L^2\sqrt{\mathbf{F}}_s\right)\delta\mathbf{z} \\
&\vdots
\end{aligned}$$

with the Lie derivatives $L^j\sqrt{\mathbf{F}}_s(\mathbf{x},t)$ (Lovelock and Rund, 1989)

$$\begin{aligned}
L^o\sqrt{\mathbf{F}}_s &= \sqrt{\mathbf{F}}_s \\
L^{j+1}\sqrt{\mathbf{F}}_s &= L^j\sqrt{\mathbf{F}}_s\mathbf{F} + \frac{d}{dt}L^j\sqrt{\mathbf{F}}_s \qquad \forall j \geq 0
\end{aligned}$$

As a result $\delta\mathbf{z}^T\delta\mathbf{z}(t+T)$ along a trajectory $\mathbf{x}(t)$ can be computed with a Taylor series expansion as

$$\begin{aligned}
\delta\mathbf{z}^T\delta\mathbf{z}(t+T) &= \delta\mathbf{z}^T\delta\mathbf{z} - \delta\mathbf{z}^T\begin{pmatrix} L^o\sqrt{\mathbf{F}}_s^T & L^1\sqrt{\mathbf{F}}_s^T & \cdots \end{pmatrix}\begin{pmatrix} T & \frac{T^2}{2!} & \frac{T^3}{3!} & \cdots \\ \frac{T^2}{2!} & \frac{2T^3}{3!} & \frac{3T^4}{4!} & \cdots \\ \frac{T^3}{3!} & \frac{3T^4}{4!} & \frac{4T^5}{5!} & \cdots \\ \vdots & \vdots & \vdots & \ddots \end{pmatrix}\begin{pmatrix} L^o\sqrt{\mathbf{F}}_s \\ L^1\sqrt{\mathbf{F}}_s \\ \vdots \end{pmatrix}\delta \\
&\leq \delta\mathbf{z}^T\delta\mathbf{z} - \beta\,\delta\mathbf{z}^T\begin{pmatrix} L^o\sqrt{\mathbf{F}}_s^T & L^1\sqrt{\mathbf{F}}_s^T & \cdots \end{pmatrix}\begin{pmatrix} L^o\sqrt{\mathbf{F}}_s \\ L^1\sqrt{\mathbf{F}}_s \\ \vdots \end{pmatrix}\delta\mathbf{z} \qquad (3.10
\end{aligned}$$

where all the terms on the right hand side are computed at time t. Note that for a given constant $T > 0$ the interior matrix in (3.10) can be shown by complete induction to be uniformly positive definite, which implies a uniformly positive β. As a result we can conclude on exponential convergence of $\|\delta\mathbf{z}\|$ to zero for uniformly positive definite $\mathbb{\Phi}^T\mathbb{\Phi}$ with

$$\mathbb{\Phi} = \begin{pmatrix} L^o\sqrt{\mathbf{F}}_s \\ L^1\sqrt{\mathbf{F}}_s \\ \vdots \end{pmatrix} \qquad (3.11)$$

Contrary to linear time-invariant (LTI) systems the rank of $\mathbb{\Phi}$ can be increased with any additional Lie derivative $L^j\sqrt{\mathbf{F}}_s$. However, once $\mathbb{\Phi}^T\mathbb{\Phi}$ is uniformly positive definite for a finite number of Lie derivatives the following ones do not influence the definiteness of $\mathbb{\Phi}^T\mathbb{\Phi}$ anymore.

Consider now the corresponding semi-contracting metric dynamics

$$\frac{d}{dt}\left(\delta\mathbf{x}^T\mathbf{M}\delta\mathbf{x}\right) = -2\delta\mathbf{x}^T\mathbf{O}\delta\mathbf{x} \qquad (3.12)$$

with positive semi-definite $\mathbf{O} = \frac{\partial \mathbf{f}}{\partial \mathbf{x}}^T \mathbf{M} + \mathbf{M}\frac{\partial \mathbf{f}}{\partial \mathbf{x}} + \dot{\mathbf{M}}$. Factorizing $\mathbf{O}$ as $\sqrt{\mathbf{O}}^T\sqrt{\mathbf{O}}$, say with a Cholesky factorization, and a similar argumentation to the previous discussion allows to conclude on exponential convergence of $\|\delta\mathbf{x}\|_M = \sqrt{\delta\mathbf{x}^T\mathbf{M}\delta\mathbf{x}}$ to zero for uniformly positive definite $\bar{\Phi}^T\bar{\Phi}$ with

$$\bar{\Phi} = \begin{pmatrix} L^o\sqrt{\mathbf{O}} \\ L^1\sqrt{\mathbf{O}} \\ \vdots \end{pmatrix} \tag{3.13}$$

and the Lie derivatives $L^j\sqrt{\mathbf{O}}(\mathbf{x},t)$

$$\begin{aligned} L^o\sqrt{\mathbf{O}} &= \sqrt{\mathbf{O}} \\ L^{j+1}\sqrt{\mathbf{O}} &= L^j\sqrt{\mathbf{O}}\,\frac{\partial \mathbf{f}}{\partial \mathbf{x}} + \frac{d}{dt}L^j\sqrt{\mathbf{O}} \qquad \forall j \geq 0 \end{aligned}$$

This leads to the following definition:

Definition 3 *Given the globally analytic system equations $\dot{\mathbf{x}} = \mathbf{f}(\mathbf{x},t)$, a semi-contraction region of the state space is called a weak-contraction region if $\Phi^T\Phi$ in (3.11) or $\bar{\Phi}^T\bar{\Phi}$ in (3.13) is uniformly positive definite in that region.*

This leads with equation (3.10) to:

Theorem 3 *Given the system equations $\dot{\mathbf{x}} = \mathbf{f}(\mathbf{x},t)$, any trajectory, which starts in a ball of constant radius with respect to the metric $\mathbf{M}(\mathbf{x},t)$, centered at a given trajectory and contained at all times in a weak contraction region with respect to $\mathbf{M}(\mathbf{x},t)$, remains in that ball and converges exponentially to this trajectory.*

Furthermore global exponential convergence to the given trajectory is guaranteed if the whole state space is a contraction region with respect to the metric $\mathbf{M}(\mathbf{x},t)$.

Example 3.2: Consider linear parameter adaptation (Narendra and Annaswamy, 1989)

$$\dot{\tilde{\mathbf{a}}} = -\mathbf{W}^T\mathbf{W}\tilde{\mathbf{a}}$$

with parameter error $\tilde{\mathbf{a}}$, and where $\mathbf{W}(\mathbf{x},t)$ might not only depend on time t but also on different states $\mathbf{x}$. A typical Lyapunov function candidate is $V = \tilde{\mathbf{a}}^T\tilde{\mathbf{a}}$ leading to

$$\frac{d}{dt}\left(\tilde{\mathbf{a}}^T\tilde{\mathbf{a}}\right) = -2\tilde{\mathbf{a}}^T\mathbf{W}^T\mathbf{W}\tilde{\mathbf{a}}$$

Replacing $\delta\mathbf{x}$ in (3.12) with $\tilde{\mathbf{a}}$ and Theorem 3 guarantees exponential parameter convergence for uniformly positive definite $\bar{\Phi}^T\bar{\Phi}$ with

$$\bar{\Phi} = \begin{pmatrix} L^o\mathbf{W} \\ L^1\mathbf{W} \\ \vdots \end{pmatrix}$$

and

$$L^o\mathbf{W} = \mathbf{W}$$

$$L^{j+1}\mathbf{W} \;=\; -L^j\mathbf{W}\,\mathbf{W}^T\mathbf{W} + \frac{d}{dt}L^j\mathbf{W} \qquad \forall j \geq 0$$

Note that this result simply represents a Taylor series expansion of the uniform positive definiteness requirement on $\int_t^{t+T} \mathbf{W}\mathbf{W}^T d\tau$ with $T > 0$ in (Narendra and Annaswamy, 1989). Note that similar parameter convergence guarantees can be given in gradient-descent function approximation designs as e.g. back-propagation. □

3.8 Linear properties of generalized contraction analysis

Introductions to nonlinear control generally start with the warning that the behavior of general nonlinear non-autonomous systems is fundamentally different from that of linear systems. While this is unquestionably the case, contraction analysis extends a number of desirable properties of linear system analysis to general nonlinear non-autonomous systems.

1. Solutions in $\delta\mathbf{z}(t)$ can be *superimposed*, since $\frac{d}{dt}\,\delta\mathbf{z} = \mathbf{F}(\mathbf{x},t)\delta\mathbf{z}$ around a specific trajectory $\mathbf{x}(t)$ represents a linear time-varying (LTV) system in local $\delta\mathbf{z}$ coordinates. Note that the system needs not be contracting for this result to hold.

2. Using this point of view, Theorem 2 can also be applied to *other norms*, such as $\|\delta\mathbf{z}\|_\infty = \max_i |\delta z_i|$ and $\|\delta\mathbf{z}\|_1 = \sum_i |\delta z_i|$, with associated balls defined accordingly. Using the same reasoning as in standard matrix measure results (Vidyasagar, 1992, page 71), the corresponding convergence results are

$$\frac{d}{dt}\|\delta\mathbf{z}\|_\infty \leq \max_i(F_{ii}+\sum_{j\neq i}|F_{ij}|)\;\|\delta\mathbf{z}\|_\infty \qquad \frac{d}{dt}\|\delta\mathbf{z}\|_1 \leq \max_j(F_{jj}+\sum_{i\neq j}|F_{ij}|)\;\|\delta\mathbf{z}\|_1$$

3. Global contraction precludes *finite escape*, under the very mild assumption

$$\exists\, \mathbf{x}^* \;,\; \exists\, c \geq 0,\; \forall t \geq 0 \;,\; \|\mathbf{f}(\mathbf{x}^*,t)\|_M \leq c$$

with the velocity norm $\|\mathbf{f}\|_M = \sqrt{\mathbf{f}^T\mathbf{M}\mathbf{f}}$. Indeed, no trajectory can diverge faster from $\mathbf{x}^*$ than the bounded velocity norm $\|\mathbf{f}(\mathbf{x}^*,t)\|_M$ and thus cannot become unbounded in finite time. The result can be extended to the case where $\mathbf{x}^*$ may itself depend on time, as long as it remains in an *a priori* bounded region.

4. In a globally contracting *autonomous* system, all trajectories converge exponentially to a unique equilibrium point. While we know from Theorem 2 that all trajectories converge exponentially to a single trajectory we now show that they converge to an equilibrium point $\mathbf{x}_{EP}$ with $\mathbf{f}(\mathbf{x}_{EP}) = \mathbf{0}$. Indeed, using

the squared velocity norm $V(\mathbf{x}) = \mathbf{f}(\mathbf{x})^T \mathbf{M}(\mathbf{x})\ \mathbf{f}(\mathbf{x})$ as a Lyapunov function (Hartmann, 1982) yields

$$\dot{V} = \mathbf{f}(\mathbf{x})^T \left(\dot{\mathbf{M}} + \mathbf{M}\frac{\partial \mathbf{f}}{\partial \mathbf{x}} + \frac{\partial \mathbf{f}}{\partial \mathbf{x}}^T \mathbf{M} \right) \mathbf{f}(\mathbf{x}) \ \leq \ -\beta_M V$$

which shows that $\dot{\mathbf{x}} = \mathbf{f}(\mathbf{x})$ tends to $\mathbf{0}$ exponentially. Since no trajectory with an exponentially decaying velocity can blow up to ∞ we even know that we converge to a finite equilibrium point $\mathbf{x}_{EP}$.

5. The output of any time-invariant contracting system driven by a *periodic input* tends exponentially to a periodic signal with the same period. Indeed, consider a time-invariant nonlinear system driven by a periodic input $\omega(t)$ of period $T > 0$,

$$\dot{\mathbf{x}} = \mathbf{f}(\mathbf{x},\ \omega(t)) \tag{3.14}$$

Let $\mathbf{x}_o(t)$ be the system trajectory corresponding to the initial condition $\mathbf{x}_o(0) = \mathbf{x}_I$, and let $\mathbf{x}_T(t)$ be the system trajectory corresponding to the system being initialized instead at $\mathbf{x}_T(T) = \mathbf{x}_I$ in Figure 3-1. Since $\mathbf{f}$ is time-invariant and $\omega(t)$ has period T, $\mathbf{x}_T(t)$ is simply as shifted version of $\mathbf{x}_o(t)$,

$$\forall t \geq T, \qquad \mathbf{x}_T(t) = \mathbf{x}_o(t - T) \tag{3.15}$$

Furthermore, if we now assume that the dynamics (3.14) is contracting, then initial conditions are exponentially forgotten, and thus $\mathbf{x}_T(t)$ tends to $\mathbf{x}_o(t)$ exponentially. Therefore, from (3.15), $\mathbf{x}_o(t-T)$ tends towards $\mathbf{x}_o(t)$ exponentially. By recursion, this implies that $\forall t,\ 0 \leq t < T$, the sequence $\mathbf{x}_o(t + nT)$ is a Cauchy sequence, and therefore the limiting function $lim_{n \to +\infty}\ \mathbf{x}_o(t+nT)$ exists, which completes the proof.

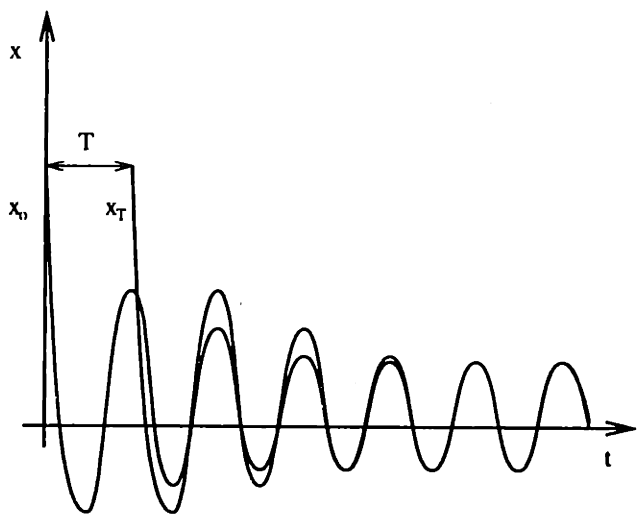

Figure 3-1: Two trajectories in a contracting periodic system

6. Any contracting system is *robust* to bounded disturbances. Indeed, consider the distance $R = \int_{P_1}^{P_2} \|\delta \mathbf{z}\|$ between two trajectories P_1 and P_2 , contained at all times in a contraction region characterized by maximal eigenvalues $\lambda_{max}(\mathbf{x}, t) \leq -\beta < 0$ of $\mathbf{F}$. The relative velocity between these trajectories verifies

$$\dot{R} + |\lambda_{max}| R \leq 0$$

Assume now, instead, that P_1 represents a desired system trajectory and P_2 the actual system trajectory in a *disturbed flow field* $\dot{\mathbf{x}} = \mathbf{f}(\mathbf{x}, t) + \mathbf{d}(\mathbf{x}, t)$. The relative velocity between these trajectories verifies then $\dot{R} + |\lambda_{max}| R \leq \|\mathbf{d}\|_M$. For disturbance $\|\mathbf{d}\|_M < (|\lambda_{max}| - \beta)R + d$ with bounded $d(\mathbf{x}, t) > 0$ and constant $\beta > 0$ any trajectory remains in a boundary ball of

$$\dot{R} + \beta R \leq d \tag{3.16}$$

around the desired trajectory. Since initial conditions $R(t = 0)$ are exponentially forgotten, we can also state that any trajectory converges exponentially to a ball of radius R in (3.16) with arbitrary initial condition $R(t = 0)$. Equation (3.16) also implies that *frequencies* larger than β are filtered out.

7. The above can be used to describe a contracting dynamics at multiple resolutions using multi scale approximation of the dynamics with bounded basis functions, as e.g., in wavelet analysis. The radius R with respect to the metric $\mathbf{M}$ of the boundary ball to which all trajectories converge exponentially becomes smaller as resolution is increased, making precise the usual "coarse grain" to "fine grain" terminology.

3.9 Additional Remarks

In addition to the simple properties above, we can make a few more technical remarks and extensions on Theorem 2.

- Theorem 2 may be viewed as a more precise version of Gauss theorem in fluid mechanics

$$\frac{d}{dt} \delta V = \mathrm{div}(\frac{d}{dt}\delta \mathbf{z})\, \delta V$$

which shows that any volume element δV shrinks exponentially to zero for uniformly negative definite $\mathrm{div}(\frac{d}{dt}\delta \mathbf{z})$, implying convergence to an $(n-1)$-dimensional manifold rather than to a single trajectory. Indeed, $\mathrm{div}(\frac{d}{dt}\delta \mathbf{z})$ is just the trace of $\mathbf{F}$.

- Theorem 2 still holds if the radius R of the ball is time-varying, as long as trajectories starting in the ball can be guaranteed to remain in the ball. Given (3.4) and $\mathbf{F} \leq -\beta\, \mathbf{I} < 0$ this is the case if $\forall t \geq 0,\ \dot{R} + \beta \geq 0$.

- In the case that the metric $\mathbf{M}$ is only positive semi-definite exponential convergence of only $\delta \mathbf{x}^T \mathbf{M} \delta \mathbf{x}$ to zero can still be concluded.

- Consider now a system with uniformly positive definite metric $\mathbf{M}$ and negative semi-definite bounded $\mathbf{F}$, with also $\dot{\mathbf{F}}$ bounded. Since in this case $\delta\mathbf{z}$ and hence $\frac{d}{dt}\left(\delta\mathbf{z}^T\mathbf{F}\delta\mathbf{z}\right)$ are bounded, Barbalat's lemma (see, e.g., (Slotine and Li, 1991), page 122) implies asymptotic convergence of $\delta\mathbf{z}^T\mathbf{F}\delta\mathbf{z}$ to zero.

- Assume that $\mathbf{F}$ is not uniformly negative definite, but rather that $\exists\,\kappa > 0, \exists\,t_o > 0, \forall t \geq t_o, \mathbf{F} \leq -\frac{1}{t}\kappa\mathbf{I}$. Since $\int_{t_o}^{t} \frac{1}{\tau}\kappa\, d\tau$ tends to $+\infty$ as $t \to +\infty$, any infinitesimal length converges asymptotically (although not necessarily exponentially) to zero, and thus asymptotic convergence to a single trajectory can be concluded.

- Since trajectories can rotate or oscillate around each other, overshoots may occur in the elongated principal directions of the metric $\mathbf{M}(\mathbf{x}, t)$.

- In the case that an *explicit* $\mathbf{z}(\mathbf{x}, t)$ exists, we can alternatively compute the virtual velocity from $\dot{\mathbf{z}} = \frac{\partial \mathbf{z}}{\partial \mathbf{x}}\mathbf{f} + \frac{\partial \mathbf{z}}{\partial t}$, since then

$$\delta\dot{\mathbf{z}} = \delta\left(\frac{\partial \mathbf{z}}{\partial \mathbf{x}}\mathbf{f} + \frac{\partial \mathbf{z}}{\partial t}\right) = \frac{\partial^2 \mathbf{z}}{\partial \mathbf{x}^2}\delta\mathbf{x}\,\mathbf{f} + \frac{\partial \mathbf{z}}{\partial \mathbf{x}}\frac{\partial \mathbf{f}}{\partial \mathbf{x}}\delta\mathbf{x} + \frac{\partial \mathbf{z}^2}{\partial t \partial \mathbf{x}}\delta\mathbf{x} = \frac{d}{dt}\delta\mathbf{z}$$

- Contraction analysis can also be applied to differential coordinates $\delta\mathbf{z}$ whose dimension is not the same as that of $\mathbf{x}$. We will use lower-dimensional coordinates extensively in Chapter 4.

- Theorem 2 can also be used to show exponential *divergence* of two neighboring trajectories. Indeed, if the minimal eigenvalue $\lambda_{min}(\mathbf{x}, t)$ of the symmetric part of the $\mathbf{F}$ is strictly positive, then equation (2.2) implies exponential divergence of two neighboring trajectories.

Chapter 4

Combinations of contracting systems

The classical passivity formalism (Popov, 1973) analyze combinations of systems of the form

$$\dot{V}_i = \mathbf{y}_i^T \mathbf{u}_i + g_i$$

with positive V_i, input $\mathbf{u}_i$ and output $\mathbf{y}_i$, and $g_i \geq 0$ (see e.g., (Slotine and Li, 1991)). Parallel or feedback combinations then lead to the augmented Lyapunov dynamics

$$\frac{d}{dt} \sum_i V_i = \sum_i g_i$$

In geometric terms, this simply corresponds to constructing a total length $\sum_i V_i$ out of length elements V_i. This chapter discusses corresponding differential closure properties of contracting systems.

4.1 Parallel combination

Consider two systems of the same dimension

$$\begin{aligned} \dot{\mathbf{x}}_1 &= \mathbf{f}_1(\mathbf{x}_1, t) \\ \dot{\mathbf{x}}_2 &= \mathbf{f}_2(\mathbf{x}_2, t) \end{aligned}$$

with virtual dynamics

$$\begin{aligned} \delta\dot{\mathbf{z}}_1 &= \mathbf{F}_1 \, \delta\mathbf{z} \\ \delta\dot{\mathbf{z}}_2 &= \mathbf{F}_2 \, \delta\mathbf{z} \end{aligned}$$

and connect them in a parallel combination. If both systems are contracting in the same metric, so is any uniformly positive superposition

$$\alpha_1(t) \, \delta\dot{\mathbf{z}}_1 + \alpha_2(t) \, \delta\dot{\mathbf{z}}_2 \qquad \text{where } \exists \, \alpha > 0, \ \forall t \geq 0, \ \alpha_i(t) \geq \alpha \tag{4.1}$$

Example 4.1: In the biological motor control community, there has been considerable interest recently in analyzing feedback controllers for biological motor systems as combinations of simpler elements, or motion primitives. For instance (Bizzi, et al., 1993; Mussa-Ivaldi, et al., 1994) have experimentally studied the hypothesis that stimulating a small number of areas in a frog's spinal cord generates corresponding force fields at the frog's ankle, and furthermore that these force fields simply add when different areas are stimulated at the same time. Interpreting each of these force fields as a contracting flow in joint-space is consistent with experimental data, and likely candidates for the $\alpha_i(t)$ in (4.1) would then be sigmoids and pulses – so-called "tonic" and "phasic" signals (Mussa-Ivaldi, 1997; Berthoz, 1993). A simplified architecture may thus consist of weighted contracting fields generated at the spinal chord level through high-bandwidth few-synapse feedback connections, combined with the natural viscoelastic properties of the muscles, and added open-loop terms generated by the brain, with some time advance because of the significant nerve transmission delays. □

4.2 Feedback Combination

If two systems, of possibly different dimensions

$$\begin{aligned} \dot{\mathbf{x}}_1 &= \mathbf{f}_1(\mathbf{x}_1, \mathbf{x}_2, t) \\ \dot{\mathbf{x}}_2 &= \mathbf{f}_2(\mathbf{x}_1, \mathbf{x}_2, t) \end{aligned}$$

are connected in the feedback combination

$$\frac{d}{dt}\begin{pmatrix} \delta\mathbf{z}_1 \\ \delta\mathbf{z}_2 \end{pmatrix} = \begin{pmatrix} \mathbf{F}_1 & \mathbf{G} \\ -\mathbf{G}^T & \mathbf{F}_2 \end{pmatrix}\begin{pmatrix} \delta\mathbf{z}_1 \\ \delta\mathbf{z}_2 \end{pmatrix}$$

then the augmented system is contracting if the separated plants are contracting.

4.3 Hierarchical Combination

Consider a smooth virtual dynamics of the form

$$\frac{d}{dt}\begin{pmatrix} \delta\mathbf{z}_1 \\ \delta\mathbf{z}_2 \end{pmatrix} = \begin{pmatrix} \mathbf{F}_{11} & \mathbf{0} \\ \mathbf{F}_{21} & \mathbf{F}_{22} \end{pmatrix}\begin{pmatrix} \delta\mathbf{z}_1 \\ \delta\mathbf{z}_2 \end{pmatrix}$$

The first equation does not depend on the second, so that exponential convergence of $\delta\mathbf{z}_1$ to zero can be concluded for uniformly negative definite $\mathbf{F}_{11}$. In turn for bounded $\mathbf{F}_{21}$, $\mathbf{F}_{21}\delta\mathbf{z}_1$ represents an exponentially decaying disturbance in the second equation. Thus, uniform negative definitiveness of $\mathbf{F}_{22}$ implies exponential convergence of $\delta\mathbf{z}_2$ to zero - The augmented system is contracting as well. By recursion, this result can be extended to systems similarly partitioned in more than two equations. An identical reasoning shows that when $\delta\mathbf{z}_1$ converges only asymptotically to zero, so does $\delta\mathbf{z}_2$ for uniformly negative definite $\mathbf{F}_{22}$. This technique may be viewed as providing a common framework for sliding control concepts (e.g., (Slotine and Li, 1991)), singular

perturbations (e.g., (Khalil, 1995)), and triangular systems (e.g., (Ezal, et al., 1997)), where such hierarchical analysis can be found (see also (Simon, 1981) in a broader context). Note while backstepping and sliding control transforms a dynamic system into a hierarchical structure with the help of a control input $\mathbf{u}$, a hierarchical stability analysis can be applied directly on the closed-loop dynamics.

Consider again the system above, but now with bounded disturbances in the $\delta\mathbf{z}_1$ and $\delta\mathbf{z}_2$ dynamics. With the robustness remark in Section 3.9 the first dynamics converges exponentially to a bounded ball around the desired trajectory. This introduces an additional bounded disturbance to the second dynamics. Hence the second dynamics converges as well to a bounded ball around the desired trajectory.

Example 4.2: Contraction analysis may be used as a more precise alternative to zero-dynamics analysis (Isidori, 1995). Consider an n-dimensional system $\dot{\mathbf{x}} = \mathbf{f}(\mathbf{x}, \mathbf{u}, t)$ with measurement $\mathbf{y} = \mathbf{h}(\mathbf{x}, t)$. Assume that repeated differentiation of the measurement leads to $\mathbf{y}^{(p)} = \mathbf{g}(\mathbf{x}, \mathbf{u}, t)$ with $p \leq n$, where we can choose a control input that leads to a contracting linear design in $\mathbf{y}, ..., \mathbf{y}^{(p)}$.

Contracting behavior of the $(n-p)$-dimensional remaining states $\mathbf{z}$ and thus of the whole system can then be concluded according to Section 4.3 for uniformly negative definite $\mathbf{F}$. □

Note that the properties above can be arbitrarily combined.

Example 4.3: Using the hierarchical property, the open-loop signal generated by the brain in the biological motor control model of Example 4.1 may itself be the output of a contracting dynamics. So can be the $\alpha_i(t)$, since the corresponding primitives are bounded. In principle, the contraction property would also enable this term to be learned (see also (Droulez, et al., 1983; Flash, 1995; Mussa-Ivaldi, 1997)) by making the system's behavior consistent in the presence of disturbances or variations in initial conditions.

In this context, the remark (5) on periodic inputs in Section 3.8 may also be relevant to the periodic phenomena pervasive in physiology. These include, for instance, the rhythmic motor behaviors used in locomotion and driven by central pattern generators, as in walking, swimming, or flying (Kandel, et al., 1991; Dowling, 1992), as well as automatic mechanisms such as breathing and heart cycles. □

In the following four sections we assume for the brief of simplicity the explicit existence of $\mathbf{z}$. The derivations can be extended to the general case by replacing $\tilde{\mathbf{z}}$ with $\int_{x_d}^{x} \delta\mathbf{z}$.

4.4 Adaptation

It is straightforward to incorporate adaptive techniques in contraction-based designs if part of the system's uncertainty consists of unknown but constant (or slowly-varying) parameters $\mathbf{a}$. Consider a closed-loop plant error dynamics

$$\dot{\tilde{\mathbf{z}}} = \mathbf{f}(\mathbf{z}, t) - \mathbf{f}(\mathbf{z}_d, t) + \mathbf{W}(\mathbf{z}, t)\mathbf{a} - \mathbf{W}(\mathbf{z}, t)\hat{\mathbf{a}}$$

with parameter estimate vector $\hat{\mathbf{a}}$, state vector $\mathbf{z}$, desired state vector $\mathbf{z}_d$, and $\tilde{\mathbf{z}} = \mathbf{z} - \mathbf{z}_d$. Choosing the parameter adaptation

$$\dot{\tilde{\mathbf{a}}} = \dot{\hat{\mathbf{a}}} = -\mathbf{W}^T(\mathbf{z}, t)\ \tilde{\mathbf{z}}$$

with $\tilde{\mathbf{a}} = \hat{\mathbf{a}} - \mathbf{a}$ shows with Barbalat's lemma (Slotine and Li, 1991) and the Lyapunov analysis

$$\dot{V} = \frac{d}{dt}\left(\tilde{\mathbf{z}}^T\tilde{\mathbf{z}} + \tilde{\mathbf{a}}^T\tilde{\mathbf{a}}\right) = 2\ \tilde{\mathbf{z}}^T \int_o^1 \frac{\partial \mathbf{f}}{\partial \mathbf{z}}(\mathbf{z}_d + \lambda\tilde{\mathbf{z}})d\lambda\ \tilde{\mathbf{z}}$$

asymptotic convergence of $\tilde{\mathbf{z}}$ to zero for uniformly negative definite $\frac{\partial \mathbf{f}}{\partial \mathbf{z}}$ and bounded $\ddot{V}$. Note that $V = \tilde{\mathbf{z}}^T\tilde{\mathbf{z}} + \tilde{\mathbf{a}}^T\tilde{\mathbf{a}}$ only represent a Lyapunov function when $\mathbf{z}$ exists explicitly since otherwise V not only depends on $\mathbf{x}$ and t but also on the chosen path between $\mathbf{x}_d$ and $\mathbf{x}$.

4.5 Separation Principle

Similarly, consider now an observer

$$\dot{\hat{\mathbf{z}}} = \mathbf{f}(\hat{\mathbf{z}}, t) - (\mathbf{e}(\hat{\mathbf{z}}) - \mathbf{e}(\mathbf{z})) + \mathbf{G}(\mathbf{z}, t)\mathbf{u}(\hat{\mathbf{z}}, t)$$

combined with the plant dynamics

$$\dot{\mathbf{z}} = \mathbf{f}(\mathbf{z}, t) + \mathbf{G}(\mathbf{z}, t)\mathbf{u}(\hat{\mathbf{z}}, t)$$

with control input $\mathbf{u}(\hat{\mathbf{z}}, t)$, state vector $\mathbf{z}$, and state estimate vector $\hat{\mathbf{z}}$. Subtracting the plant dynamics from the observer dynamics, leads with $\tilde{\mathbf{z}} = \hat{\mathbf{z}} - \mathbf{z}$ to

$$\dot{\tilde{\mathbf{z}}} = \mathbf{f}(\hat{\mathbf{z}}, t) - \mathbf{e}(\hat{\mathbf{z}}) - (\mathbf{f}(\mathbf{z}, t) - \mathbf{e}(\mathbf{z})) = \int_o^1 \frac{\partial(\mathbf{f} - \mathbf{e})}{\partial \mathbf{z}}(\mathbf{z} + \lambda\tilde{\mathbf{z}})\ d\lambda\ \tilde{\mathbf{z}}$$

The Lyapunov analysis

$$\frac{d}{dt}\left(\tilde{\mathbf{z}}^T\tilde{\mathbf{z}}\right) = 2\ \tilde{\mathbf{z}}^T \int_o^1 \frac{\partial(\mathbf{f} - \mathbf{e})}{\partial \mathbf{z}}\ d\lambda\ \tilde{\mathbf{z}}$$

then shows that the convergence rate of $\hat{\mathbf{z}}$ to $\mathbf{z}$ is given by $\frac{\partial(\mathbf{f}-\mathbf{e})}{\partial \hat{\mathbf{z}}}$. For bounded $\mathbf{G}$ this system is a hierarchy, and thus the convergence rate of the plant is given by $\frac{\partial(\mathbf{f}-\mathbf{Gu})}{\partial \mathbf{z}}$. This result generalizes the standard linear separation principle in (Luenberger, 1979).

4.6 Adaptive Separation Principle

The previous two results may be combined for time-dependent $\mathbf{W}(t)$, and measured $\mathbf{W}^T\mathbf{z}$. Consider an adaptive observer

$$\dot{\hat{\mathbf{z}}} = \mathbf{f}(\hat{\mathbf{z}}, t) + \mathbf{W}(t)\hat{\mathbf{a}} - (\mathbf{e}(\hat{\mathbf{z}}) - \mathbf{e}(\mathbf{z})) + \mathbf{G}(\mathbf{z}, t)\mathbf{u}(\hat{\mathbf{z}}, t)$$

$$\dot{\hat{\mathbf{a}}} \;=\; -\mathbf{W}^T(t)\;(\hat{\mathbf{z}}-\mathbf{z})$$

and a corresponding plant dynamics

$$\dot{\mathbf{z}} = \mathbf{f}(\mathbf{z},t) + \mathbf{W}(t)\mathbf{a} + \mathbf{G}(\mathbf{z},t)\mathbf{u}(\hat{\mathbf{z}},t)$$

where we have used the notation from above. Subtracting the plant dynamics from the observer dynamics leads to

$$\dot{\tilde{\mathbf{z}}} = \mathbf{f}(\hat{\mathbf{z}},t) - \mathbf{e}(\hat{\mathbf{z}}) - (\mathbf{f}(\mathbf{z},t) - \mathbf{e}(\mathbf{z})) + \mathbf{W}\tilde{\mathbf{a}} = \int_z^{\hat{z}} \frac{\partial(\mathbf{f}-\mathbf{e})}{\partial \mathbf{z}}(\mathbf{z}+\lambda\tilde{\mathbf{z}},t)d\lambda\;\tilde{\mathbf{z}} + \mathbf{W}\tilde{\mathbf{a}}$$

The following Lyapunov analysis

$$\dot{V} = \frac{d}{dt}\left(\tilde{\mathbf{z}}^T\tilde{\mathbf{z}} + \tilde{\mathbf{a}}^T\tilde{\mathbf{a}}\right) = 2\;\tilde{\mathbf{z}}^T\int_o^1 \frac{\partial(\mathbf{f}-\mathbf{e})}{\partial \mathbf{z}}\;d\lambda\;\tilde{\mathbf{z}}$$

then shows with Barbalat's lemma asymptotic convergence of $\tilde{\mathbf{z}}$ to zero for uniformly negative definite $\frac{\partial(\mathbf{f}-\mathbf{e})}{\partial \mathbf{z}}$ and bounded $\ddot{V}$. For bounded $\mathbf{G}$ this system is a hierarchy so that the convergence rate of the plant is given by $\frac{\partial(\mathbf{f}-\mathbf{G}\mathbf{u})}{\partial \mathbf{z}}$.

4.7 Time-delayed transmission channels

Many practical applications involve multiple systems with time-delayed feedback connections, due to transmission or computation delays. In robotics for instance, this is the case in force-reflecting teleoperation, underwater vehicle control through acoustic transmissions, and hand-eye coordination.

Consider two such systems, of possibly different dimensions in $\mathbf{z}_1$ and $\mathbf{z}_2$ (Figure 4-1),

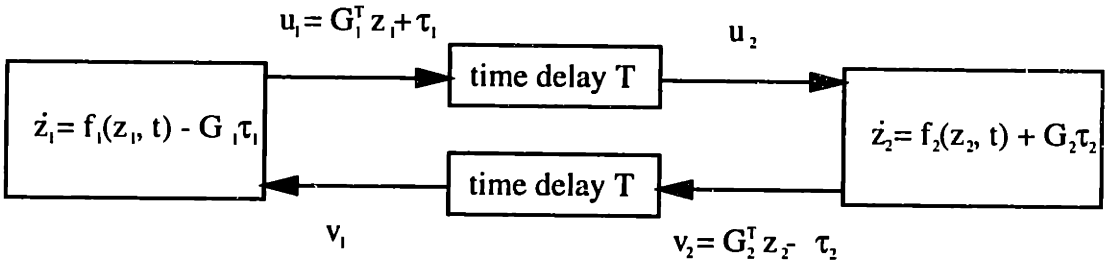

Figure 4-1: Time-delayed transmission channel

$$\begin{aligned}\dot{\mathbf{z}}_1 &= \mathbf{f}_1(\mathbf{z}_1,t) - \mathbf{G}_1\tau_1\\ \dot{\mathbf{z}}_2 &= \mathbf{f}_2(\mathbf{z}_2,t) + \mathbf{G}_2\tau_2\end{aligned}$$

where $\mathbf{G}_i$ is constant and τ_1 and τ_2 have the same dimension. While delays are inherent to the system physics or the computational limitations, the designer is free

to choose which variables are actually transmitted. Directly inspired by the use of wave variables in force-reflecting teleoperation (Niemeyer and Slotine, 1991), define intermediate variables

$$\begin{aligned} \mathbf{u}_1 &= \mathbf{G}_1^T \mathbf{z}_1 + \tau_1 \\ \mathbf{v}_1 &= \mathbf{G}_1^T \mathbf{z}_1 - \tau_1 \\ \mathbf{u}_2 &= \mathbf{G}_2^T \mathbf{z}_2 + \tau_2 \\ \mathbf{v}_2 &= \mathbf{G}_2^T \mathbf{z}_2 - \tau_2 \end{aligned}$$

and transmit these in place of the more obvious $\mathbf{z}_i$,

$$\begin{aligned} \mathbf{u}_2(t) &= \mathbf{u}_1(t-T) \\ \mathbf{v}_1(t) &= \mathbf{v}_2(t-T) \end{aligned}$$

The rate of change of differential length can then be computed similarly to (Niemeyer and Slotine, 1991)

$$\dot{\delta V} = \frac{1}{2}\frac{d}{dt}\left(\delta \mathbf{z}_1^T \delta \mathbf{z}_1 + \delta \mathbf{z}_2^T \delta \mathbf{z}_2 + \frac{1}{2}\int_{t-T}^{t} \left(\delta \mathbf{u}_1^T \delta \mathbf{u}_1 + \delta \mathbf{v}_2^T \delta \mathbf{v}_2\right)\, d\tau\right) = \delta \mathbf{z}_1 \frac{\partial \mathbf{f}_1}{\partial \mathbf{z}_1}\delta \mathbf{z}_1 + \delta \mathbf{z}_2 \frac{\partial \mathbf{f}_2}{\partial \mathbf{z}_2}\delta \mathbf{z}_2$$

We have used

$$\begin{aligned} & \int_{t-T}^{t} \left(\delta \mathbf{u}_1^T \delta \mathbf{u}_1(\tau) + \delta \mathbf{v}_2^T \delta \mathbf{v}_2(\tau)\right)\, d\tau - \int_{-T}^{0} \left(\delta \mathbf{u}_1^T \delta \mathbf{u}_1(\tau) + \delta \mathbf{v}_2^T \delta \mathbf{v}_2(\tau)\right)\, d\tau \\ = & \int_{o}^{t} \left(\delta \mathbf{u}_1^T \delta \mathbf{u}_1(\tau) - \delta \mathbf{u}_1^T \delta \mathbf{u}_1(\tau - T) + \delta \mathbf{v}_2^T \delta \mathbf{v}_2(\tau) - \delta \mathbf{v}_2^T \delta \mathbf{v}_2(\tau - T)\right)\, d\tau \\ = & \int_{o}^{t} \left(\left(\delta \mathbf{u}_1^T \delta \mathbf{u}_1(\tau) - \delta \mathbf{v}_1^T \delta \mathbf{v}_1(\tau)\right) - \left(\delta \mathbf{u}_2^T \delta \mathbf{u}_2(\tau) - \delta \mathbf{v}_2^T \delta \mathbf{v}_2(\tau)\right)\right)\, d\tau \\ = & \; 4\int_{o}^{t} \left(\delta \mathbf{z}_1^T \mathbf{G}_1 \delta \tau_1(\tau) - \delta \mathbf{z}_2^T \mathbf{G}_2 \delta \tau_2(\tau)\right)\, d\tau \end{aligned}$$

where the time arguments apply to the whole dot-products and $\mathbf{u}_1 = \mathbf{v}_2 = 0, \forall t \leq 0$. Applying Barbalat's lemma to $\dot{\delta V}$ shows asymptotic convergence of $\delta \mathbf{z}_1$ and $\delta \mathbf{z}_1$ to zero for contracting separate dynamics $\mathbf{f}_1$ and $\mathbf{f}_2$ and bounded $\ddot{\delta V}$. This derivation can be extended straightforwardly to different transmission time delays T_i, and to feedback loops composed of more than two systems. Note that in the special case $T = 0$, the above reduces to $\mathbf{G}_1^T \mathbf{z}_1 - \mathbf{G}_2^T \mathbf{z}_2 = \mathbf{0}$.

4.8 Continuous switching

Consider an arbitrary number of continuously differentiable flow fields

$$\dot{\mathbf{x}} = \mathbf{f}_i(\mathbf{x}, t)$$

which are all contracting with respect to the *same* continuous $\Theta(\mathbf{x}, t)$. Now switch arbitrarily among these different flow fields $\mathbf{f}_i$, but impose the requirement that the

resulting flow is *continuous in* $\mathbf{x}$ for any time $t \geq 0$ – typical examples of such continuous switching are the min and max operators on field components, and higher processes switching the $\mathbf{f}_i$ as a function of time only. Any such continuous switching of contracting systems is itself contracting, as we now show.

Indeed, consider the distance $\int_{P_1}^{P_2} \|\delta \mathbf{z}\|$ between two trajectories P_1 and P_2, which is simply the sum of the distances $\int_i \|\delta \mathbf{z}_i\|$ in the flow fields $\mathbf{f}_i$. Since any $\|\delta \mathbf{z}_i\|$ converges exponentially to zero and no jump in $\dot{\mathbf{x}}$ can occur, the trajectories P_1 and P_2 converge exponentially to each other. This result may be regarded as a generalization of the stability analysis of linear switching systems in (Shorten and Narendra, 1998).

4.9 Switching between local controller designs

Consider an arbitrary number of continuously differentiable flow fields

$$\dot{\mathbf{x}} = \mathbf{f}_i(\mathbf{x}, t)$$

that are all locally contracting with respect to possibly different $\Theta_i(\mathbf{x}, t)$ around one specific trajectory $\mathbf{x}_i(t)$. Typical examples of such systems are gain-scheduling designs (Lawrence and Rugh, 1995). If a trajectory $\mathbf{x}$ is at the same time in two contracting balls, centered at the trajectories $\mathbf{x}_i(t)$ and $\mathbf{x}_j(t)$ with respect to the metric $\mathbf{M}_i$ and $\mathbf{M}_j$ then we can stably switch with Theorem 2 from $\dot{\mathbf{x}} = \mathbf{f}_i(\mathbf{x}, t)$ to $\dot{\mathbf{x}} = \mathbf{f}_j(\mathbf{x}, t)$. As a result we will leave the region around $\mathbf{x}_i(t)$ and converge to $\mathbf{x}_j(t)$.

4.10 Algebraic constraints

Consider an n-dimensional dynamics $\dot{\mathbf{z}} = \mathbf{f}(\mathbf{z}, t)$ constrained to an m-dimensional manifold $\mathbf{z}(\mathbf{x})$. The constraint $\mathbf{z}(\mathbf{x})$ incorporates an error term $\mathbf{e}$ into the n-dimensional dynamics

$$\dot{\mathbf{z}} = \mathbf{f}(\mathbf{z}, t) + \mathbf{e} \tag{4.2}$$

We can minimize $\mathbf{e}$ by requiring $\frac{\partial \mathbf{z}}{\partial \mathbf{x}}^T \mathbf{e} = \mathbf{0}$ resulting in

$$\mathbf{M}\dot{\mathbf{x}} = \frac{\partial \mathbf{z}}{\partial \mathbf{x}}^T \mathbf{f}$$

with $\mathbf{M} = \frac{\partial \mathbf{z}}{\partial \mathbf{x}}^T \frac{\partial \mathbf{z}}{\partial \mathbf{x}}$. Taking the variation of (4.2) and $\delta(\frac{\partial \mathbf{z}}{\partial \mathbf{x}}^T \mathbf{e}) = \mathbf{0}$ lead to

$$\frac{1}{2}\frac{d}{dt}(\delta \mathbf{x}^T \mathbf{M} \delta \mathbf{x}) = \delta \mathbf{x}^T \frac{\partial \mathbf{z}}{\partial \mathbf{x}}^T \frac{\partial \mathbf{f}}{\partial \mathbf{z}} \frac{\partial \mathbf{z}}{\partial \mathbf{x}} \delta \mathbf{x} - \delta \mathbf{x} \frac{\partial^2 \mathbf{z}}{\partial \mathbf{x}^2}^T \mathbf{e}\, \delta \mathbf{x}$$

This dynamics can be simplified with the largest eigenvalue λ_{max} of $\frac{\partial \mathbf{z}}{\partial \mathbf{x}}^T \frac{\partial \mathbf{f}}{\partial \mathbf{z}} \frac{\partial \mathbf{z}}{\partial \mathbf{x}}$ with respect to the metric $\mathbf{M}$, and the maximal principal curvature $|\kappa|_{max}$ of $\mathbf{z}(\mathbf{x})$ to

$$\frac{1}{2}\frac{d}{dt}(\delta \mathbf{x}^T \mathbf{M} \delta \mathbf{x}) \leq (\lambda_{max} + \|\mathbf{e}\| |\kappa|_{max})\, \delta \mathbf{x}^T \mathbf{M} \delta \mathbf{x}$$

If we assume $\mathbf{x}$ to be a minimal realization of $\mathbf{z}$, i.e. require $\mathbf{M}$ to be uniformly positive definite then exponential convergence of $\delta\mathbf{x}^T\mathbf{M}\delta\mathbf{x}$ to zero implies exponential convergence of $\delta\mathbf{x}^T\delta\mathbf{x}$ to zero. The contraction behavior is hence unchanged in regions of small $\|\mathbf{e}\|\|\kappa\|_{max}$.

4.11 Coordinate feedback

Observer design using contraction analysis can be simplified by prior coordinate transformations similar to those used in linear reduced-order observer design (Luenberger, 1979). Consider the system

$$\begin{aligned} \dot{\mathbf{x}} &= \mathbf{f}(\mathbf{x}, t) \\ \mathbf{y} &= \mathbf{h}(\mathbf{x}, t) \end{aligned}$$

where $\mathbf{x}$ is the state vector and $\mathbf{y}$ the measurement vector. Define a state observer with

$$\begin{aligned} \dot{\bar{\mathbf{x}}} &= \mathbf{f}(\hat{\mathbf{x}}, t) - \mathbf{K}\dot{\hat{\mathbf{y}}} \\ \hat{\mathbf{x}} &= \bar{\mathbf{x}} + \mathbf{K}\mathbf{y} \end{aligned} \tag{4.3}$$

where $\hat{\mathbf{y}} = \hat{\mathbf{h}}(\hat{\mathbf{x}}, t)$ and $\dot{\hat{\mathbf{y}}} = \dot{\mathbf{h}}(\hat{\mathbf{x}}, t) + \frac{\partial \mathbf{h}}{\partial t}$. By differentiation, this leads to the observer dynamics

$$\dot{\hat{\mathbf{x}}} = \mathbf{f}(\hat{\mathbf{x}}, t) - \mathbf{K}\left(\dot{\hat{\mathbf{y}}} - \dot{\mathbf{y}}\right)$$

Thus the dynamics of $\hat{\mathbf{x}}$ contains $\dot{\mathbf{y}}$, although the actual computation is done using equation (4.3) and hence $\dot{\mathbf{y}}$ is not explicitly used. This coordinate error feedback can of course be combined with a normal error feedback.

Chapter 5

Mechanical systems

This chapter presents immediate applications of the above discussion to specific mechanical control and estimation problems. Before doing so, however, let us first remark that in nonlinear, non-autonomous, mechanical systems, PD terms alone do not guarantee convergence, even locally.

Example 5.1: Consider two point masses on a rotational hyperboloid as in Figure

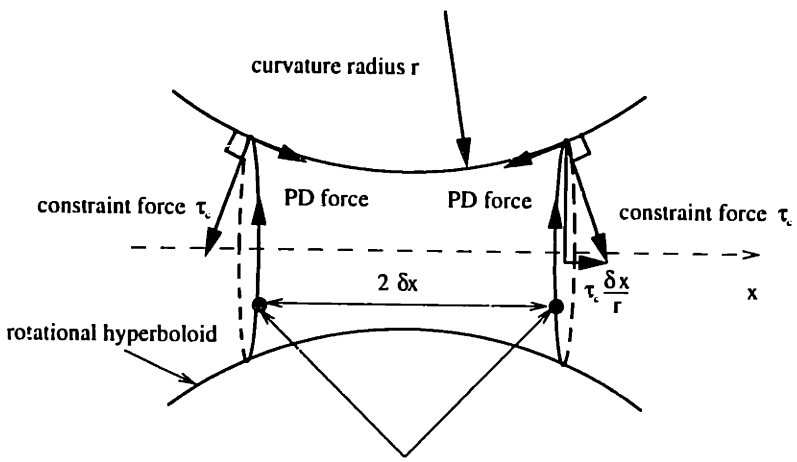

Figure 5-1: Two point masses on a curved surface

5-1. The constraint force τ_c, which guarantees that each point mass remains on the hyperboloid, induces the radial force component $\tau_c \frac{\delta x}{r}$, where r corresponds to the curvature radius of the hyperboloid. If $\frac{\tau_c}{r}$ is larger than the spring constant then the resulting overall spring gain is negative, and this nonlinear non-autonomous mechanical system is locally unstable. Thus, independent of any additional open-loop input, stable tracking convergence of a nonlinear mechanical PD system can in general not be concluded. □

By contrast, in the following we describe classes of mechanical controller and observer problems for which global convergence can be guaranteed very simply since no constraint forces occur.

5.1 An aircraft controller

Figure 5-2 describes a simplified model of the longitudinal motion of a high-performance aircraft, possibly at high angle of attack

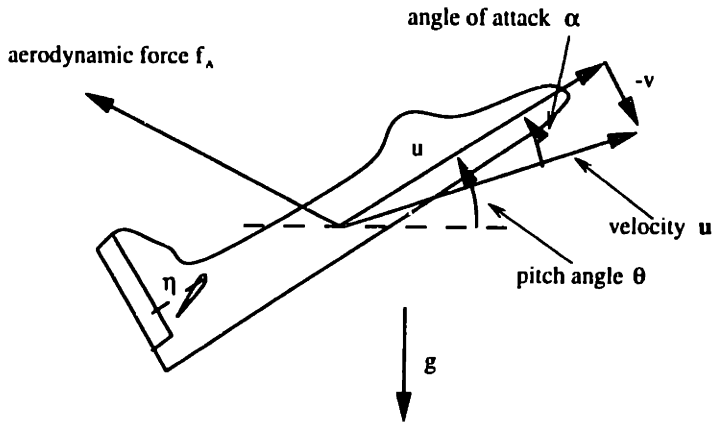

Figure 5-2: Longitudinal aircraft dynamics

$$\dot{\mathbf{u}} = \begin{pmatrix} \dot{u} \\ \dot{v} \end{pmatrix} = \begin{pmatrix} 0 & \dot{\theta} \\ -\dot{\theta} & 0 \end{pmatrix} \mathbf{u} + \frac{1}{m}\mathbf{f}_A + \frac{1}{m}\begin{pmatrix} \xi \\ 0 \end{pmatrix} + g\begin{pmatrix} -\sin\theta \\ -\cos\theta \end{pmatrix}$$
$$\ddot{\theta} = \frac{1}{I}(M + \eta)$$

with the body fixed velocity $\mathbf{u}$, pitch angle θ, mass m, inertia I, gravity constant g, constant thrust ξ, elevator torque η and external torque $M(\mathbf{u}, \theta, \dot{\theta})$ around the center of mass, and the aerodynamic force $\mathbf{f}_A(\mathbf{u}, \eta)$. A simple hierarchical rotational controller

$$\eta = -M + I\left(\ddot{\theta}_d - \dot{\theta} + \theta_d - \theta + \ddot{\theta}_d\right)$$

guarantees exponential convergence of θ to θ_d. The virtual velocity dynamics

$$\delta\dot{\mathbf{u}} = \left[\begin{pmatrix} 0 & \dot{\theta} \\ -\dot{\theta} & 0 \end{pmatrix} + \frac{1}{m}\frac{\partial \mathbf{f}_A}{\partial \mathbf{u}}\right]\delta\mathbf{u}$$

is contracting under the mild physical assumption that $\frac{\partial \mathbf{f}_A}{\partial \mathbf{u}}$ is uniformly negative definite – this control-motivated requirement may actually guide aerodynamic design for high angle of attack aircraft. The convergence rate may be improved with a thrust controller. Exponential convergence to a desired trajectory in $\alpha_d(t) = -\arctan\frac{v_d(t)}{u_d(t)}$ or $\mathbf{u}_d(t)$ can be guaranteed by selecting a corresponding time-varying $\theta_d(t)$.

Example 5.2: The aerodynamic force in body fixed coordinates can be computed from the lift and drag force

$$\mathbf{f}_A = \begin{pmatrix} \sin\alpha & -\cos\alpha \\ \cos\alpha & \sin\alpha \end{pmatrix}\begin{pmatrix} L \\ D \end{pmatrix}$$

with effective angle of attack $\alpha = -\arctan\frac{v}{u}$, and the lift and drag forces $L(\mathbf{u},\eta)$ and $D(\mathbf{u},\eta)$. A reasonable approximation for the $\frac{\alpha}{\pi}$ periodic lift force and $\frac{2\alpha}{\pi}$ periodic drag force is

$$\begin{aligned} L &= \frac{\rho S}{2}\left(u^2+v^2\right)c_{Lmax}\sin\alpha\cos\alpha = -\frac{\rho S}{2}c_L uv \\ D &= \frac{\rho S}{2}\left(u^2+v^2\right)\left(c_o + c_{imax}\sin^2\alpha\right) = \frac{\rho S}{2}\left(c_o u^2 + (c_{imax}+c_o)v^2\right) \end{aligned}$$

with air density ρ, wing area S, maximal lift coefficient $c_{Lmax} > 0$, frictional drag coefficients $c_o > 0$, and maximal induced drag coefficient $c_{imax} > 0$. The aerodynamic force can be rewritten as

$$\mathbf{f}_A = -\frac{\rho S}{2}\frac{1}{\sqrt{u^2+v^2}}\begin{pmatrix} c_o u^3 + (c_{imax}+c_o-c_{Lmax})uv^2 \\ (c_{Lmax}+c_o)vu^2 + (c_{imax}+c_o)v^3 \end{pmatrix}$$

whose variation is with $c_1 = c_{imax}+c_o-c_{Lmax}$, $c_2 = c_{Lmax}+c_o$, and $c_3 = c_{imax}+c_o$

$$\begin{aligned} \frac{\partial \mathbf{f}_A}{\partial \mathbf{u}} &= -\frac{\rho S}{2\sqrt{u^2+v^2}^3}\left(\left(u^2+v^2\right)\begin{pmatrix} 3c_o u^2 + c_1 v^2 & 2c_1 uv \\ 2c_2 vu & c_2 u^2 + 3c_3 v^2 \end{pmatrix} - \begin{pmatrix} u & v \end{pmatrix}\begin{pmatrix} c_o u^3 + c_1 uv^2 \\ c_2 vu^2 + c_3 v^3 \end{pmatrix}\right) \\ &= -\frac{\rho S}{2}\sqrt{u^2+v^2}\begin{pmatrix} 2c_o u^4 + 3c_o u^2 v^2 + c_1 v^4 & (-c_o+2c_1)u^3 v + c_1 uv^3 \\ c_2 vu^3 + (-c_3+2c_2)v^3 u & c_2 u^4 + 3c_3 v^2 u^2 + 2c_3 v^4 \end{pmatrix} \\ &= -\frac{\rho S}{2}\sqrt{u^2+v^2}\begin{pmatrix} 2c_o\cos^4\alpha + 3c_o\cos^2\alpha\sin^2\alpha + c_1\sin^4\alpha & (c_o-2c_1)\cos^3\alpha\sin\alpha + c_1\cos\alpha\sin^3\alpha \\ -c_2\sin\alpha\cos^3\alpha + (c_3-2c_2)\sin^3\alpha\cos\alpha & c_2\cos^4\alpha + 3c_3\sin^2\alpha\cos^2\alpha + 2c_3\sin^4\alpha \end{pmatrix} \end{aligned} \tag{5.1}$$

The contraction behavior of the translational motion is only a function of the angle of attack α. Consider now a typical high performance aircraft such as the Eurofighter, and a complete turn around maneuver, with air density $\rho = 0.6$ kg/m^3, mass $m = 1.5\cdot 10^4$ kg, wing area $S = 50$ m^2, constant thrust $\xi = 6\cdot 10^4$ N, extrapolated lift and drag coefficients $c_o = 0.05$, $c_{imax} = 2$, and $c_{lmax} = 3$, and gravity constant $g = 9.81$ N/kg. The eigenvalues of the symmetric part of $\frac{\partial \mathbf{f}_A}{\partial \mathbf{u}}$ divided by $\frac{1}{2}\rho S\sqrt{u^2+v^2}$ are illustrated in Figure 5-3 as functions of $|\alpha|$. Since both are uniformly negative, the system is naturally contracting. Note that the contraction behavior increases with the energy dissipation at high angle of attack.

Consider the rotational dynamics

$$I\ddot{\theta} = -\frac{1}{2}\rho S\sqrt{u^2+v^2}c_q\bar{c}^2\dot{\theta} + \eta$$

with unknown rotational inertia $I = 8\cdot 10^3$ kgm^2 and damping coefficient $c_q = 3$, reference length $\bar{c}$, and elevator angle η. We first design an adaptive stabilization controller (Slotine and Li, 1991) with sliding variable $s = \dot{\theta} + \lambda(\theta - 2\pi)$, $\lambda = 1$ rad/s, $K_D = 10^4$ kgm^2, and control input

$$\eta = -\lambda\hat{I}\dot{\theta} + \frac{1}{2}\rho S\sqrt{u^2+v^2}\hat{c}_q\bar{c}^2\dot{\theta} - K_D s$$

and parameter adaptation with $\gamma_I = 500$ 1/kgs^{4}and $\gamma_{c_q} = 10^{-3}$ s^3/kg

$$\begin{aligned} \dot{\hat{I}} &= \gamma_I\lambda\dot{\theta}s \\ \dot{\hat{c}}_q &= \gamma_{c_q}\frac{1}{2}\rho S\sqrt{u^2+v^2}\bar{c}^2\dot{\theta}s \end{aligned}$$

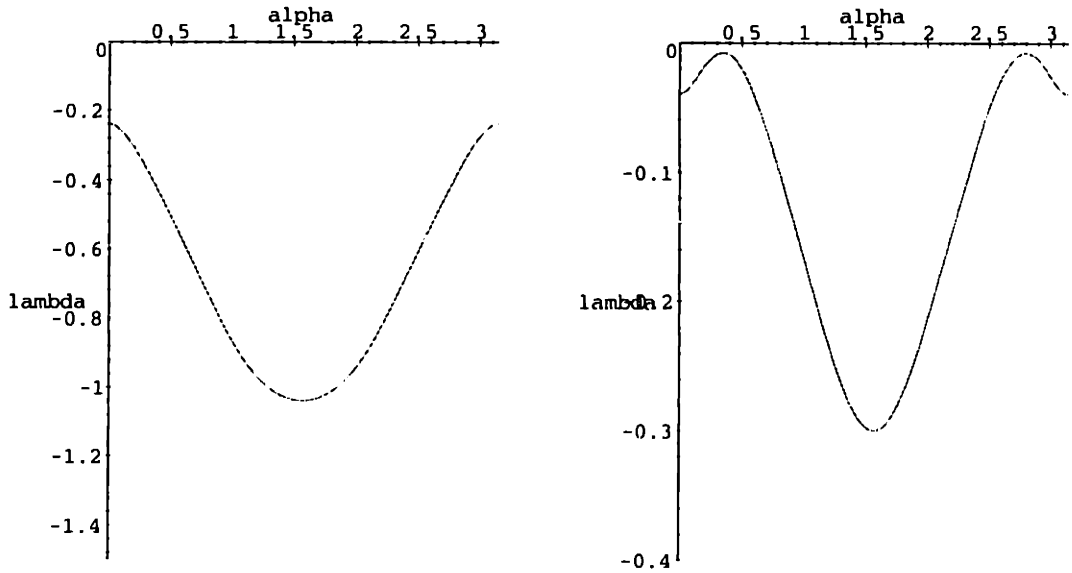

Figure 5-3: Natural contraction behavior of a high performance aircraft

Asymptotic convergence of θ to 2π can be shown with the Lyapunov function candidate $V = \frac{1}{2}Is^2 + \frac{1}{2}\gamma_I(I - \hat{I})^2 + \frac{1}{2}\gamma_{c_q}(c_q - \hat{c}_q)^2$ whose time derivative is $\dot{V} = -K_D s^2$ and $\ddot{V}$ is bounded. The hierarchical structure of the system then implies asymptotic convergence of $\mathbf{u}$.

System responses with initial conditions $\theta(0) = 0$ rad, $\dot{\theta}(0) = 0$ rad/s, $u(0) = 300$ m/s, $v(0) = -10$ m/s, $\hat{I}(0) = 12 \cdot 10^3$ kgm^2, and $\hat{c}_q(0) = -2$ are illustrated in Figure 5-4. Note that parameter estimates do not converge to actual values as the system is not persistently exciting. □

Note that in this approach non-minimum phase characteristics are irrelevant to the stability discussion, but rather they simply affect the planning of the desired trajectory. Additional unknown aerodynamic parameters appearing linearly can be adapted upon similarly to Section 4.4. Also note that any stable rotational controller for the 3-dimensional case also guarantees contraction behavior for the translational motion since for free moving objects inertia forces always correspond to a skew-symmetric Jacobian. Similar derivations can be performed for depth control of underwater vehicles and planar control of ship motions.

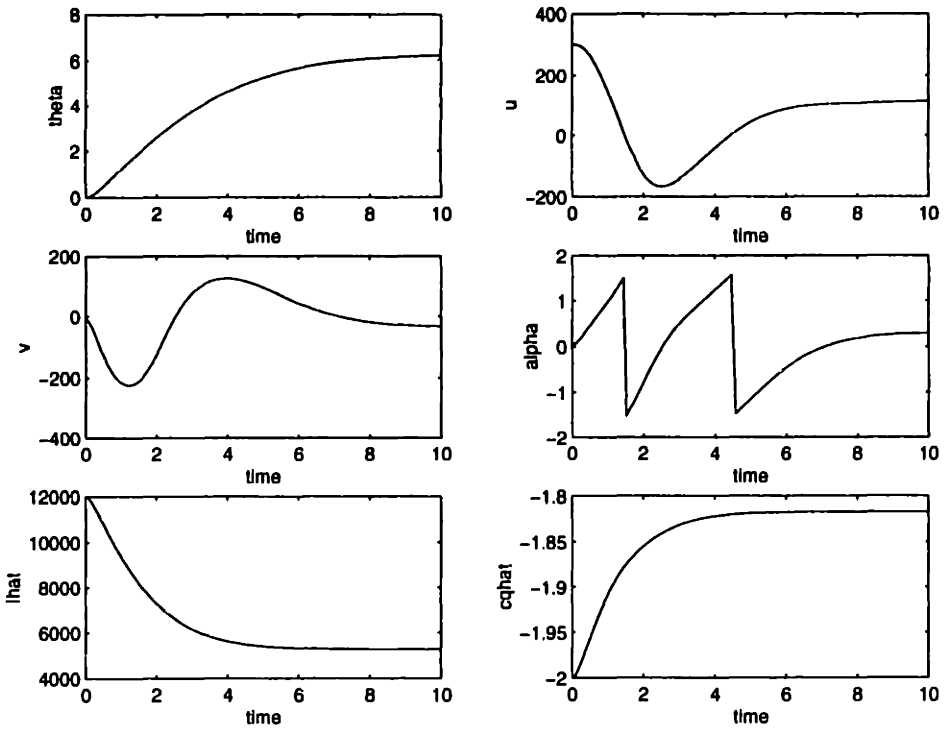

Figure 5-4: 360^o turn around maneuver of a high-performance aircraft

5.2 Time-delayed underwater vehicle controller

As an application of Section 4.7, consider the simple underwater vehicle model in Figure 5-5

$$\begin{pmatrix} \dot{\omega} \\ \dot{v} \end{pmatrix} = \begin{pmatrix} \tau_\omega - c\,\omega\,|\omega| - 10\omega \\ -10\,v\,|v| + \omega\,|\omega| \end{pmatrix}$$

with unknown drag coefficient $c = 3$ and assume that the underwater vehicle is controlled over a time-delayed sonar transmission channel, with

$$\dot{x} = -10x - (\tau_x - \tau_d)$$

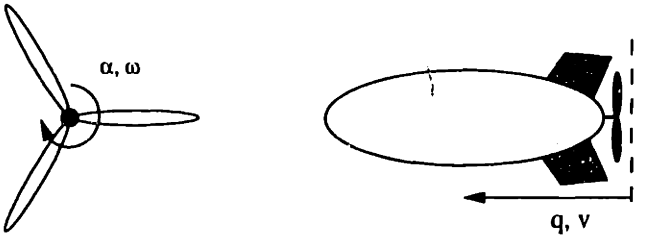

Figure 5-5: Underwater vehicle

where τ_x connects the master dynamics x to the vehicle dynamics, and τ_d implicitly specifies the desired vehicle velocity $v_d(t)$. Similarly to Section 4.7 we use wave variables

$$\begin{aligned} u_x &= x + \tau_x \\ v_x &= x - \tau_x \\ u_\omega &= \omega + \tau_\omega \\ v_\omega &= \omega - \tau_\omega \end{aligned}$$

and transmit these

$$\begin{aligned} u_\omega &= u_x(t-T) \\ v_x &= v_\omega(t-T) \end{aligned}$$

The open-loop term τ_d can be computed from the desired vehicle velocity $v_d(t)$ with $\omega_d(t) = \sqrt{|\dot{v}_d + 10\, v_d|v_d||}sign(\dot{v}_d + 10 v_d|v_d|)$, $\tau_{\omega d}(t) = \dot{\omega}_d + \hat{c}\omega_d|\omega_d| + 10\omega_d$, $u_{\omega d}(t) = \omega_d + \tau_{\omega d}$, $v_{\omega d}(t) = \omega_d - \tau_{\omega d}$, $x_d(t) = \frac{1}{2}(u_{\omega d}(t+T) + v_{\omega d}(t-T))$, $\tau_{xd}(t) = \frac{1}{2}(u_{\omega d}(t+T) - v_{\omega d}(t-T))$, $\tau_d(t) = \dot{x}_d + 10x_d + \tau_{xd}$, where an omitted time index corresponds to time t. The unknown drag coefficient $\hat{c}$ can be adapted according to Section 4.4 with

$$\dot{\hat{c}} = -\gamma W(x - x_d)$$

where $\gamma = 10^{-4}$ and

$$\begin{aligned} W &= \frac{1}{2}\frac{d}{dt}\left(\omega_d(t+T)|\omega_d(t+T)| - \omega_d(t-T)|\omega(t-T)|\right) \\ &+ 5\left(\omega_d(t+T)|\omega_d(t+T)| - \omega_d(t-T)|\omega(t-T)|\right) \\ &+ \frac{1}{2}\left(\omega_d(t+T)|\omega_d(t+T)| + \omega_d(t-T)|\omega(t-T)|\right) \end{aligned}$$

is the gain of $\hat{c}$ in the x dynamics. Due to the hierarchical structure of the underwater vehicle let us first analyze the contraction behavior of the propeller dynamics with the results in Section 4.4 and 4.7

$$\frac{1}{2}\frac{d}{dt}\left(\delta x^2 + \delta\omega^2 + \frac{1}{\gamma}\delta\hat{c}^2 + \frac{1}{2}\int_{t-T}^{t}\left(\delta u_1^2 + \delta v_2^2\right)\, d\tau\right) = -10\delta x^2 - \delta\omega^2(10 + c|\omega|)$$

which guarantees asymptotic tracking convergence of x and ω for positive unknown c. Since the velocity dynamics is contracting with $\frac{\partial \dot{v}}{\partial v} = -10|v|$ for $v \neq 0$ (which is left in finite time for the following open-loop input $\tau_d(t)$) asymptotic convergence of v and hence of the total system can be concluded.

Note that local feedback loops, as say an altitude stabilization controller, are irrelevant to the stability discussion since they are not transmitted over the time-delayed channel.

System responses for the initial conditions $\omega(0) = 0$, $v(0) = 0$, $x(0) = 0$, $\hat{c}(0) = 2$, and $v_\omega(0) = v_x(0) = u_\omega(0) = u_x(0)$ in the complete transmission channel are

illustrated in Figure 5-6, with $T = 2$ and $v_d(t) = 5 \sin \frac{\pi}{10} t$. The dashed line represents the desired velocity and the solid line the actual system response. Note that the sharp wave reflections (Niemeyer and Slotine, 1991) in Figure 5-6 attenuate asymptotically.

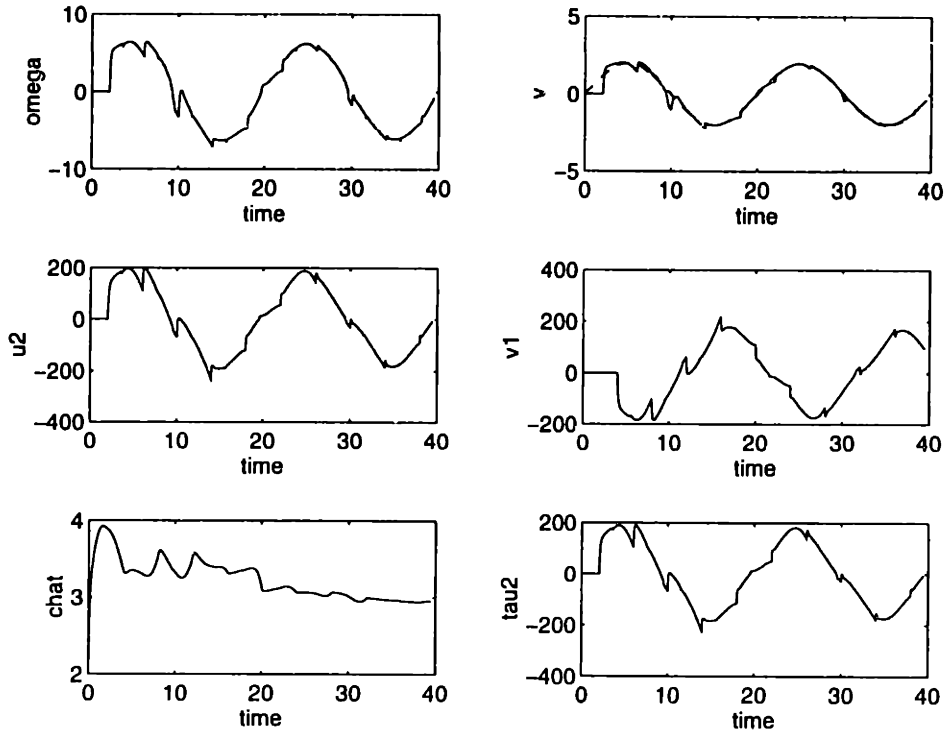

Figure 5-6: Time-delayed underwater vehicle tracking controller

5.3 A simple underwater vehicle observer

Consider again the underwater vehicle in Figure 5-5

$$\begin{pmatrix} \dot{\omega} \\ \dot{v} \end{pmatrix} = \begin{pmatrix} \tau - 3\,\omega\,|\omega| \\ -10\,v\,|v| + \omega\,|\omega| \end{pmatrix}$$
$$\begin{pmatrix} \dot{\alpha} \\ \dot{q} \end{pmatrix} = \begin{pmatrix} \omega \\ v \end{pmatrix}$$

with propeller velocity ω, vehicle velocity v, measured propeller position α, measured vehicle position q, propeller thrust $\omega\,|\omega|$, propeller drag $-3\omega\,|\omega|$, vehicle drag $-10\,v\,|v|$, and torque input to the propeller $\tau(t)$. The system dynamics is heavily damped for large $|\omega|$ and $|v|$. However, this natural damping is ineffective at low velocities. This suggests using a coordinate error feedback in the reduced-order

observer

$$\begin{pmatrix} \dot{\hat{\omega}} \\ \dot{\hat{v}} \end{pmatrix} = \begin{pmatrix} \tau(t) - 3\hat{\omega}\,|\hat{\omega}| - k_\omega \hat{\omega} \\ -10\,\hat{v}\,|\hat{v}| + \hat{\omega}\,|\hat{\omega}| - k_v \hat{v} \end{pmatrix}$$
$$\begin{pmatrix} \hat{\omega} \\ \hat{v} \end{pmatrix} = \begin{pmatrix} \bar{\omega} + k_\omega \alpha \\ \bar{v} + k_v q \end{pmatrix}$$

where k_ω and k_v are strictly positive constants. This leads to the hierarchical dynamics

$$\begin{pmatrix} \dot{\hat{\omega}} \\ \dot{\hat{v}} \end{pmatrix} = \begin{pmatrix} \tau(t) - 3\hat{\omega}\,|\hat{\omega}| - k_\omega(\hat{\omega} - \dot{\alpha}) \\ -10\,\hat{v}\,|\hat{v}| + \hat{\omega}\,|\hat{\omega}| - k_v(\hat{v} - \dot{q}) \end{pmatrix}$$

The uniform negative definiteness of $\frac{\partial \dot{\hat{\omega}}}{\partial \hat{\omega}} = (-3\,|\hat{\omega}| - k_\omega)$ and $\frac{\partial \dot{\hat{v}}}{\partial \hat{v}} = (-10\,|\hat{v}| - k_v)$ (which is implied by our choice of strictly positive constants k_v and k_ω) guarantees exponential convergence to the actual system trajectory, which is indeed a particular solution.

System responses to the input

$$\tau = \begin{pmatrix} 5 & \text{for } 0 \le t < 1 \\ -10 & \text{for } 1 \le t < 2 \end{pmatrix}$$

with initial conditions $\omega(0) = 0, \hat{\omega}(0) = 4$ or $-4, v(0) = 5, \hat{v}(0) = -10$ or 20 and feedback gains $k_v = k_\omega = 5$ are illustrated in Figure 5-7. The solid line represents the actual plant and the dashed lines the observer estimates.

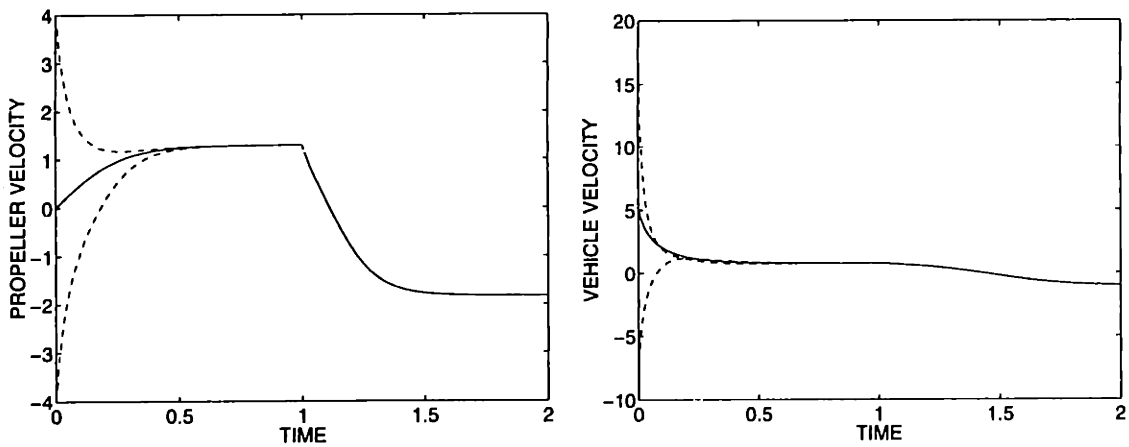

Figure 5-7: Underwater vehicle observer

5.4 A more advanced underwater vehicle observer

Let us illustrate observer design for mechanical systems on the underwater vehicle of Figure 5-5, but now using the recent detailed hydrodynamic model of (Withcomb and Yoerger, 1998)

$$\begin{aligned} m\dot{v} &= T - c_D v|v| \\ I\dot{\omega} &= -k_1\omega + k_2 U - Q \end{aligned}$$

with propeller velocity ω, vehicle velocity v, vehicle mass $m = 400$ kg, propeller inertia $I = 0.01$ kgm^2, vehicle drag coefficient $c_D = 10^4$ Ns^2/m^2, motor back-emf $k_1 = 0.01$ Nms, motor gain $k_2 = 0.1$ Nm/V, vehicle thrust T, and propeller drag Q. The vehicle thrust and propeller drag are

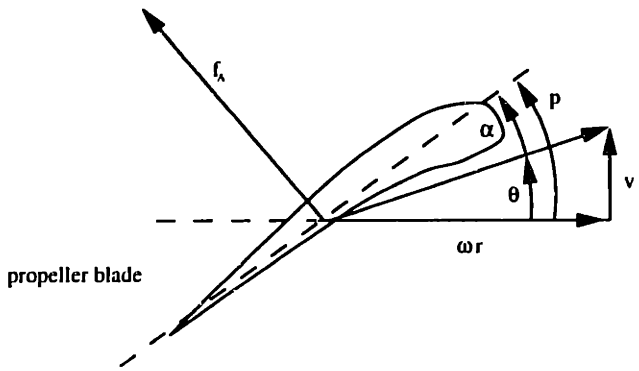

Figure 5-8: Propeller geometry

$$\begin{aligned} T &= L\cos\theta - D\sin\theta \\ Q &= L\sin\theta + D\cos\theta \end{aligned}$$

where the blade lift L and drag forces D can in turn be expressed as

$$\begin{aligned} L &= 500(v^2 + r^2\omega^2)c_{Lmax}\sin\alpha\cos\alpha \\ D &= 500(v^2 + r^2\omega^2)(c_o + c_{imax}\sin^2\alpha) \end{aligned}$$

with angle of attack $\alpha = p - \theta$, blade angle $p = 0.4$ rad, pitch angle $\theta = \arctan\frac{v}{r\omega}$, and effective propeller radius $r = 0.1$ m in Figure 5-8. Using inertia as the metric, the Jacobian of this dynamics is

$$\mathbf{F} = \begin{pmatrix} -10000|v| & 0 \\ 0 & -0.01 \end{pmatrix} + \begin{pmatrix} \cos p & \sin p \\ -\sin p & \cos p \end{pmatrix} \frac{\partial \mathbf{f}_A}{\partial \mathbf{u}} \begin{pmatrix} \cos p & -\sin p \\ \sin p & \cos p \end{pmatrix}$$

where $\frac{\partial \mathbf{f}_A}{\partial \mathbf{u}}$ is given in equation (5.1). The eigenvalues of the symmetric part of $\frac{\partial \mathbf{f}_A}{\partial \mathbf{u}}$ divided by $500\sqrt{v^2 + 0.01\omega^2}$ are illustrated in Figure 5-9 for $c_o = 0.1$, $c_{imax} = 2.5$,

and $c_{Lmax} = 1.1$. Since both are negative the system is naturally contracting. Note that the contraction behavior increases with the energy dissipation at high angle of attack.

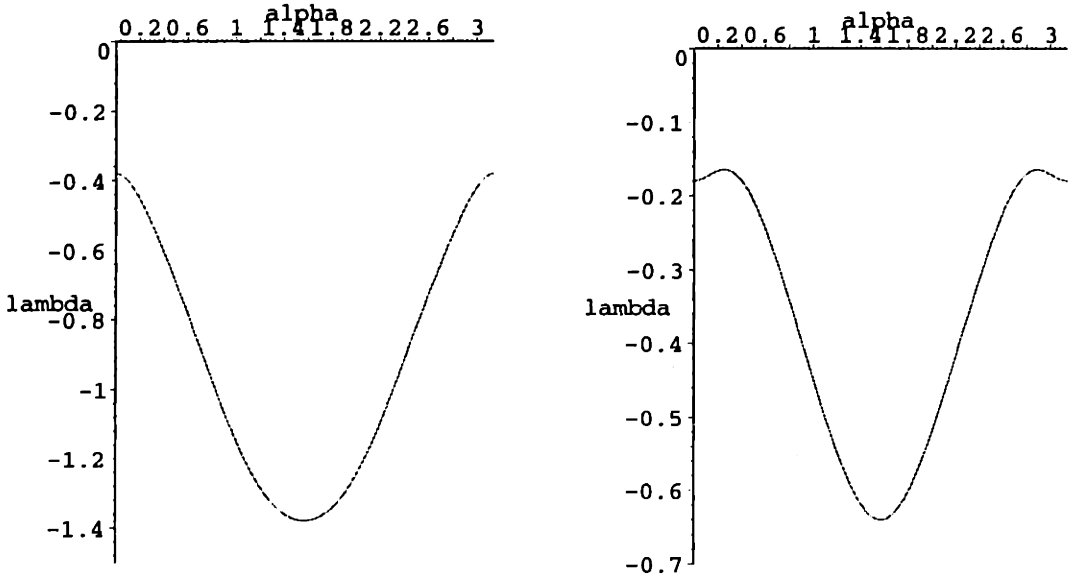

Figure 5-9: Natural contraction behavior of propeller blades

Assuming that the vehicle position q and propeller angle α are measured, the following coordinate error feedback observer (see Section 4.11)

$$\begin{aligned} m\dot{\hat{v}} &= T - c_D\hat{v}|\hat{v}| - k_q\hat{v} \\ I\dot{\hat{\omega}} &= -k_1\hat{\omega} + k_2U - Q - k_\alpha\hat{\omega} \\ \hat{v} &= \bar{v} + k_q q \\ \hat{\omega} &= \bar{\omega} + k_\alpha\alpha \end{aligned}$$

leads to the exponentially convergent observer dynamics

$$\begin{aligned} m\dot{\hat{v}} &= T - c_D\hat{v}|\hat{v}| - k_q(\hat{v} - \dot{q}) \\ I\dot{\hat{\omega}} &= -k_1\hat{\omega} + k_2U - Q - k_\alpha(\hat{\omega} - \dot{\alpha}) \end{aligned}$$

hence augmenting the natural contraction behavior of the system.

System responses to the input

$$U = \begin{pmatrix} 100V & \text{for } 0 \le t < 1 \\ 300V & \text{for } 1 \le t < 2 \end{pmatrix}$$

with initial conditions $v(0) = 0.5$ m/s, $\hat{v}(0) = 1$ m/s, $\omega(0) = 2$ 1/s, $\hat{\omega}(0) = 3$ 1/s and feedback gains $k_q = 1$ Ns/m and $k_\alpha = 1$ Nms are illustrated in Figure 5-10. The solid line represents the actual plant and the dashed lines the observer estimates.

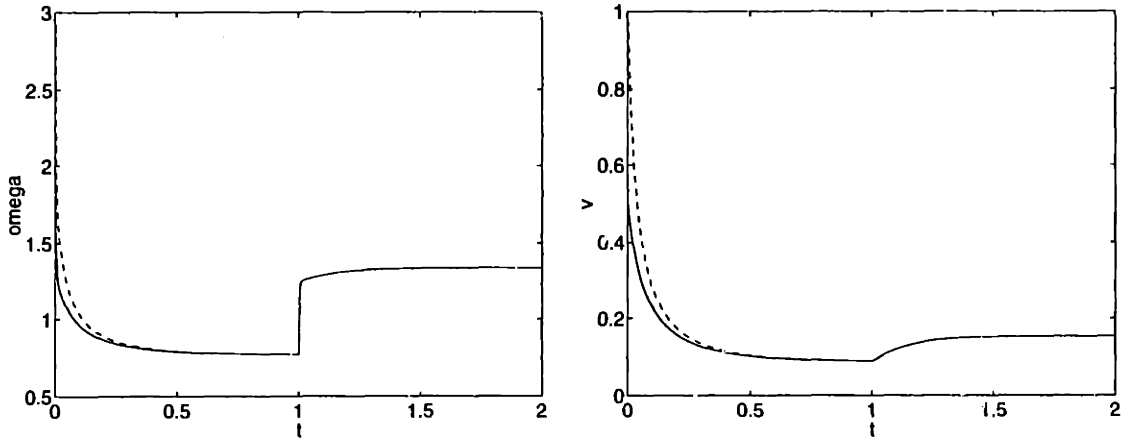

Figure 5-10: Underwater vehicle observer

5.5 Mechanical PD observer design

This Section provides a simple dissipative PD observer design for nonlinear mechanical systems, that uses only position measurements. Indeed consider a general nonlinear mechanical system (Slotine and Li, 1991)

$$\mathbf{H}\ddot{\mathbf{q}} + \mathbf{C}\dot{\mathbf{q}} + \mathbf{g} = \tau$$

with the generalized position vector $\mathbf{q}$, inertia matrix $\mathbf{H}(\mathbf{q})$, Coriolis and centripetal forces $\mathbf{C}(\mathbf{q}, \dot{\mathbf{q}})\dot{\mathbf{q}}$, gravitational forces $\mathbf{g}(\mathbf{q})$, and external forces τ. Assume now that only $\mathbf{q}$ is measured and design the full-state observer

$$\begin{aligned} \hat{\mathbf{H}}\,\dot{\bar{\mathbf{q}}} + \hat{\mathbf{C}}\hat{\mathbf{q}} &= -\mathbf{K}_p\left(\hat{\mathbf{q}} - \mathbf{q}\right) - k_d\hat{\mathbf{H}}\hat{\mathbf{q}} \\ \hat{\mathbf{q}} &= \bar{\mathbf{q}} + k_d\,\mathbf{q} \end{aligned}$$

with symmetric, uniformly positive definite $\mathbf{K}_p$ and k_d, and where a $\hat{}$ describes the corresponding estimate. The observer dynamics can with the coordinate feedback in Section 4.11 be rewritten as

$$\hat{\mathbf{H}}\dot{\hat{\mathbf{q}}} + \hat{\mathbf{C}}\hat{\mathbf{q}} = -\mathbf{K}_p\left(\hat{\mathbf{q}} - \mathbf{q}\right) - k_d\hat{\mathbf{H}}\left(\dot{\hat{\mathbf{q}}} - \dot{\mathbf{q}}\right)$$

The energy of this PD observer design is

$$V = \frac{1}{2}\dot{\hat{\mathbf{q}}}^T\hat{\mathbf{H}}\dot{\hat{\mathbf{q}}} + \frac{1}{2}\left(\mathbf{q} - \hat{\mathbf{q}}\right)^T\mathbf{K}_p\left(\mathbf{q} - \hat{\mathbf{q}}\right) \tag{5.2}$$

whose time derivative can be computed to be

$$\dot{V} = -g + \dot{\mathbf{q}}^T \tau^*$$

The proposed PD observer is dissipative (Popov, 1973) with internal power dissipation $g = k_d \dot{\hat{\mathbf{q}}}^T \hat{\mathbf{H}} \dot{\hat{\mathbf{q}}}$ and external power input $\dot{\mathbf{q}}^T \tau^* = \dot{\mathbf{q}}^T \left(k_d \hat{\mathbf{H}} \dot{\hat{\mathbf{q}}} + \mathbf{K}_p (\mathbf{q} - \hat{\mathbf{q}}) \right)$. Note that uncertainties in the inertia forces do not affect the dissipative properties of this observer design, as long as an energy function V in equation (5.2) can be constructed.

We can combine this observer with the PD stabilization controller in (Takegaki and Arimoto, 1981)

$$\tau = \mathbf{g} - \mathbf{K}_P^* (\mathbf{q} - \mathbf{q}_d) - \tau^*$$

with symmetric uniformly positive definite $\mathbf{K}_P^*$ and the desired constant position vector $\mathbf{q}_d$. Applying the global invariant set theorem (Slotine and Li, 1991) to the augmented system then shows global asymptotic convergence of $\mathbf{q}$, and $\hat{\mathbf{q}}$ to $\mathbf{q}_d$.

Example 5.3: Consider for instance the two-link robot in Figure 5-11

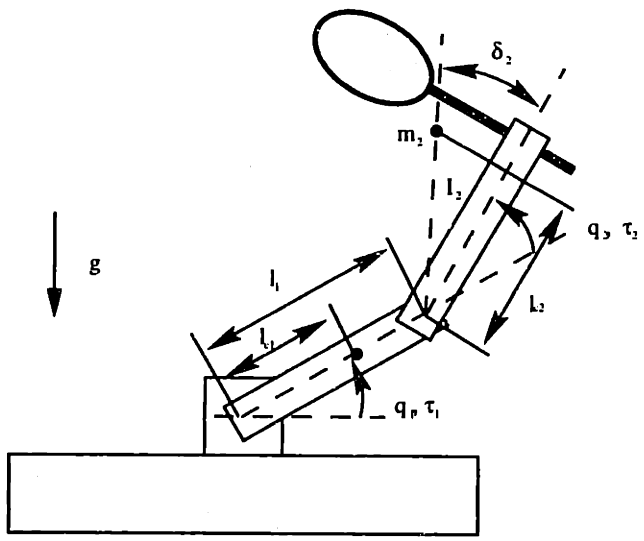

Figure 5-11: Two-link robot

$$\mathbf{H}\ddot{\mathbf{q}} + \mathbf{C}\dot{\mathbf{q}} + \mathbf{g} = \tau$$

with measured positions $\mathbf{q} = (q_1 \; q_2)^T$, unknown velocities $\dot{\mathbf{q}} = (\dot{q}_1 \; \dot{q}_2)^T$, control inputs $\tau = (\tau_1 \; \tau_2)^T$, gravity vector $\mathbf{g}$, inertia matrix $\mathbf{H}$, and centripetal forces $\mathbf{C}\dot{\mathbf{q}}$ with

$$\mathbf{g} = \begin{pmatrix} -gm_1 l_{c1} \cos q_1 - gm_2 (l_{c2} \cos(q_1 + q_2 + \delta_2) + l_1 \cos q_1) \\ -gm_2 l_{c2} \cos(q_1 + q_2 + \delta_2) \end{pmatrix}$$

$$\mathbf{H} = \begin{pmatrix} a_1 + 2a_3 \cos q_2 + 2a_4 \sin q_2 & a_2 + a_3 \cos q_2 + a_4 \sin q_2 \\ a_2 + a_3 \cos q_2 + a_4 \sin q_2 & a_2 \end{pmatrix}$$

$$
\begin{aligned}
\mathbf{C}\dot{\mathbf{q}} &= \begin{pmatrix} -h\dot{q}_2(2\dot{q}_1 + \dot{q}_2) \\ h\dot{q}_1^2 \end{pmatrix} \\
h &= a_3 \sin q_2 - a_4 \cos q_2 \\
a_1 &= I_1 + m_1 l_{c1}^2 + I_2 + m_2 l_{c2}^2 + m_2 l_1^2 \\
a_2 &= I_2 + m_2 l_{c2}^2 \\
a_3 &= m_2 l_1 l_{c2} \cos \delta_2 \\
a_4 &= m_2 l_1 l_{c2} \sin \delta_2
\end{aligned}
$$

The full-state observer

$$
\begin{aligned}
\hat{\mathbf{H}}\,\dot{\bar{\mathbf{q}}} + \hat{\mathbf{C}}\hat{\dot{\mathbf{q}}} &= -k_p\,(\hat{\mathbf{q}} - \mathbf{q}) - k_d \hat{\mathbf{H}}\hat{\dot{\mathbf{q}}} \\
\hat{\dot{\mathbf{q}}} &= \bar{\dot{\mathbf{q}}} + k_d\,\mathbf{q}
\end{aligned}
$$

is according to the previous analysis for uniformly positive definite k_p and k_d dissipative. The combination with the PD stabilization controller

$$
\tau = \mathbf{g} - k_p\,(\mathbf{q} - \mathbf{q}_d) - \left(k_d \hat{\mathbf{H}}\hat{\dot{\mathbf{q}}} - \mathbf{K}_p\,(\hat{\mathbf{q}} - \mathbf{q})\right)
$$

is hence globally asymptotically stable.

System responses with $g = 9.81$ N/kg, $m_1 = 1$ kg, $m_2 = 2$ kg, $I_1 = 0.12$ kgm^2, $I_2 = 0.25$ kgm^2, $l_1 = 1$ m, $l_{c1} = 0.5$ m, $l_{c2} = 0.6$ m, $\delta_2 = 30^o$, $k_p = 20$ N/m, $k_d = 20$ Ns/m, $q_{1d} = 0$ and $q_{2d} = 0$, and initial conditions $q_1(0) = 1$ rad, $q_2(0) = -1$ rad, $\hat{q}_1(0) = 2$ rad, $\hat{q}_2(0) = -1$ rad, $\dot{q}_1(0) = -2$ rad/s, $\dot{q}_2(0) = -1$ rad/s, $\hat{\dot{q}}_1(0) = 1$ rad/s, $\hat{\dot{q}}_2(0) = -2$ rad/s are illustrated in Figure 5-12. The dashed lines represent the observer estimates and the solid lines the actual system responses. □

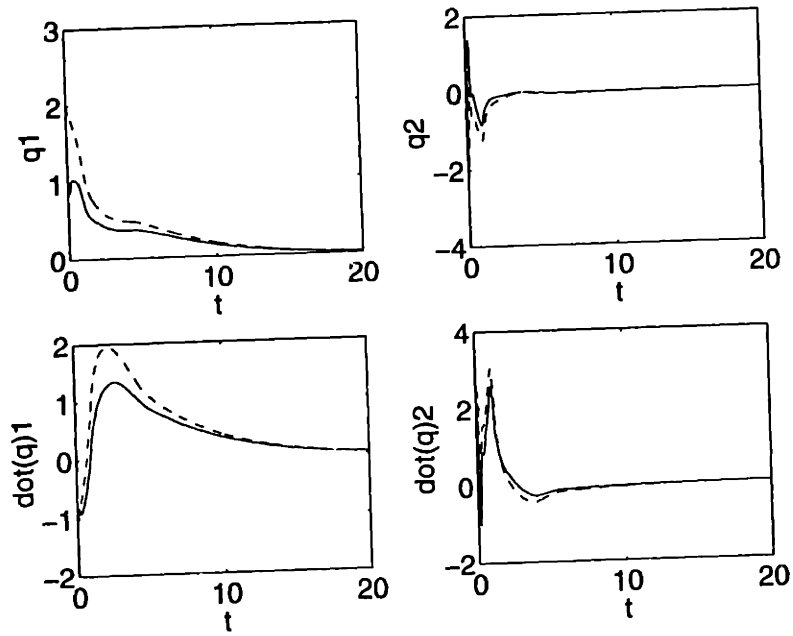

Figure 5-12: Two-link robot stabilization observer

This approach provides a simple alternative to current locally convergent mechanical observer design methods (see e.g., Berghuis and Nijmeyer, 1993; Marino and Tomei, 1995).

Chapter 6

Chemical systems

In the following we analyze the contraction behavior of nonlinear chemical reactions. As an illustration we propose an observer for a standard polymerization process. We then analyze a typical mixture process including input constraints.

6.1 Chemical reactions

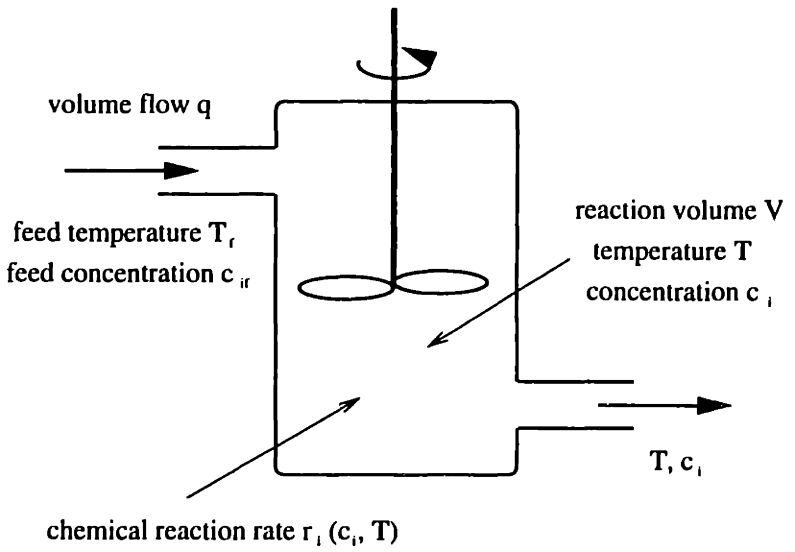

Figure 6-1: Open stirred tank

Figure 6-1 describes a general n-dimensional reaction dynamics in an open stirred tank (Henson and Seborg, 1997)

$$\dot{\mathbf{x}} = \frac{q}{V}(\mathbf{x}_f - \mathbf{x}) - \mathbf{G}\mathbf{r} \tag{6.1}$$

with the state vector $\mathbf{x} = (c_1 \ \ldots \ c_{n-1} \ \ T)^T$ consisting of the chemical concentrations

$0 \leq c_i \leq 1$ and the temperature $T > 0$, and the corresponding feed values $\mathbf{x}_f$. $q \geq 0$ represents the volume flow, and $V > 0$ the reaction volume. The positive stoichiometric coefficients ν_1 and ν_2 of the p chemical reactions

$$\nu_1 \, \mathbf{c} \rightarrow \nu_2 \, \mathbf{c}$$

and the reaction enthalpies ΔH_i define

$$\mathbf{G} = \begin{pmatrix} \nu_1^T - \nu_2^T \\ \Delta H_1 \ \ldots \ \Delta H_p \end{pmatrix}$$

The reaction rate vector $\mathbf{r}(\mathbf{x})$ consists of p reactions $r_i = k_i e^{-\frac{E_i}{RT}} c_j^{\nu_1 ij}$ with the activation energies $E_i \geq 0$, the reaction constants $k_i \geq 0$, and the general gas constant $R \geq 0$. Heat transfer can be simply added to $\frac{q}{V}(\mathbf{x}_f - \mathbf{x})$.

Contraction behavior of (6.1) can be concluded for uniformly negative definite $\frac{\partial \dot{\mathbf{x}}}{\partial \mathbf{x}} = -\frac{q}{V} - \mathbf{G}\frac{\partial \mathbf{r}}{\partial \mathbf{x}}$. Chain reactions can often be treated as hierarchies (see Section 4.3) as the following example illustrates.

Example 6.1: Consider the nuclear chain reaction

$$\begin{aligned} U_{92}^{238} + n_0^1 &\rightarrow U_{92}^{239} + \gamma \\ U_{92}^{239} &\rightarrow Np_{93}^{239} + e^- \\ Np_{93}^{239} &\rightarrow Pu_{94}^{239} + e^- \end{aligned}$$

whose reaction dynamics is with the reaction constants k_i and the control input $n_0^1(t) \geq \beta > 0$

$$\begin{aligned} \dot{U}_{92}^{238} &= -k_1 n_0^1 U_{92}^{238} \\ \dot{U}_{92}^{239} &= k_1 n_0^1 U_{92}^{238} - k_2 U_{92}^{239} \\ \dot{Np}_{93}^{239} &= k_2 U_{92}^{239} - k_3 Np_{93}^{239} \end{aligned}$$

The Jacobian of this dynamics is a left triangular matrix with uniformly negative definite main diagonal - The chain reaction

$$\begin{array}{ccccccc} U_{92}^{238} & \rightarrow & U_{92}^{239} & \rightarrow & Np_{93}^{239} & \rightarrow & Pu_{94}^{239} \\ n_0^1 & & \gamma & & e^- & & e^- \end{array}$$

is a contracting hierarchy. □

6.2 Chemical observer design

Consider the chemical reaction dynamics (6.1)

$$\dot{\mathbf{x}} = \frac{q}{V}(\mathbf{x}_f - \mathbf{x}) - \mathbf{G}\mathbf{r}$$

with measurement $\mathbf{y} = \mathbf{C}\mathbf{x}$ and constant $\mathbf{C}$. A chemical observer design

$$\dot{\hat{\mathbf{x}}} = \frac{q}{V}(\mathbf{x}_f - \hat{\mathbf{x}}) - \mathbf{G}\mathbf{r}(\hat{\mathbf{x}})$$

can

- modify $\mathbf{r}$ by replacing estimates $\hat{x}_i$ with actual measurements $y_i = x_i$.
- modify $\mathbf{G}$ by using a coordinate error feedback observer (see Section 4.11)

$$\begin{aligned}\dot{\bar{\mathbf{x}}} &= \frac{q}{V}(\mathbf{x}_f - \hat{\mathbf{x}}) - \mathbf{G}\mathbf{r}(\hat{\mathbf{x}}) + \mathbf{E}\mathbf{C}\left(\frac{q}{V}(\mathbf{x}_f - \mathbf{x}) - \mathbf{G}\mathbf{r}(\hat{\mathbf{x}})\right)\\ \hat{\mathbf{x}} &= \bar{\mathbf{x}} - \mathbf{E}\mathbf{y}\end{aligned}$$

leading to the observer dynamics

$$\dot{\hat{\mathbf{x}}} = \frac{q}{V}(\mathbf{x}_f + \mathbf{E}\mathbf{C}\mathbf{G}\mathbf{r}(\mathbf{x}) - \hat{\mathbf{x}}) - (\mathbf{G} + \mathbf{E}\mathbf{C}\mathbf{G})\,\mathbf{r}(\hat{\mathbf{x}})$$

Contraction behavior can the be concluded for uniformly negative definite $\frac{\partial \dot{\mathbf{x}}}{\partial \mathbf{x}} = -\frac{q}{V} - (\mathbf{G} + \mathbf{E}\mathbf{C}\mathbf{G})\frac{\partial \mathbf{r}}{\partial \mathbf{x}}$.

The following example illustrates this observer design for a standard industrial polymerization process.

Example 6.2: Consider the methyl methacrylate polymerization process in (Adebekun and Schork, 1989) in an open stirred tank

$$\begin{aligned}\dot{I} &= \frac{q}{V}(I_f - I) - k_1 e^{-\frac{E_1}{RT}} I\\ \dot{M} &= \frac{q}{V}(M_f - M) - k_2 e^{-\frac{E_2}{RT}} M\sqrt{I}\\ \dot{T} &= \frac{q}{V}(T_f - T) + \frac{hA_c}{V\rho c_p}(T_c - T) + \frac{\Delta H}{\rho c_p} k_2 e^{-\frac{E_2}{RT}} M\sqrt{I}\end{aligned}$$

with initiator concentration I, monomer concentration M, temperature T, coolant temperature $T_c = 310$ K, volume flow $q = 1$ l/s, reaction volume $V = 900$ l, general gas constant $R = 2$ cal/molT, activation energies $E_1 = 30000$ cal/mol, $E_2 = 19000$ cal/mol, reaction constants $k_1 = 1.69\ 10^{17}$ 1/s, $k_2 = \frac{1}{\sqrt{g_t}} 2.05\ 10^8$ $1/(\mathrm{s}\sqrt{mol})$, reaction enthalpy $\frac{\Delta H}{\rho c_p} = 33.24$ K/mol, heat transfer constant $\frac{hA_c}{V\rho c_p} = 0.001$ 1/s, and the Schmidt-Ray correlation for the gel effect

$$g_t = \begin{cases} 0.106 e^{-0.017(T-273.2)} & for\ T > 300K \\ 2.3\ 10^{-6} & for\ T \leq 300K \end{cases}$$

Consider now the coordinate feedback observer with temperature T measurement

$$\begin{aligned}\dot{\hat{I}} &= \frac{q}{V}\left(I_f - \hat{I}\right) - k_1 e^{-\frac{E_1}{RT}} \hat{I}\\ \dot{\hat{M}} &= \frac{q}{V}\left(M_f - \hat{M}\right) - k_2 e^{-\frac{E_2}{RT}} \hat{M}\sqrt{\hat{I}} - k_M\left(\frac{q}{V}(T_f - T) + \frac{hA_c}{V\rho c_p}(T_c - T) + \frac{\Delta H}{\rho c_p} k_2 e^{-\frac{E_2}{RT}} \hat{M}\sqrt{\hat{I}}\right)\end{aligned}$$

$$\begin{aligned}\dot{\hat{T}} &= \frac{q}{V}\left(T_f - \hat{T}\right) + \frac{hA_c}{V\rho c_p}\left(T_c - \hat{T}\right) + \frac{\Delta H}{\rho c_p} k_2 e^{-\frac{E_2}{RT}} \hat{M}\sqrt{\hat{I}} - k_T\left(\hat{T} - T\right) \\ \hat{M} &= \bar{M} + k_M T\end{aligned}$$

leading to the observer dynamics

$$\begin{aligned}\dot{\hat{I}} &= \frac{q}{V}\left(I_f - \hat{I}\right) - k_1 e^{-\frac{E_1}{RT}} \hat{I} \\ \dot{\hat{M}} &= \frac{q}{V}\left(M_f - \hat{M}\right) - k_2 e^{-\frac{E_2}{RT}} \hat{M}\sqrt{\hat{I}} - k_M \frac{\Delta H}{\rho c_p} k_2 e^{-\frac{E_2}{RT}} \left(\hat{M}\sqrt{\hat{I}} - M\sqrt{I}\right) \\ \dot{\hat{T}} &= \frac{q}{V}\left(T_f - \hat{T}\right) + \frac{hA_c}{V\rho c_p}\left(T_c - \hat{T}\right) + \frac{\Delta H}{\rho c_p} k_p(T) \hat{M}\sqrt{\hat{I}} - k_T\left(\hat{T} - T\right)\end{aligned}$$

This chain reaction dynamics represents a hierarchy $\hat{I} \to \hat{M} \to \hat{T}$, that can be extended with further intermediate chemicals. We can conclude on contraction behavior since $\frac{\partial \dot{\hat{I}}}{\partial \hat{I}}$, $\frac{\partial \dot{\hat{M}}}{\partial \hat{M}}$, $\frac{\partial \dot{\hat{M}}}{\partial \hat{M}}$ are uniformly negative definite. The monomer and temperature convergence rate can be arbitrarily improved with the feedback gains k_T and k_M, whereas the initiator convergence rate is given by the natural convergence rate.

Observer and plant responses with $k_M = 50$ mol/K, $k_T = 0.1$ 1/s, $I_f = 0.1 + 0.1 \sin 0.1t$ mol, $M_f = 0.8$ mol, $T_f = 340$ K, initial conditions $I(0) = 0.005$ mol, $M(0) = 0.8$ mol, $T(0) = 340$ K, $\hat{I}(0) = 0.01$ mol, $\hat{M}(0) = 0.5$ mol, $\hat{T}(0) = 360$ K are illustrated in Figure 6-2. The corresponding responses without feedback, i.e. $k_M = 0$ mol/K, $k_T = 0$ 1/s, are illustrated in Figure 6-3. The solid lines represent the real plant and the dashed lines the observer estimate. □

Finally, let us illustrate on a simple mixture process the incorporation of physical constraints and adaptation.

6.3 Mixture process

Consider the stirred tank in Figure 6-4, fed with two incoming flows with controllable flow rate q_1 and constant flow rate $q_2 = 1$ (Kwakernaak and Sivan, 1972). Both flows contain dissolved material with constant concentrations $c_1 = 0.1$ and $c_2 = 0.3$. The outgoing flow has a flow rate $q = k\sqrt{V}$, with the fluid volume V in the tank and an unknown outflow constant k. The partial volume of the dissolved material in the tank is V_c. The dynamic equations are

$$\begin{aligned}\dot{V} &= q_1 + q_2 - k\sqrt{V} \\ \dot{V}_c &= c_1 q_1 + c_2 q_2 - k V_c \frac{1}{\sqrt{V}}\end{aligned}$$

The dynamics is a hierarchy from V to V_c , and it is contracting since $\frac{\partial \dot{V}}{\partial V} = -\frac{k}{2\sqrt{V}}$ and $\frac{\partial \dot{V}_c}{\partial V_c} = -\frac{k}{\sqrt{V}}$ are uniformly negative. The adaptive tracking controller

$$q_1 = V_d - V - q_2 + \hat{k}\sqrt{V_d} + \dot{V}_d$$

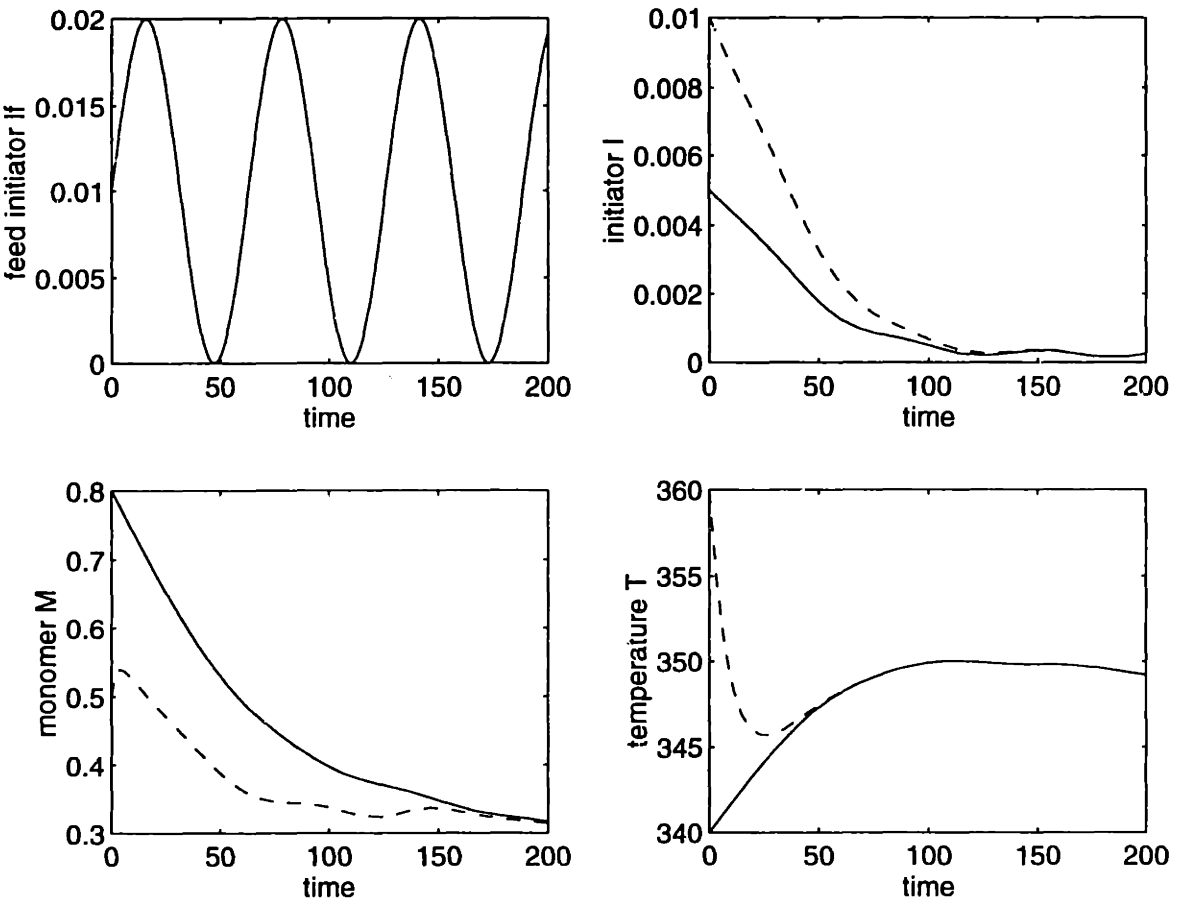

Figure 6-2: Polymerization observer

$$\dot{\hat{k}} \;=\; -0.1(V - V_d)\sqrt{V_d}$$

preserves the hierarchy from V to V_c. It guarantees with the adaptation results in Section 4.4 asymptotic convergence of V to $V_d(t)$ since $\frac{\partial \dot{V}}{\partial V} = -1 - k\frac{1}{2\sqrt{V}}$ is uniformly negative. Asymptotic tracking convergence of V_c can then be concluded for uniformly negative $\frac{\partial \dot{V}_c}{\partial V_c} = -k\frac{1}{\sqrt{V}}$.

To complete the design, we must also account for the physical input constraint $q_1 \geq 0$, leading to the actual control input

$$q_1 = \max(0, V_d - V - q_2 + \hat{k}\sqrt{V_d} + \dot{V}_d)$$

If we turn off adaptation for $q_1 = 0$ then the system switches continuously between two semi-contracting systems in the same coordinates V, V_c, and $\hat{k}$. The switching system is hence from Section 4.8 contracting as well. Note that the actual trajectory cannot necessarily follow any arbitrary trajectory, since a suitable open loop input may not exist due to the input constraint $q_1 \geq 0$.

Plant responses and control input, with $V_d(t) = \sin t + 3$, and initial conditions

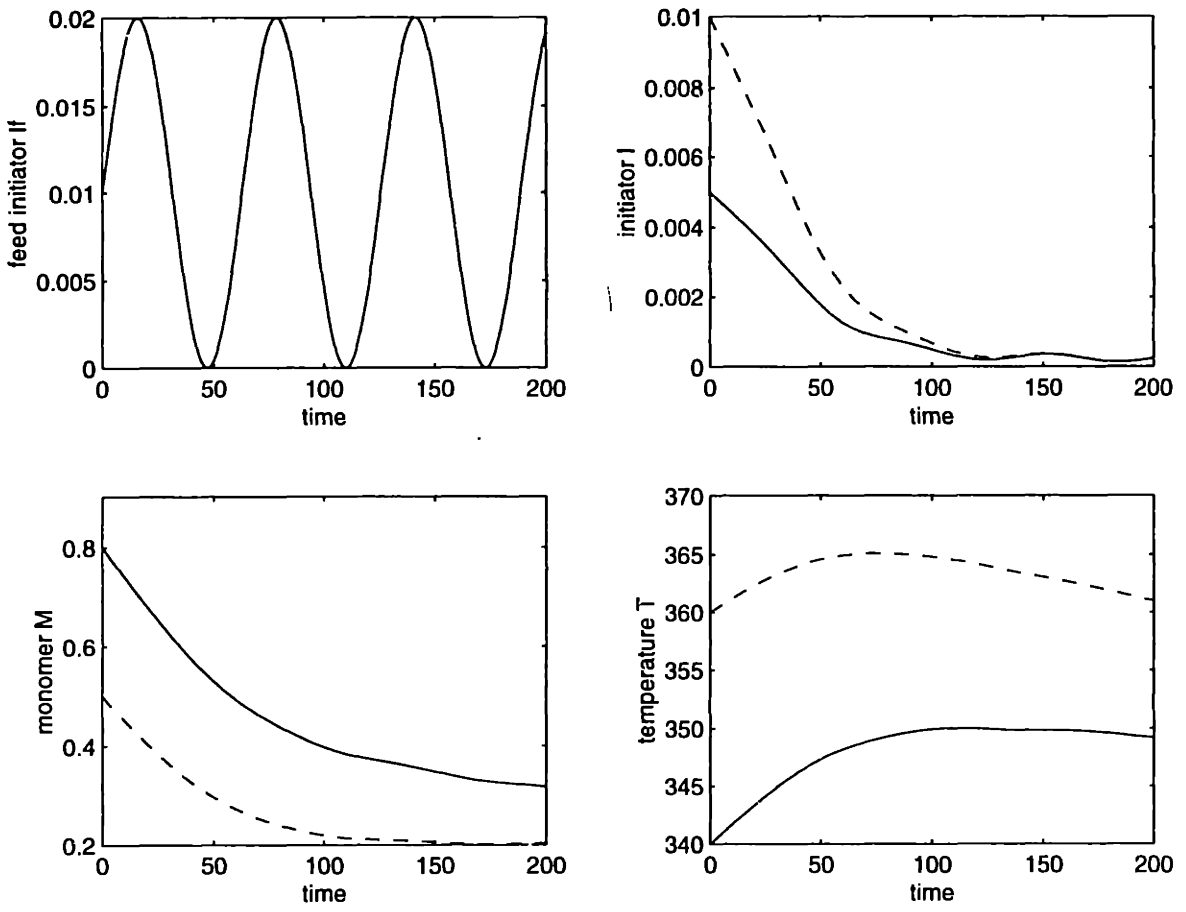

Figure 6-3: Polymerization observer without feedback

$V(0) = 5$, $V_c(0) = 5$, $\hat{k}(0) = 0.7$ and $k = 1$, are illustrated in Figure 6-5. The dashed line represents the desired trajectory and the solid lines the actual plant responses. Note that the actual trajectory cannot completely follow the desired trajectory due to the input constraint $q_1 \geq 0$.

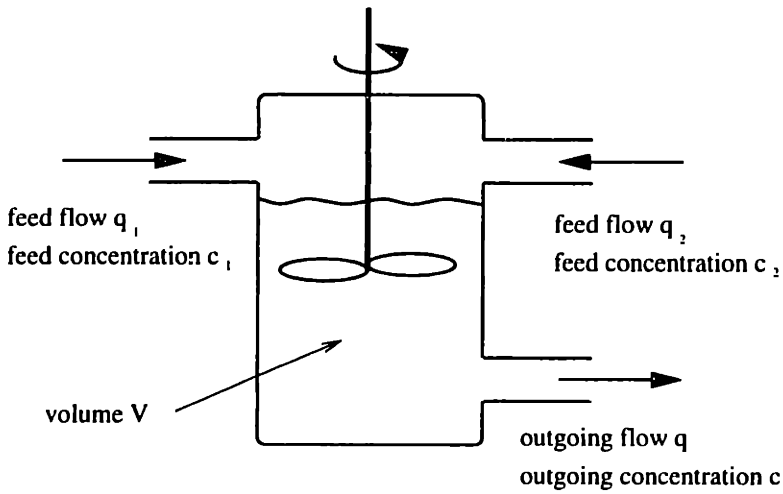

Figure 6-4: Stirred tank

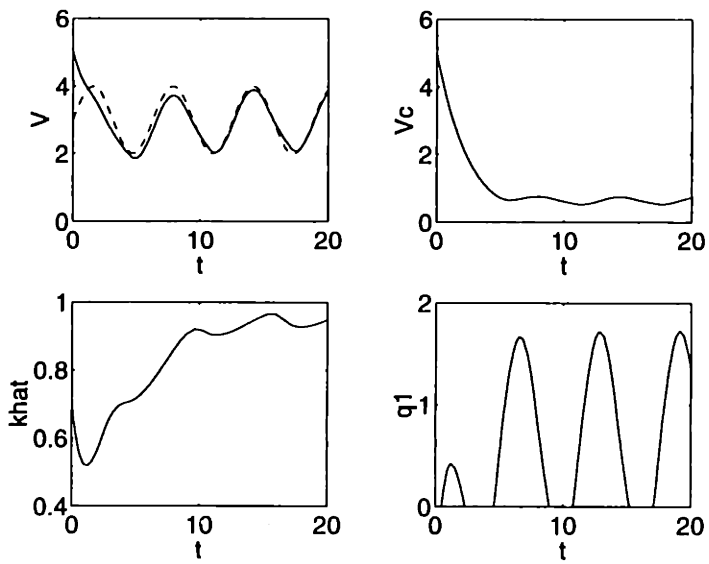

Figure 6-5: Mixture process controller

Chapter 7

Nonlinear partial differential equations

We now extend and apply the above results to practical classes of physical systems described by nonlinear partial differential equations. We shall use continuous state vectors Φ in Cartesian coordinates $\mathbf{x}$, defined on a bounded m-dimensional region V. Bold characters will denote the continuous state-space quantities corresponding to pointwise terms. For instance, $\dot{\Phi}$ will denote the state-space vector of components $\frac{\partial \phi}{\partial t}$, and $\nabla^k \Phi$ the state-space vector of components $\nabla^k \phi$.

Formally, Φ now lives on the Hilbert space $L^2(V)$, and differential length is defined by $\int_V \delta\phi^2 dV$, so that the above derivation extends immediately. Furthermore, continuous state-space quantities can be computed as the limits of regularly discretized versions, as the discretization step tends to zero. For instance, on a one-dimensional continuum of length l

$$\int_V \delta\phi^2 dV = \lim_{n \to +\infty} \frac{l^2}{n^2} \sum_{i=1}^{n} \delta\phi_i^T \delta\phi_i$$

where the $\delta\phi_i$'s are the discretized values. This limiting process will be our main computation tool in assessing and quantifying the stability properties of the systems.

Specifically, in Section 7.1 and 7.2 we analyze the contraction properties of the Laplace (∇^2) operator. Section 7.3 analyzes and quantifies the convergence rate of the heat equation including nonlinear source terms. Corresponding discretized partial differential equations are analyzed in Section 7.4.

7.1 One-dimensional Laplace operator

Consider now the one-dimensional Laplace operator on the continuum, with given $\phi_l(t)$ and $\phi_r(t)$. We can write

$$\nabla^2\Phi = \lim_{n\to+\infty} \frac{(n+1)^2}{l^2} \left(\begin{pmatrix} -2 & 1 & 0 & 0 & \ddots \\ 1 & -2 & 1 & \ddots & \ddots \\ 0 & 1 & \ddots & \ddots & 0 \\ 0 & \ddots & \ddots & -2 & 1 \\ \ddots & \ddots & 0 & 1 & -2 \end{pmatrix} \Phi + \begin{pmatrix} \phi_l \\ 0 \\ \vdots \\ 0 \end{pmatrix} + \begin{pmatrix} 0 \\ \vdots \\ 0 \\ \phi_r \end{pmatrix} \right) \tag{7.1}$$

The corresponding Jacobian is

$$\frac{\partial\nabla^2\Phi}{\partial\Phi} = \lim_{n\to+\infty} \frac{(n+1)^2}{l^2} \begin{pmatrix} -2 & 1 & 0 & 0 & \ddots \\ 1 & -2 & 1 & \ddots & \ddots \\ 0 & 1 & \ddots & \ddots & 0 \\ 0 & \ddots & \ddots & -2 & 1 \\ \ddots & \ddots & 0 & 1 & -2 \end{pmatrix} \tag{7.2}$$

whose largest eigenvalue is shown in the Appendix to be upper bounded by $-\frac{2\pi^2}{l^2}$. Thus, the one-dimensional Laplace operator $\nabla^2\Phi$ with given boundary elements $\phi_l(t)$ and $\phi_r(t)$ is contracting.

Consider instead the Laplace operator with given boundary elements $\phi_l(t)$ and $\nabla\phi_r(t)$ along a continuum of length l. By adding a mirror image of the system to the right we get a continuum of length $2l$ and given boundary elements $\phi_l(t)$ and $\phi_r(t)$. Thus the largest eigenvalue of the Jacobian is $-\frac{\pi^2}{2l^2}$.

If instead, $\nabla\phi_l(t)$ and $\nabla\phi_r(t)$ are given on the left and right boundary, then in (7.2) the upper left and lower right corners become -1. A similar derivation in the Appendix shows that the resulting matrix is only negative semi-definite, i.e. the resulting Laplacian is only semi-contracting. Note that this can be expected physically, since the system might simply converge to a specific Φ with a constant error over the continuum.

7.2 Multi-dimensional Laplace operator

Consider now the m-dimensional Laplacian

$$\nabla^2\Phi = \sum_{i=1}^{m} \frac{\partial^2\Phi}{\partial x_i^2}$$

defined in a general region with Cartesian orthonormal coordinates x_i, and given $\phi_b(t)$ on the boundary of that region. Discretizing that region similar to the previous

section along x_i, the largest eigenvalue of $\frac{\partial^2 \Phi}{\partial x_i^2}$ is $-\frac{2\pi^2}{l_{i,max}^2}$, where $l_{i,max}$ is the diameter (maximal thickness) of the region in direction x_i. Computing the largest eigenvalues along the remaining coordinates x_j, $j \neq i$ and noting that a discretization in x_i can be transformed to another discretization in x_j with an orthonormal coordinate transformation, not influencing the contraction rate the largest eigenvalue of $\nabla^2 \Phi = \sum_{i=1}^{m} \frac{\partial^2 \Phi}{\partial x_i^2}$ is at most

$$\lambda_{\nabla^2} = -\sum_{i=1}^{m} \frac{2\pi^2}{l_{i,max}^2} \tag{7.3}$$

The multi-dimensional Laplace operator $\nabla^2 \Phi$ with given boundary elements $\phi_b(t)$ is contracting. If instead $\nabla \phi_b(t)$ is given on the complete boundary, then the Laplacian is only semi-contracting with

$$\lambda_{\nabla^2} = 0 \tag{7.4}$$

Example 7.1: Consider the Laplace operator in spherical coordinates

$$\nabla^2 \Phi = \frac{\partial^2 \Phi}{\partial r^2} + \frac{2}{r}\frac{\partial \Phi}{\partial r} + \frac{1}{r^2}\frac{\partial^2 \Phi}{\partial \nu^2} + \frac{\cos \nu}{r^2 \sin \nu}\frac{\partial \Phi}{\partial \nu} + \frac{1}{r^2 \sin^2 \nu}\frac{\partial^2 \Phi}{\partial \theta^2}$$

with angles θ, ν, and radius r, and assume that $\phi_b(t)$ is given on the sphere $r = r_o$. The diameter of that sphere is $2r_o$, so that the largest eigenvalue of this Laplacian is $\lambda_{\nabla^2} = -\frac{3}{2}\frac{\pi^2}{r_o^2}$. □

7.3 Reaction-diffusion equation

Collecting the above results and using Theorem 2 thus yields

Theorem 4 *Given the reaction-diffusion equation*

$$\frac{\partial \phi}{\partial t} = h\ \nabla^2 \phi + f(\phi, \mathbf{x}, t) \tag{7.5}$$

with positive h, any trajectory Φ converges exponentially to a single trajectory $\Phi_d(\mathbf{x}, t)$ for uniformly negative

$$h\ \lambda_{\nabla^2} + \frac{\partial f}{\partial \phi}$$

with minimal convergence rate $|h\lambda_{\nabla^2} + \frac{\partial f}{\partial \phi}|$, where λ_{∇^2} is defined by equation (7.3) or (7.4) depending on the boundary conditions.
In the autonomous case, Φ_d simply represents the solution of the generalized Poisson equation

$$0 = h\ \nabla^2 \phi_d + f(\phi_d, \mathbf{x})$$

Note that the reaction-diffusion equation also describes heat transfer and is used in machine vision. Also many other practical nonlinear partial differential equations

as the Burgers equation (Evans, 1998) can be transformed to the reaction diffusion equation.

The Schroedinger equation

$$i\hbar\frac{\partial\phi}{\partial t} = -\frac{\hbar^2}{2m}\nabla^2\phi + V(\phi, \mathbf{x}, t)$$

can be studied with minor modifications, where $\hbar$ is the reduced Planck constant, m the mass, and $\frac{\partial V}{\partial \phi}$ the potential, all reals. Defining squared length as $\delta\Phi^T\delta\Phi^*$ (where $*$ indicates complex conjugation), using

$$i\hbar\delta\dot{\Phi} \;=\; -\frac{\hbar^2}{2m}\frac{\partial\nabla^2\Phi}{\partial\Phi}\delta\Phi + \frac{\partial \mathbf{V}}{\partial\Phi}\delta\Phi$$

leads to

$$\frac{d}{dt}\left(\delta\Phi^T\delta\Phi^*\right) = \delta\dot{\Phi}^T\delta\Phi^* + \delta\Phi^T\delta\dot{\Phi}^* = 0$$

Thus the system is indifferent, a well-known result in the linear time-invariant case.

The above also implies that all the system combination results can be extended to contracting diffusion processes. In particular, any autonomous contracting diffusion equation, if unforced, will tend exponentially to a unique equilibrium solution, and if driven by an input periodic in time, will tend exponentially to a periodic solution of the same period. Also the convergence is robust to bounded or linearly increasing disturbances.

Example 7.2: Consider a wafer disk of radius $r_o = 20$ cm in Figure 7-1 whose temperature is controlled with a continuous external light source (Cho and Gyugyi, 1997). The dynamic equations in radial coordinates θ and r are (Groeber, et al., 1988):

$$\dot{T} = -h\nabla^2 T - f\left(T^4 - T_o^4\right) = -h\left(\frac{1}{r}\frac{\partial}{\partial r}\left(r\frac{\partial T}{\partial r}\right) + \frac{1}{r^2}\frac{\partial^2 T}{\partial\theta^2}\right) - f\left(T^4 - T_o^4\right)$$

with wafer temperature $T > 0$, externally controlled temperature $T_o 0$, heat transfer constant $h = 1$ cm^2/s, radiation constant $f = 10^{-9}$ 1/K^{3}s, and boundary conditions $\frac{\partial T}{\partial r}_{r_o} = 0$. Note that, in contrast to the Laplacian, the radiation $-f(T^4 - T_o^4)$ represents the only "genuine" nonlinearity in this dynamics. The system is according to Theorem 4 naturally contracting with minimal convergence rate $4fT^3$. The natural contraction behavior can be augmented with additional source terms or different boundary conditions.

Two plant responses with $T_o = 500 + 200\sin\frac{\pi t}{20s}$ K, and continuous initial conditions $T_1(0) = 900 - 200\cos\frac{2\pi r}{r_0}$ K, $T_2(0) = 300 + 200\cos\frac{2\pi r}{r_0}$ K are illustrated in Figure 7-2. For computational simplicity the simulation assumes rotational symmetry in θ. □

7.4 Discretized diffusion equation

This section briefly discusses some of the implications of the previous results for the numerical simulation of partial differential equations. Let us discretized equation (7.5) by approximating the continuous state vector Φ with $\Phi(\Psi, \mathbf{x})$, where Ψ is a

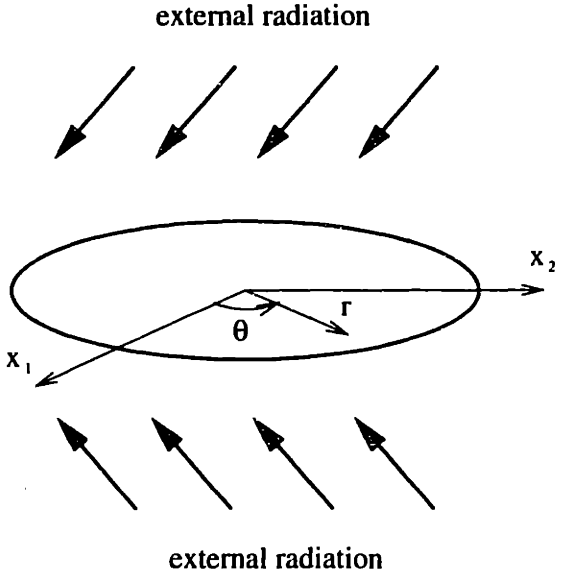

Figure 7-1: Thermal processing of a wafer

finite-dimensional state vector. This discretization leads to an error $\mathbf{e}$ in equation (7.5)

$$\dot{\Phi} = h\nabla^2\Phi + \mathbf{f}(\Phi, \mathbf{x}, t) + \mathbf{e} \tag{7.6}$$

We can minimize $\mathbf{e}$ by requiring $\frac{\partial\Phi}{\partial\Psi}^T\mathbf{e} = \mathbf{0}$ resulting in

$$\mathbf{M}\dot{\Psi} = \frac{\partial\Phi}{\partial\Psi}^T\left(h\nabla^2\Phi + \mathbf{f}\right)$$

with $\mathbf{M} = \frac{\partial\Phi}{\partial\psi}^T\frac{\partial\Phi}{\partial\psi}$. Taking the variation of (7.6) and $\delta(\frac{\partial\Phi}{\partial\Psi}^T\mathbf{e}) = \mathbf{0}$ lead to

$$\frac{1}{2}\frac{d}{dt}(\delta\Psi^T\mathbf{M}\delta\Psi) = \delta\Psi^T\frac{\partial\Phi}{\partial\Psi}^T\frac{\partial(h\nabla^2\Phi + \mathbf{f})}{\partial\Phi}\frac{\partial\Phi}{\partial\Psi}\delta\Psi - \delta\Psi\frac{\partial^2\Phi}{\partial\Psi^2}^T\mathbf{e}\,\delta\Psi$$

This dynamics can be simplified with the largest eigenvalue λ_{max} of $\frac{\partial\Phi}{\partial\Psi}^T\frac{\partial(h\nabla^2\Phi+\mathbf{f})}{\partial\Phi}\frac{\partial\Phi}{\partial\Psi}$ with respect to $\mathbf{M}$, and the maximal principal curvature $|\kappa|_{max}$ of $\Phi(\Psi, \mathbf{x})$

$$\frac{1}{2}\frac{d}{dt}(\delta\Psi^T\mathbf{M}\delta\Psi) \leq (\lambda_{max} + \|\mathbf{e}\||\kappa|_{max})\,\delta\Psi^T\mathbf{M}\delta\Psi$$

If we assume Ψ to be a minimal realization of Φ, i.e. require $\mathbf{M}$ to be uniformly positive definite then exponential convergence of $\delta\Psi^T\mathbf{M}\delta\Psi$ to zero implies exponential convergence of $\delta\Psi^T\delta\Psi$ to zero. The contraction behavior is hence unchanged in regions of small $\|\mathbf{e}\||\kappa|_{max}$. This simply means that we have to approximate regions with large $|\kappa|_{max}$ more precisely.

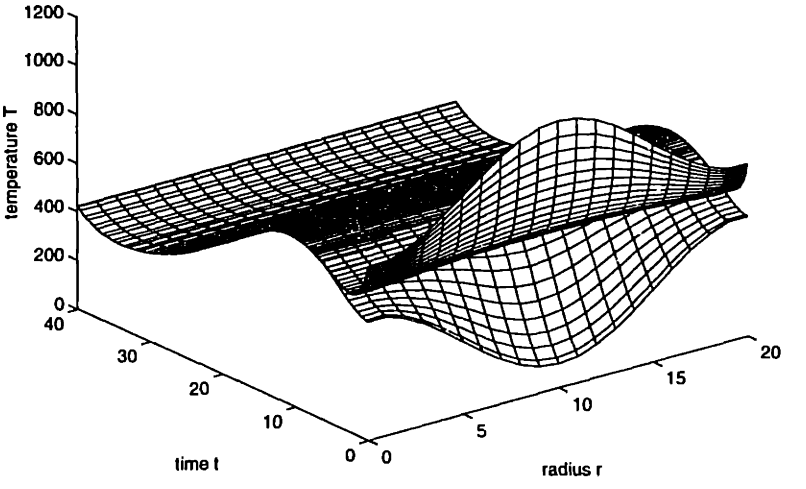

Figure 7-2: Wafer temperature as a function of time

Appendix[1]

Let us compute an upper bound on the largest eigenvalue λ of the $n \times n$ matrix

$$-\frac{(n+1)^2}{l^2}\begin{pmatrix} 2 & -1 & 0 & 0 & \ddots \\ -1 & 2 & -1 & \ddots & \ddots \\ 0 & -1 & \ddots & \ddots & 0 \\ 0 & \ddots & \ddots & 2 & -1 \\ \ddots & \ddots & 0 & -1 & 2 \end{pmatrix} \tag{7.7}$$

as $n \to +\infty$. Since λ is the largest eigenvalue of (7.7), the $n \times n$ matrix

$$\begin{pmatrix} 2-2\eta & -1 & 0 & 0 & \ddots \\ -1 & 2-2\eta & -1 & \ddots & \ddots \\ 0 & -1 & \ddots & \ddots & 0 \\ 0 & \ddots & \ddots & 2-2\eta & -1 \\ \ddots & \ddots & 0 & -1 & 2-2\eta \end{pmatrix} \tag{7.8}$$

[1]We are grateful to Christophe Bernard for his help in this derivation.

is positive semi-definite, where $\eta = -\frac{l^2}{2(n+1)^2}\lambda$. Now the principal minors Δ_k of (7.8), which must all be positive or zero, can be computed recursively

$$\Delta_k^2 = (2-2\eta)\Delta_{k-1}^2 - \Delta_{k-2}^2$$

with $\Delta_1 = 2-2\eta$ and $\Delta_2 = (2-2\eta)^2 - 1$. Noticing that $\Delta_1 \geq 0$ implies $\eta \leq 1$, this yields

$$\Delta_k = \frac{\left(1-\eta+\sqrt{(1-\eta)^2-1}\right)^{k+1} - \left(1-\eta-\sqrt{(1-\eta)^2-1}\right)^{k+1}}{2\sqrt{(1-\eta)^2-1}}$$

Thus, letting $\cos\alpha = 1-\eta$ and $\sin\alpha = \sqrt{1-(1-\eta)^2}$, with $0 \leq \alpha \leq \frac{\pi}{2}$, one can write

$$\Delta_k = \frac{(\cos\alpha + i\sin\alpha)^{k+1} - (\cos\alpha - i\sin\alpha)^{k+1}}{2i\sin\alpha} = \frac{\sin(k+1)\alpha}{\sin\alpha}$$

Thus, $\Delta_k \geq 0$ implies that $\alpha \leq \frac{\pi}{k+1}$, for any $k \geq 1$. This in turn implies that

$$1-\eta = \cos\alpha \geq 1 - \alpha^2 \geq 1 - \frac{\pi^2}{(k+1)^2}$$

and thus that $\eta \leq \frac{\pi^2}{(n+1)^2}$. As $n \to +\infty$, the largest eigenvalue of (7.7) thus verifies

$$\lambda_{\nabla^2} = -\lim_{n\to+\infty} \frac{2(n+1)^2}{l^2}\eta \leq -\frac{2\pi^2}{l^2}$$

In the simpler case of boundary conditions in $\nabla\phi_l(t)$ and $\nabla\phi_r(t)$, the corresponding $n \times n$ matrix is

$$\frac{(n+1)^2}{l^2}\begin{pmatrix} -1 & 1 & 0 & 0 & \ddots \\ 1 & -2 & 1 & \ddots & \ddots \\ 0 & 1 & \ddots & \ddots & 0 \\ 0 & \ddots & \ddots & -2 & 1 \\ \ddots & \ddots & 0 & 1 & -1 \end{pmatrix} \tag{7.9}$$

To show that this matrix is negative semi-definite as $n \to +\infty$ it suffices to show that

$$\begin{pmatrix} 1 & -1 & 0 & 0 & \ddots \\ -1 & 2 & -1 & \ddots & \ddots \\ 0 & -1 & \ddots & \ddots & 0 \\ 0 & \ddots & \ddots & 2 & -1 \\ \ddots & \ddots & 0 & -1 & 1 \end{pmatrix} \tag{7.10}$$

is positive semi-definite. Computing by induction the principal minors Δ_k of the

above matrix leads to $\Delta_k = 1$ for $1 \leq k \leq n-1$, and $\Delta_n = 0$, hence the result. $\square$

Chapter 8

Nonlinear eigenvalue analysis

This Chapter introduces a generalization of linear eigenvalue analysis to nonlinear systems $\dot{\mathbf{x}} = \mathbf{f}(\mathbf{x})$. We assume that the system possesses at least one equilibrium point $\mathbf{x}_e$. The principle is simple: rather than performing linearized analysis at each point in a coordinate system defined a priori, *we compute a suitable differential coordinate transformation* $\Theta(\mathbf{x})$ *such that the corresponding generalized Jacobian* $\mathbf{F}$ *is constant,* and equal to the (coordinate-invariant) Jordan form of the linearized system at the equilibrium point $\mathbf{x}_e$. In the case of several equilibrium points, the corresponding Θ will have singularities, thus partitioning the state-space into distinct regions.

8.1 Nonlinear eigenvector computation

Let us first illustrate that in general, in contrast to linear systems, only the eigenvalues of the generalized Jacobian $\mathbf{F}$ around an equilibrium point $\mathbf{x}_e$ (with $\mathbf{f}(\mathbf{x}_e) = \mathbf{0}$) are guaranteed to be coordinate invariant.

Example 8.1: Consider again the example of equation (1.2). The generalized Jacobian F, which is equivalent to the eigenvalue λ in this case, is represented in z and x coordinates by the solid and dashed lines in Figure 8-1. They are identical around the equilibrium point $x_e = 0$ but differ in the rest of the state space – only the eigenvalue around an equilibrium point is coordinate invariant. Note more specifically that it is the term $\dot{\Theta}$ in (3.4) which causes the discrepancy. □

In order to guarantee coordinate invariance of our computations, a simple approach is to use the constant eigenvalues λ from $\det|\frac{\partial \dot{\mathbf{x}}}{\partial \mathbf{x}}(\mathbf{x}_e) - \lambda \mathbf{I}| = 0$ around an equilibrium point $\mathbf{x}_e$ to define the constant Jordan matrix Λ of the eigenvector computation. The eigenvector matrix Θ can then be computed from (3.4)

$$\mathbf{F} = \left(\dot{\Theta} + \Theta \frac{\partial \mathbf{f}}{\partial \mathbf{x}}\right) \Theta^{-1} = \Lambda$$

which can be rewritten as

$$\frac{\partial \Theta}{\partial \mathbf{x}} \mathbf{f} + \Theta \frac{\partial \mathbf{f}}{\partial \mathbf{x}} = \Lambda \Theta \tag{8.1}$$

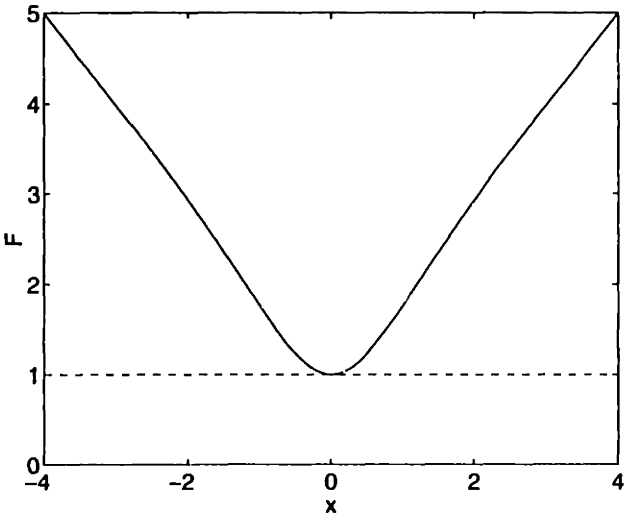

Figure 8-1: Generalized Jacobian in different coordinate systems

Unlike $\mathbf{z}(\mathbf{x})$, the solution $\Theta(\mathbf{x})$ of equation (8.1) is guaranteed to exist, from Frobenius theorem (Lovelock and Rund, 1989). Indeed, $\Theta_e = \Theta(\mathbf{x}_e)$ is given by the left eigenvector matrix of the linearized system, and the remaining $\Theta(\mathbf{x})$ can be computed numerically by solving (8.1) along the system trajectories.

If Λ is diagonal then the computations in (8.1) can be simplified to $\frac{\partial \theta}{\partial \mathbf{x}}\mathbf{f} + \theta\left(\frac{\partial \mathbf{f}}{\partial \mathbf{x}} - \lambda \mathbf{I}\right) = \mathbf{0}$, where θ corresponds to a row vector of Θ.

8.2 Coordinate invariance

The preceding calculation explicitly guarantees the coordinate invariance of Λ. Let us now show that under a coordinate transformation $\mathbf{x}^*(\mathbf{x})$, the computed eigenvector field transforms linearly, with $\Theta^* = \Theta\frac{\partial \mathbf{x}}{\partial \mathbf{x}^*}$.

Indeed, consider the eigenvector field of the plant dynamics $\dot{\mathbf{x}}^* = \mathbf{f}^* = \frac{\partial \mathbf{x}^*}{\partial \mathbf{x}}\mathbf{f}$ in $\mathbf{x}^*(\mathbf{x})$ coordinates

$$\frac{\partial \Theta^*}{\partial \mathbf{x}^*}\mathbf{f}^* + \Theta^*\frac{\partial \mathbf{f}^*}{\partial \mathbf{x}^*} = \Lambda\Theta^*$$

that is with $\Theta^* = \Theta\frac{\partial \mathbf{x}}{\partial \mathbf{x}^*}$

$$\left(\Theta\frac{\partial}{\partial \mathbf{x}}\left(\frac{\partial \mathbf{x}}{\partial \mathbf{x}^*}\right)\frac{\partial \mathbf{x}}{\partial \mathbf{x}^*} + \frac{\partial \Theta}{\partial \mathbf{x}}\frac{\partial \mathbf{x}}{\partial \mathbf{x}^*}\frac{\partial \mathbf{x}}{\partial \mathbf{x}^*}\right)\frac{\partial \mathbf{x}^*}{\partial \mathbf{x}}\mathbf{f} + \Theta\frac{\partial \mathbf{x}}{\partial \mathbf{x}^*}\left(\frac{\partial \mathbf{x}^*}{\partial \mathbf{x}}\frac{\partial \mathbf{f}}{\partial \mathbf{x}} + \frac{\partial \mathbf{x}^{*2}}{\partial \mathbf{x}^2}\mathbf{f}\right)\frac{\partial \mathbf{x}}{\partial \mathbf{x}^*} = \Lambda\Theta\frac{\partial \mathbf{x}}{\partial \mathbf{x}^*}$$

and $\frac{\partial}{\partial \mathbf{x}}\left(\frac{\partial \mathbf{x}}{\partial \mathbf{x}^*}\frac{\partial \mathbf{x}^*}{\partial \mathbf{x}}\right) = \mathbf{0}$

$$\frac{\partial \Theta}{\partial \mathbf{x}}\mathbf{f} + \Theta\frac{\partial \mathbf{f}}{\partial \mathbf{x}} = \Lambda\Theta$$

which proves the result.

8.3 Nonlinear modal analysis

Once the left eigenvector matrix Θ is found, the modal coordinate dynamics

$$\frac{d}{dt}\delta\mathbf{z} = \Lambda\delta\mathbf{z}$$

with initial condition $\delta\mathbf{z}_o = \Theta(\mathbf{x}_o)\delta\mathbf{x}_o$ at initial position $\mathbf{x}_o$ and initial time t_o can be solved

$$\delta\mathbf{z}(t) = e^{\Lambda(t-t_o)}\delta\mathbf{z}_o$$

By path integration this implies that any trajectory with initial finite distance to the manifold through $\mathbf{x}_e$ and span by the unstable eigenvectors directions converges exponentially to this manifold. On this unstable manifold any trajectory with $\mathbf{x}_o \neq \mathbf{x}_e$ diverges exponentially to a set with ∞ distance to $\mathbf{x}_e$.

We can also solve for the $\mathbf{x}$ dynamics directly from

$$\delta\mathbf{x}(\mathbf{x}, t) = \Phi(\mathbf{x}, t)\delta\mathbf{x}_o$$

where $\Phi(\mathbf{x}, t) = \Theta^{-1}(\mathbf{x})e^{\Lambda(t-t_o)}\Theta(\mathbf{x}_o)$ represents a nonlinear transition matrix, leading to

$$\mathbf{x} - \mathbf{x}_e = \int_{\mathbf{x}_e}^{\mathbf{x}_o} \Phi(\mathbf{x}, t)\delta\mathbf{x}_o$$

where the path integral is defined along the forward image of an initial connecting path between $\mathbf{x}_e$ and $\mathbf{x}_o$.

8.4 Nonlinear eigenvalue analysis and chaos theory

We can now more specifically interpret Lyapunov exponents in chaos theory (Ruelle, 1982; Guckenheimer and Holmes, 1983; Strogatz, 1994) in this context. Chaos theory analyzes numerically the time limit of a virtual displacement along a system trajectory $\mathbf{x}(t)$

$$\lim_{t\to\infty} \delta\mathbf{x} = \lim_{t\to\infty} \Phi(\mathbf{x}(t), t)\delta\mathbf{x}_o$$

The n independent Lyapunov exponents σ_j describing this limit behavior are then defined as (see e.g. (Argyris, *et al.*, 1994))

$$\sigma_j = \lim_{t\to\infty} \frac{1}{t} \ln|\text{Eig } \Phi(\mathbf{x}(t), t)|$$

if this limit exists. Since the Θ matrices in $\Phi(\mathbf{x}, t) = \Theta^{-1}(\mathbf{x})e^{\Lambda t}\Theta(\mathbf{x}_o)$ are computed at different positions $\mathbf{x}$ and $\mathbf{x}_o$, the eigenvalues of Φ and hence *the Lyapunov exponents are not coordinate invariant.* Accordingly Lyapunov exponents do not represent intrinsic properties of a dynamic system.

8.5 Two simple nonlinear eigenvector fields

Let us now illustrate the nonlinear eigenvector computation with two elementary examples, highlighting the role of singularities in Θ. The proposed method applies in principle to systems of any dimension.

Example 8.2: Consider the plant

$$\dot{x} = -\sin x$$

whose linearized eigenvalue at the equilibrium point $x_e = 0$ is $\lambda = -1$. The nonlinear eigenvector field can be computed from

$$F = \left(-\frac{\partial\theta}{\partial x}\sin x - \theta\cos x\right)\theta^{-1} = -1 \qquad \theta_e = 1$$

leading to $\theta = \frac{1}{1+\cos x}$. Figure 8-2 shows that the distance between x_e and $x = \pm\pi$ is $\int_o^{\pm\pi}\|\delta z\| = \infty$. This means that a trajectory starting at $x = \pm\pi$ will never converge to x_e or $]-\pi,\ \pi[$ is the complete region of convergence of x_e. □

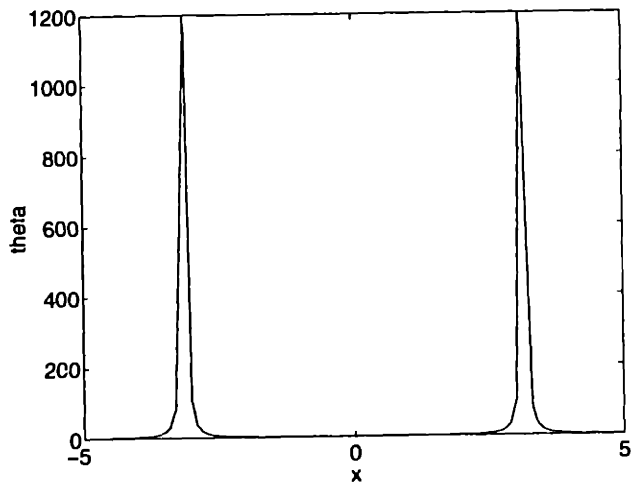

Figure 8-2: One-dimensional eigenvector field

Note that this analytic eigenvector computation can be extended recursively to systems with triangular Jacobian. In general, however, the eigenvector computation must be performed numerically, as we now illustrate.

Example 8.3: Consider the Van der Pol equation

$$\begin{aligned}\ddot{x} &= -(x^2-1)\dot{x} - x\\ \dot{x} &= \dot{x}\end{aligned}$$

The constant real Jordan form $\mathbf{\Lambda}$ in the whole state space and the left eigenvector matrix $\mathbf{\Theta}_e$ around the equilibrium point $\mathbf{x}_e = (0\ 0)^T$ are

$$\mathbf{\Lambda} = \begin{pmatrix} \frac{1}{2} & -\frac{\sqrt{3}}{2} \\ \frac{\sqrt{3}}{2} & \frac{1}{2} \end{pmatrix} \qquad \mathbf{\Theta}_e = \begin{pmatrix} 1 & -\frac{1}{2} - \frac{\sqrt{3}}{2} \\ 1 & -\frac{1}{2} - \frac{1}{2\sqrt{3}} + \frac{2}{\sqrt{3}} \end{pmatrix}$$

The nonlinear eigenvector field $\mathbf{\Theta}(x, \dot{x})$ can be computed recursively by solving numerically

$$\frac{\partial \mathbf{\Theta}}{\partial \mathbf{x}} \begin{pmatrix} -(x^2-1)\dot{x} - x \\ \dot{x} \end{pmatrix} + \mathbf{\Theta} \begin{pmatrix} -(x^2-1) & -2\dot{x}x - 1 \\ 1 & 0 \end{pmatrix} = \mathbf{\Lambda}\mathbf{\Theta}$$

along system trajectories. The result is illustrated in Figure 8-3, where we have stopped integration at the singularities of $\mathbf{\Theta}$. Also note that in the plot we have saturated $\mathbf{\Theta}$ (which becomes infinite) at the boundary of the eigenvector field.

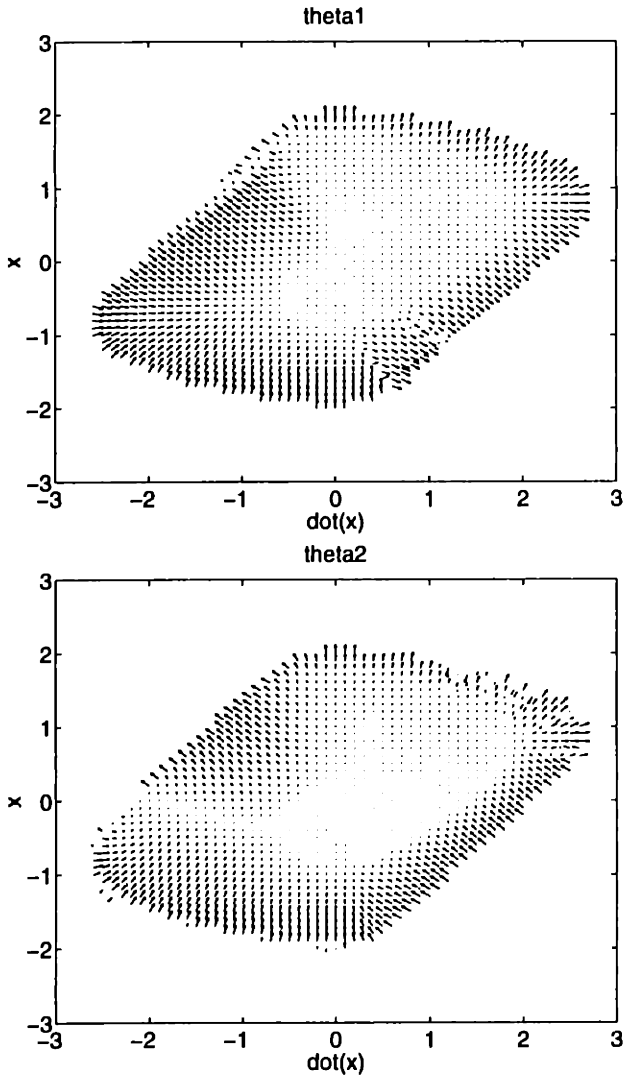

Figure 8-3: Eigenvector field of the Van der Pol equation

For unstable $\mathbf{\Lambda}$, any trajectory which does not start at $\mathbf{x}_e$ diverges to a set with infinite distance to the equilibrium point $\mathbf{x}_e$, i.e., to the boundary of the eigenvector field in Figure 8-3.

Since the boundary of the eigenvector field itself is not in the range of $\mathbf{\Theta}$, nothing can be said on the contraction behavior of two trajectories on this boundary.

Of course, in this simple example much of this information could be inferred from the phase portrait of the system itself, but the method applies systematically to higher order systems as well. □

Chapter 9

Continuous-time controller and observer designs

This Chapter explicitly exploits the fact that contraction analysis only requires a local coordinate transformation $\delta \mathbf{z} = \Theta \delta \mathbf{x}$ in order to guarantee exponential convergence. This leads in Section 9.1 to a generalization of feedback linearization. For the completion of the discussion Section 9.2 gives a brief derivation of the corresponding observer design, that turns out to be the extended Luenberger observer in (Zeitz, 1987).

9.1 Continuous-time controllers

In this Section we consider $\forall t \geq 0$ a smooth dynamic system

$$\dot{\mathbf{x}} = \mathbf{f}(\mathbf{x}, u, t) \tag{9.1}$$

with control input u. First we analyze the virtual dynamics around a general trajectory $\mathbf{x}(t)$

$$\delta \dot{\mathbf{x}} = \mathbf{A} \delta \mathbf{x} + \mathbf{b} \delta u$$

with $\mathbf{A}(\mathbf{x}, u, t) = \frac{\partial \mathbf{f}}{\partial \mathbf{x}}$, and $\mathbf{b}(\mathbf{x}, u, t) = \frac{\partial \mathbf{f}}{\partial u}$ and focus on choosing the gain $\mathbf{K}$ of the virtual control input

$$\delta u = \mathbf{K} \delta \mathbf{x} \tag{9.2}$$

so as to achieve contraction behavior around this general trajectory. Once $\mathbf{K}$ is found we perform a path integration between the actual trajectory $\mathbf{x}$ and the desired trajectory $\mathbf{x}_d$ leading to a finite control input u.

First, we need to find a coordinate transformation $\delta \mathbf{z} = \Theta \delta \mathbf{x}$ and a virtual control

input δu that leads $\forall t \geq 0$ to the generalized Jacobian

$$\mathbf{F} = \left(\dot{\Theta} + \Theta\left(\mathbf{A} + \mathbf{bK}\right)\right)\Theta^{-1} = \begin{pmatrix} 0 & 1 & 0 & \cdots & 0 \\ 0 & 0 & 1 & \cdots & 0 \\ \vdots & \vdots & \vdots & \ddots & \vdots \\ 0 & 0 & 0 & 0 & 1 \\ -a_o & -a_1 & -a_2 & \cdots & -a_{n-1} \end{pmatrix}$$

with the desired stable characteristic coefficients a_i. Exponential convergence of $\delta\mathbf{z}$ to zero can then be concluded with Theorem 2 under a second coordinate transformation $\delta\mathbf{z}^* = \mathbf{T}\delta\mathbf{z}$ ($\mathbf{T} = const$) transforming $\mathbf{F}$ into a uniformly negative definite real Jordan form. Note that an eventual normalization factor in the Jordan form can be scaled below the real part of the corresponding eigenvalue.

The above equation can be rewritten in terms of the row vectors θ_j ($j = 1, \cdots, n$) of Θ as

$$\dot{\theta}_j + \theta_j\left(\mathbf{A} + \mathbf{bK}\right) = \theta_{j+1} \qquad j = 1, \cdots, n-1 \tag{9.3}$$

$$\dot{\theta}_n + \theta_n\left(\mathbf{A} + \mathbf{bK}\right) = -\mathbf{a}\begin{pmatrix} \theta_1 \\ \vdots \\ \theta_n \end{pmatrix} \tag{9.4}$$

with $\mathbf{a} = (a_1, ..., a_n)$. In order to make Θ independent of δu, let us impose recursively, $\forall t \geq 0$, the following constraints on θ_j

$$\begin{aligned} 0 &= \theta_1\mathbf{b} = \theta_1 L^o\mathbf{b} \\ 0 &= \theta_2\mathbf{b} = \left(\dot{\theta}_1 + \theta_1\mathbf{A}\right)\mathbf{b} - \frac{d}{dt}\left(\theta_1\mathbf{b}\right) = \theta_1 L^1\mathbf{b} \\ 0 &= \theta_3\mathbf{b} = \left(\dot{\theta}_2 + \theta_2\mathbf{A}\right)\mathbf{b} - \frac{d}{dt}\left(\theta_2\mathbf{b}\right) = \theta_2 L^1\mathbf{b} \\ &= \left(\dot{\theta}_1 + \theta_1\mathbf{A}\right)L^1\mathbf{b} - \frac{d}{dt}\left(\theta_1 L^1\mathbf{b}\right) = \theta_1 L^2\mathbf{b} \\ &\vdots \\ 1 &= \theta_n\mathbf{b} = \theta_1 L^{n-1}\mathbf{b} \end{aligned} \tag{9.5}$$

The $L^j\mathbf{b}$ are *Lie derivatives* (Lovelock and Rund, 1989)

$$\begin{aligned} L^o\mathbf{b} &= \mathbf{b} \\ L^{j+1}\mathbf{b} &= \mathbf{A}\,L^j\mathbf{b} - \frac{d}{dt}L^j\mathbf{b} \qquad j = 0, ..., n-2 \end{aligned} \tag{9.6}$$

For uniformly positive definite $\mathfrak{C}\mathfrak{C}^T$ with

$$\mathfrak{C}(\mathbf{x}, u, ..., u^{(n-1)}, t) = \left(L^o\mathbf{b} \ ... \ L^{n-1}\mathbf{b}\right) \tag{9.7}$$

equation (9.5) can be solved algebraically for θ_1. From (9.3) the remaining θ_j can be

computed analytically using the recursion

$$\theta_{j+1} = \dot{\theta}_j + \theta_j \mathbf{A} \qquad j = 1, \cdots, n-1$$

The feedback gain $\mathbf{K}$ along a general trajectory can then be computed from (9.4)

$$\mathbf{K}(\mathbf{x}, u, ..., u^{(2n-2)}, t) = -\mathbf{a}\ \Theta - \dot{\theta}_n - \theta_n \mathbf{A} \tag{9.8}$$

Let us now perform a path integration from $\mathbf{x}$ to $\mathbf{x}_d$ through a region of uniformly positive definite $\mathfrak{C}\mathfrak{C}^T$ leading to the control input

$$u = u_d + \int_{x_d}^{x} \mathbf{K} dx \tag{9.9}$$

where $u_d(t)$ specifies the desired trajectory $\mathbf{x}_d(t)$.

If the differential relation $\delta u = \mathbf{K}\delta\mathbf{x}$ in (9.2) is not exact then u in (9.9) not only depends on $\mathbf{x}$, $\mathbf{x}_d$ and t, but also on the chosen path from $\mathbf{x}_d$ to $\mathbf{x}$. However, if the path integral $\int_{x_d}^{x} \mathbf{K} dx$ is computed along the forward image of an initial path from $\mathbf{x}_d$ to $\mathbf{x}$ then contraction behavior between neighboring trajectories on this path can still concluded, which implies exponential convergence of $\mathbf{x}$ to $\mathbf{x}_d$. Also note although $\mathbf{K}$ in (9.9) depends on $u, ..., u^{(n-1)}$ it does not depend on δu or its time-derivatives. As a result (9.2) represents an explicit differential relation in δu and can therefore be solved by path integration.

Note that a smooth system dynamics (9.1) implies bounded Lie derivatives $L^j\mathbf{b}$ that results with a uniformly positive definite $\mathfrak{C}\mathfrak{C}^T$ in bounded Θ and $\mathbf{K}$. Multiplying equation (9.5) with itself and dividing by $\mathfrak{C}$ on both sides leads to

$$\Theta^T\Theta = \mathfrak{C}^{-T} \begin{pmatrix} \cdot^{\cdot} & \cdot^{\cdot} & 0 & 1 \\ 0 & \cdot^{\cdot} & \cdot^{\cdot} & * \\ 0 & 1 & \cdot^{\cdot} & \cdot^{\cdot} \\ 1 & * & * & \cdot^{\cdot} \end{pmatrix} \begin{pmatrix} \cdot^{\cdot} & 0 & 0 & 1 \\ \cdot^{\cdot} & \cdot^{\cdot} & 1 & * \\ 0 & \cdot^{\cdot} & \cdot^{\cdot} & * \\ 1 & * & \cdot^{\cdot} & \cdot^{\cdot} \end{pmatrix} \mathfrak{C}^{-1} \geq \left(\mathfrak{C}\mathfrak{C}^T\right)^{-1}$$

where the product of the two interior matrices can be shown by complete induction to be greater or equal than $\mathbf{I}$. The metric $\Theta^T\mathbf{T}^T\mathbf{T}\Theta$ is uniformly positive definite for bounded, uniformly positive definite $\mathfrak{C}\mathfrak{C}^T$. This leads with Theorem 2 to:

Theorem 5 *Given the smooth system dynamics*

$$\dot{\mathbf{x}} = \mathbf{f}(\mathbf{x}, u, t)$$

in combination with the controller

$$u = u_d + \int_{x_d}^{x} \mathbf{K} dx$$

where $\mathbf{K}$ in (9.8) is defined for stable characteristic coefficients $\mathbf{a}$ and uniformly positive definite $\mathfrak{C}\mathfrak{C}^T$ in (9.7) and the path integral $\int_{x_d}^{x} \mathbf{K} dx$ is computed along the forward image of an initial connecting path from $\mathbf{x}$ to the desired trajectory $\mathbf{x}_d(t)$.

As a result any trajectory $\mathbf{x}$ *which starts in a ball of constant radius, centered at a desired trajectory* $\mathbf{x}_d(t)$*, and contained at all times in a region of uniformly positive definite* $\mathfrak{C}\mathfrak{C}^T$ *in (9.7), remains in that ball and converges exponentially to* $\mathbf{x}_d(t)$*.*

Note, if we assume $\delta\mathbf{x}$ to be a good measure of the control effect of a virtual control input δu then the smallest singular value of $\mathfrak{C}$ defines the maximal overshoot of a control input δu and can hence be regarded as a measure of the control effectiveness of the virtual control input δu.

The terms $\dot{\theta}_i$ and $\frac{d}{dt}L^j\mathbf{b}$ distinguish this derivation from usual pole-placement in an LTI system, as well as from related gain-scheduling-like techniques (Wu, Packard, and Bals, 1995; Mracek, Cloutier, and D'Souza, 1996; Reboulet and Champetier, 1984). By letting the desired trajectory $\mathbf{x}_d$ start close enough to $\mathbf{x}$, the control law can be approximated as $u \approx u_d + \mathbf{K}(\mathbf{x}_d, u_d, ..., u_d^{(2n-2)})\Delta\mathbf{x}$. Exponential convergence of this local controller design can be concluded in the largest ball, centered at $\mathbf{x}_d$ and contained at all times in a region of uniform negative definite $\mathbf{F} = \mathbf{T}(\dot{\Theta} + \Theta\mathbf{A}(\mathbf{x},t))\Theta^{-1}\mathbf{T}^{-1}$.

9.1.1 Feedback linearization

Let us now show that Theorem 5 can be regarded as an extension of feedback linearization (Isidori, 1995), since it does not require an explicit invertible coordinate transformation $\mathbf{z} = \mathbf{z}(\mathbf{x},t)$. Indeed consider $\forall t \geq 0$ the nonlinear system

$$\dot{\mathbf{x}} = \bar{\mathbf{f}}(\mathbf{x},t) + \bar{\mathbf{g}}(\mathbf{x},t)u \tag{9.10}$$

whose virtual dynamics is

$$\delta\dot{\mathbf{x}} = \mathbf{A}\delta\mathbf{x} + \mathbf{b}\delta u$$

with $\mathrm{A} = (\frac{\partial\bar{\mathbf{f}}}{\partial\mathbf{x}} + \frac{\partial\mathbf{b}}{\partial\mathbf{x}}u)$, and $\mathbf{b} = \bar{\mathbf{g}}$. If we assume $L^j\mathbf{b}$ to be a function of $\mathbf{x}$ and t only, then $L^{j+1}\mathbf{b}$ in (9.6) results in

$$L^{j+1}\mathbf{b} = \mathbf{A}\ L^j\mathbf{b} - \frac{d}{dt}L^j\mathbf{b} = \frac{\partial\bar{\mathbf{f}}}{\partial\mathbf{x}}\ L^j\mathbf{b} - \frac{\partial L^j\mathbf{b}}{\partial\mathbf{x}}\bar{\mathbf{f}} - \frac{\partial L^j\mathbf{b}}{\partial t} + \left(\frac{\partial\mathbf{b}}{\partial\mathbf{x}}L^j\mathbf{b} - \frac{\partial L^j\mathbf{b}}{\partial\mathbf{x}}\mathbf{b}\right)u$$

If we assume in addition that $\mathbf{b}$ and $L^j\mathbf{b}$ are involutive, (i.e., $\frac{\partial\mathbf{b}}{\partial\mathbf{x}}L^j\mathbf{b} - \frac{\partial L^j\mathbf{b}}{\partial\mathbf{x}}\mathbf{b}$ is a linear combination of $\mathbf{b}$ and $L^j\mathbf{b}$) then $\theta_{j+1}L^{j+1}\mathbf{b}$ in (9.5) can be replaced with $\theta_{j+1}\bar{L}^{j+1}\mathbf{b}$ and

$$\begin{aligned}\bar{L}^o\mathbf{b} &= \mathbf{b}\\ \bar{L}^{j+1}\mathbf{b} &= \frac{\partial\bar{\mathbf{f}}}{\partial\mathbf{x}}\ \bar{L}^j\mathbf{b} - \frac{\partial\bar{L}^j\mathbf{b}}{\partial\mathbf{x}}\bar{\mathbf{f}} - \frac{\partial\bar{L}^j\mathbf{b}}{\partial t} \qquad j = 0, ..., n-2\end{aligned}$$

that guarantees that $\bar{L}^{j+1}\mathbf{b}$ is only a function of $\mathbf{x}$ and t as well. According to Frobenius theorem equation (9.5) can be solved for an explicit z_1 under a proper choice D of the normalization factor on the left-hand side of (9.5) for involutive

$\left(\bar{L}^o\mathbf{b}...\bar{L}^{n-2}\mathbf{b}\right)$ and regular

$$\bar{\mathfrak{C}} = \left(\bar{L}^o\mathbf{b} \ ... \ \bar{L}^{n-1}\mathbf{b}\right) \tag{9.11}$$

Integrating (9.3) the remaining states z_{j+1} can be computed with the recursion

$$z_{j+1} = \frac{\partial z_j}{\partial \mathbf{x}}\mathbf{f} + \frac{\partial z_j}{\partial t} \qquad i = 1, \cdots, n-1$$

Integrating (9.4) the control input u is

$$D\ u = -\mathbf{a}\ \mathbf{z} - \frac{\partial z_n}{\partial \mathbf{x}}\mathbf{f} + u_d(t) \tag{9.12}$$

where $u_d(t)$ specifies the desired trajectory $\mathbf{x}_d(t)$. This leads with Theorem 5 to:

Theorem 6 *Given the smooth system dynamics*

$$\dot{\mathbf{x}} = \bar{\mathbf{f}}(\mathbf{x}, t) + \bar{\mathbf{g}}(\mathbf{x}, t)u$$

in combination with the controller (9.12) defined for stable characteristic coefficients $\mathbf{a}$*, any trajectory* $\mathbf{x}$ *which starts in a ball of constant radius, centered at a desired trajectory* $\mathbf{x}_d(t)$*, and contained at all times in a region of uniformly positive definite* $\bar{\mathfrak{C}}\bar{\mathfrak{C}}^T$ *in (9.11) and involutive* $\left(\bar{L}^o\mathbf{b}...\bar{L}^{n-2}\mathbf{b}\right)$ *remains in that ball and converges exponentially to* $\mathbf{x}_d(t)$*.*

Note that the condition on a uniformly positive definite $\bar{\mathfrak{C}}\bar{\mathfrak{C}}^T$ simplifies the diffeomorphism requirement between $\mathbf{z}$ and $\mathbf{x}$ in (Isidori, 1995). This Theorem also represents an extension of feedback linearization to non-autonomous systems.

9.1.2 Multi-input systems

The multi-input virtual dynamics around one specific trajectory is

$$\delta\dot{\mathbf{x}} = \mathbf{A}\delta\mathbf{x} + (\mathbf{b}_1...\mathbf{b}_p)\,\delta\mathbf{u}$$

with $\mathbf{A}(\mathbf{x}, \mathbf{u}, t) = \frac{\partial \mathbf{f}}{\partial \mathbf{x}}$, $\mathbf{b}_j(\mathbf{x}, \mathbf{u}, t) = \frac{\partial \mathbf{f}}{\partial u_j}$, and the p-dimensional control input vector $\mathbf{u}$. Similar to the LTI case in (Ackermann, 1985) we can transform this system into p independent companion forms of order n_k with $n_1 + ... + n_p = n$. The starting vector θ_1^k of the k-th companion form can be computed from

$$\theta_1^k\,(L^o\mathbf{b}_1...L^{n_1}\mathbf{b}_1, ..., L^o\mathbf{b}_p...L^{n_p}\mathbf{b}_p) = \mathbf{e}^k$$

where $\mathbf{e}^k$ is a unit vector with a 1 in the $(n_1 + ... + n_k)$-th element. The remaining $\theta_j^k, 1 \leq k \leq n_k$ can recursively be computed with equation (9.3). The resulting system then consists of p independent single input companion forms whose poles can be placed with the p independent control inputs u_j. Note that a similar block companion form also exists for the observer design and the discrete case to be discussed later. Parallels to more sophisticated LTI designs (e.g., Moore, 1976) may also be derived.

9.1.3 Coordinate invariance

Let us now show that the controller and Lie derivative matrix $\mathfrak{C}$ in Theorem 5 are coordinate invariant. Indeed, consider the plant dynamics $\dot{\mathbf{x}}^* = \mathbf{f}^* = \frac{\partial \mathbf{x}^*}{\partial \mathbf{x}}\mathbf{f} + \frac{\partial \mathbf{x}^*}{\partial t}$ in different coordinates $\mathbf{x}^*(\mathbf{x}, t)$. The virtual dynamics is

$$\delta\dot{\mathbf{x}}^* = \mathbf{A}^*\delta\mathbf{x}^* + \mathbf{b}^*\delta u$$

with $\mathbf{A}^* = \frac{\partial \mathbf{f}^*}{\partial \mathbf{x}^*} = \left(\frac{\partial^2 \mathbf{x}^*}{\partial \mathbf{x}^2}\mathbf{f} + \frac{\partial \mathbf{x}^*}{\partial \mathbf{x}}\mathbf{A} + \frac{\partial^2 \mathbf{x}^*}{\partial t \partial \mathbf{x}}\right)\frac{\partial \mathbf{x}}{\partial \mathbf{x}^*}$, and $\mathbf{b}^* = \frac{\partial \mathbf{f}^*}{\partial u} = \frac{\partial \mathbf{x}^*}{\partial \mathbf{x}}\mathbf{b}$. The Lie derivatives in $\mathbf{x}^*(\mathbf{x}, t)$ coordinates can be computed by complete induction

$$\begin{aligned} L^o\mathbf{b}^* &= \mathbf{b}^* = \frac{\partial \mathbf{x}^*}{\partial \mathbf{x}}\mathbf{b} \\ L^{j+1}\mathbf{b}^* &= \mathbf{A}^*\, L^j\mathbf{b}^* - \frac{d}{dt}L^j\mathbf{b}^* = \frac{\partial \mathbf{x}^*}{\partial \mathbf{x}}L^{j+1}\mathbf{b} \end{aligned}$$

leading to $\mathfrak{C}^* = \frac{\partial \mathbf{x}^*}{\partial \mathbf{x}}\mathfrak{C}$. A similar argumentation shows that $\Theta^* = \Theta\frac{\partial \mathbf{x}}{\partial \mathbf{x}^*}$ leading to an unchanged control input in Theorem 5.

9.1.4 Robustness

Consider the distance $R = \int_{P_1}^{P_2} \|\delta\mathbf{z}\|$ between two trajectories P_1 and P_2 , contained at all times in a contraction region characterized by maximal eigenvalues $\lambda_{max}(\mathbf{x}, t) \leq -\beta < 0$ of $\mathbf{F}$. The relative velocity between these trajectories verifies

$$\dot{R} + |\lambda_{max}|\, R \leq 0$$

Assume now, instead, that P_1 represents a desired system trajectory and P_2 the actual system trajectory in a disturbed flow field $\dot{\mathbf{x}} = \mathbf{f}(\mathbf{x}, t) + \mathbf{d}(\mathbf{x}, t)$. The relative velocity between these trajectories verifies then $\dot{R} + |\lambda_{max}|\, R \leq \|\mathbf{d}\|_M$. For disturbance $\|\mathbf{d}\|_M < (|\lambda_{max}| - \beta)R + d$ with bounded $d(\mathbf{x}, t) > 0$ and constant $\beta > 0$ any trajectory remains in a boundary ball of

$$\dot{R} + \beta\, R \leq d \tag{9.13}$$

around the desired trajectory. Since initial conditions $R(t = 0)$ are exponentially forgotten, we can also state that any trajectory converges exponentially to a ball of radius R in (9.13) with arbitrary initial condition $R(t = 0)$. Equation (9.13) also implies that *frequencies* larger than β are filtered out. Note that disturbances increasing linearly with R appear at the numerical path integration in Theorem 5.

9.2 Continuous-time observers

For the completion of the discussion let us derive the corresponding locally convergent observer, that turns out to be the extended Luenberger observer in (Zeitz, 1987). Indeed consider $\forall t \geq 0$ the smooth open-loop plant dynamics and measurement

$$\dot{\mathbf{x}} = \mathbf{f}(\mathbf{x}, t)$$

$$y = h(\mathbf{x}, t)$$

where $\mathbf{x}$ might be augmented with some unknown but constant parameters in an adaptive context. Consider now the virtual observer dynamics and measurement

$$\begin{aligned} \delta\dot{\hat{\mathbf{x}}} &= \mathbf{A}\delta\hat{\mathbf{x}} - \mathbf{E}\delta\hat{\mathbf{y}} \\ \delta\hat{y} &= \mathbf{c}\delta\hat{\mathbf{x}} \end{aligned} \tag{9.14}$$

with $\mathbf{A} = \frac{\partial \mathbf{f}}{\partial \hat{\mathbf{x}}}(\hat{\mathbf{x}}, t)$, $\mathbf{c} = \frac{\partial h}{\partial \mathbf{x}}(\hat{\mathbf{x}}, t)$, and the feedback gain $\mathbf{E}$ to be computed in the following.

Similar to the controller design we need to find a coordinate transformation $\delta\hat{\mathbf{x}} = \mathbf{\Sigma}(\hat{\mathbf{x}}, t)\delta\hat{\mathbf{z}}$ and a feedback gain $\mathbf{E}(\hat{\mathbf{x}}, t)$ that leads to the generalized Jacobian

$$\mathbf{F} = \mathbf{\Sigma}^{-1}\left(-\dot{\mathbf{\Sigma}} + (\mathbf{A} - \mathbf{E}\mathbf{c})\,\mathbf{\Sigma}\right) = \begin{pmatrix} 0 & 0 & \cdots & 0 & -a_o \\ 1 & 0 & \cdots & 0 & -a_1 \\ 0 & 1 & \cdots & 0 & -a_2 \\ \vdots & \vdots & \ddots & 0 & \vdots \\ 0 & 0 & \cdots & 1 & -a_{n-1} \end{pmatrix}$$

with the desired stable characteristic coefficients a_i. The above equation can be rewritten in terms of the column vectors σ_j of $\mathbf{\Sigma}$ as

$$-\dot{\sigma}_j + (\mathbf{A} - \mathbf{E}\mathbf{c})\,\sigma_j = \sigma_{j+1} \qquad j = 1, \cdots, n-1 \tag{9.15}$$

$$-\dot{\sigma}_n + (\mathbf{A} - \mathbf{E}\mathbf{c})\,\sigma_n = -\begin{pmatrix} \sigma_1 & \cdots & \sigma_n \end{pmatrix}\mathbf{a} \tag{9.16}$$

with $\mathbf{a} = (a_1, ..., a_n)^T$. Let us proceed as before by imposing the constraints

$$\begin{aligned} L^j\mathbf{c}\;\sigma_1 &= 0 \qquad\qquad j = 0, ..., n-1 \\ L^{n-1}\mathbf{c}\;\sigma_1 &= 1 \end{aligned}$$

with the Lie derivatives

$$\begin{aligned} L^o\mathbf{c} &= \mathbf{c} \\ L^{j+1}\mathbf{c} &= L^j\mathbf{c}\;\mathbf{A} + \frac{d}{dt}L^j\mathbf{c} \qquad j = 0, ..., n-1 \end{aligned}$$

The above can be solved algebraically for σ_1 if $\mathbf{\Phi}^T\mathbf{\Phi}$ is uniformly positive definite with

$$\mathbf{\Phi}(\hat{\mathbf{x}}, t) = \begin{pmatrix} L^o\mathbf{c} \\ \vdots \\ L^{n-1}\mathbf{c} \end{pmatrix} \tag{9.17}$$

From (9.15) the remaining σ_j can be computed analytically

$$\sigma_{j+1} = -\dot{\sigma}_j + \mathbf{A}\sigma_j \qquad j = 1, \cdots, n-1$$

The feedback gain $\mathbf{E}$ can then be computed from (9.16)

$$\mathbf{E}(\hat{\mathbf{x}}, t) = \mathbf{\Sigma a} - \dot{\sigma}_n + \mathbf{A}\sigma_n \tag{9.18}$$

leading to the local observer dynamics

$$\dot{\hat{\mathbf{x}}} = \mathbf{f}(\hat{\mathbf{x}}, t) - \mathbf{E}(\hat{\mathbf{x}}, t)\,(h(\hat{\mathbf{x}}, t) - y)$$

Note that we cannot perform a path integration $\int_{\hat{x}}^{x} \mathbf{E} d\hat{x}$ as in the controller case since one end $\mathbf{x}$ of the path is unknown.

Using the same reasoning as in the controller case shows that the metric of this observer design is bounded and uniformly positive definite for uniformly positive definite $\mathbf{\Phi}^T\mathbf{\Phi}$. This leads with Theorem 2 to:

Theorem 7 *Given the smooth system dynamics and measurement*

$$\begin{aligned} \dot{\mathbf{x}} &= \mathbf{f}(\mathbf{x}, t) \\ y &= h(\mathbf{x}, t) \end{aligned}$$

in combination with the observer

$$\dot{\hat{\mathbf{x}}} = \mathbf{f}(\ddot{\mathbf{x}}, t) - \mathbf{E}(\hat{\mathbf{x}}, t)\,(h(\hat{\mathbf{x}}, t) - y)$$

where $\mathbf{E}$ *is defined in (9.18) for stable characteristic coefficients* $\mathbf{a}$*, any trajectory* $\hat{\mathbf{x}}$ *which starts in the neighborhood of* $\mathbf{x}$ *and contained at all times in a region of uniformly positive definite* $\mathbf{\Phi}^T\mathbf{\Phi}$ *in (9.17) converges exponentially to* $\mathbf{x}$*.*

Again, the terms $\dot{\sigma}_i$ and $\frac{d}{dt}L^i\mathbf{c}$ distinguish this derivation from pole-placement in LTI systems. Note that it is straightforward to extend the results from Section 9.1.1 to 9.1.4 to the observer case. Also note that the region of convergence of this observer design can be quantified by the region of uniform negative definite $\mathbf{S}^{-1}\mathbf{\Sigma}^{-1}\left(-\dot{\mathbf{\Sigma}} + (\mathbf{A} - \mathbf{Ec})\,\mathbf{\Sigma}\right)\mathbf{x}$, where $\mathbf{S}$ transforms the observer companion form into a real Jordan form.

9.2.1 Separation principle

The global controller in Theorem 5 and the extended Luenberger observer in Section 7 satisfy a separation principle. Indeed, let us combine the above controller and observer (perhaps with different coefficients $\mathbf{a}$) with

$$u = u_d + \int_{x_d}^{x} \mathbf{K}(\hat{\mathbf{x}}, u, ..., u^{(2n-2)}, t) d\mathbf{x}$$

Subtracting the plant dynamics from the observer dynamics in the neighborhood of $\mathbf{x}$ leads with $\delta\tilde{\mathbf{x}} = \delta\hat{\mathbf{x}} - \delta\mathbf{x}$ to

$$\delta\dot{\tilde{\mathbf{x}}} = (\mathbf{A}(\hat{\mathbf{x}}, t) - \mathbf{E}(\hat{\mathbf{x}}, t)\mathbf{c}(\hat{\mathbf{x}}, t))\,\delta\tilde{\mathbf{x}}$$

so that the Jacobian of the error-dynamics of the observer is unchanged. Since $\mathbf{K}$ in Section 9.1 is shown to be bounded the above represents a hierarchical system. As a result the convergence rate of the controller is unchanged as well.

Chapter 10

The discrete-time case

The previous chapters solely analyzed the contraction behavior of continuous dynamic systems. Let us now go a step further and extend Theorem 2 to discrete systems in Section 10.1 and hybrid systems in Section 10.2.

10.1 Discrete systems

Consider the discrete-time system

$$\mathbf{x}_{i+1} = \mathbf{f}_i(\mathbf{x}_i, i)$$

The associated virtual dynamics is

$$\delta\mathbf{x}_{i+1} = \frac{\partial \mathbf{f}_i}{\partial \mathbf{x}_i}\delta\mathbf{x}_i$$

so that the virtual length dynamics is

$$\delta\mathbf{x}_{i+1}^T\delta\mathbf{x}_{i+1} = \delta\mathbf{x}_i^T \frac{\partial \mathbf{f}_i}{\partial \mathbf{x}_i}^T \frac{\partial \mathbf{f}_i}{\partial \mathbf{x}_i}\delta\mathbf{x}_i$$

Thus, exponential convergence to a single trajectory is guaranteed for

$$\frac{\partial \mathbf{f}_i}{\partial \mathbf{x}_i}^T \frac{\partial \mathbf{f}_i}{\partial \mathbf{x}_i} - \mathbf{I} \leq -\beta\mathbf{I} < \mathbf{0}$$

This may be viewed as extending to non-autonomous systems the standard iterated map results based on the contraction mapping theorem. The convergence condition is equivalent to requiring that the largest singular value of the Jacobian $\frac{\partial \mathbf{f}_i}{\partial \mathbf{x}_i}$ remains smaller than 1 uniformly. A discrete-time version of Theorem 2 can be derived similarly, using the generalized virtual displacement

$$\delta\mathbf{z}_i = \Theta_i(\mathbf{x}_i, i)\delta\mathbf{x}_i$$

leading to

$$\delta \mathbf{z}_{i+1}^T \delta \mathbf{z}_{i+1} = \delta \mathbf{x}_i^T \frac{\partial \mathbf{f}_i}{\partial \mathbf{x}_i}^T \boldsymbol{\Theta}_{i+1}^T \boldsymbol{\Theta}_{i+1} \frac{\partial \mathbf{f}_i}{\partial \mathbf{x}_i} \delta \mathbf{x}_i = \delta \mathbf{z}_i^T \mathbf{F}_i^T \mathbf{F}_i \delta \mathbf{z}_i$$

with the discrete generalized Jacobian

$$\mathbf{F}_i = \boldsymbol{\Theta}_{i+1} \frac{\partial \mathbf{f}_i}{\partial \mathbf{x}_i} \boldsymbol{\Theta}_i^{-1} \tag{10.1}$$

Note the similarity and difference with the Jacobian of an LTI system. The above leads to the following generalized definition for discrete-time systems.

Definition 4 *Given the discrete-time system equations* $\mathbf{x}_{i+1} = \mathbf{f}_i(\mathbf{x}_i, i)$, *a region of the state space is called a contraction region with respect to a uniformly positive definite metric* $\mathbf{M}_i(\mathbf{x}_i, i) = \boldsymbol{\Theta}_i^T \boldsymbol{\Theta}_i$, *if in that region*

$$\exists \beta > 0, \quad \mathbf{F}_i^T \mathbf{F}_i - \mathbf{I} \leq -\beta \mathbf{I} < \mathbf{0}$$

where $\mathbf{F}_i = \boldsymbol{\Theta}_{i+1} \frac{\partial \mathbf{f}_i}{\partial \mathbf{x}_i} \boldsymbol{\Theta}_i^{-1}$ *or equivalently*

$$\frac{\partial \mathbf{f}_i}{\partial \mathbf{x}_i}^T \mathbf{M}_{i+1} \frac{\partial \mathbf{f}_i}{\partial \mathbf{x}_i} - \mathbf{M}_i \leq -\beta \mathbf{M}_i < \mathbf{0}$$

Note that if the metric is defined in a compact set than the regularity of $\boldsymbol{\Theta}_i$ implies a uniformly positive definite metric $\mathbf{M}_i$. Theorem 2 can then be immediately extended as

Theorem 8 *Given the system equations* $\mathbf{x}_{i+1} = \mathbf{f}_i(\mathbf{x}_i, i)$, *any trajectory, which starts in a ball of constant radius with respect to the metric* $\mathbf{M}_i$, *centered at a given trajectory and contained at all times in a generalized contraction region, remains in that ball and converges exponentially to this trajectory.*

Furthermore global exponential convergence to the given trajectory is guaranteed if the whole state space is a contraction region with respect to the metric $\mathbf{M}_i$.

Note that most of our earlier continuous-time can be extended to the discrete case.

Example 10.1: As in the continuous-time case, consider first the discrete-time LTI system

$$\mathbf{x}_{i+1} = \mathbf{A} \mathbf{x}_i$$

and the coordinate transformation $\mathbf{z}_i = \boldsymbol{\Theta} \mathbf{x}_i$ (where $\boldsymbol{\Theta}$ is constant) into a real Jordan form

$$\mathbf{z}_{i+1} = \boldsymbol{\Theta} \mathbf{A} \boldsymbol{\Theta}^{-1} \mathbf{z}_i = \boldsymbol{\Lambda} \mathbf{z}_i$$

It is straightforward to show that $\boldsymbol{\Lambda}^T \boldsymbol{\Lambda} - \mathbf{I}$ is uniformly negative definite if and only if the system is strictly stable.

This result allows one to compute an explicit region of exponential convergence for a controller design based on linearization about an equilibrium point, by using the corresponding constant $\boldsymbol{\Theta}_i$.

Now, consider instead a discrete-time gain-scheduled system. Let $\mathbf{A}_i(\mathbf{x}_i, i) = \frac{\partial \mathbf{f}_i}{\partial \mathbf{x}_i}$ be the Jacobian of the corresponding nonlinear, non-autonomous closed-loop system $\mathbf{x}_{i+1} = \mathbf{f}_i(\mathbf{x}_i, i)$, and define at each point a coordinate transformation $\mathbf{\Theta}_i$ as above. Uniform negative definiteness of $\mathbf{\Lambda}^T\mathbf{\Lambda} - \mathbf{I}$ then implies exponential convergence of this design. □

10.2 Hybrid systems

Let us now give a simple stability condition for hybrid systems, i.e., systems that combine continuous and discrete dynamics (Branicky, 1994). Indeed consider a continuous system

$$\dot{\mathbf{x}} = \mathbf{f}(\mathbf{x}, t)$$

that is switched to a discrete system

$$\mathbf{x}_{i+1} = \mathbf{f}_i(\mathbf{x}_i, i)$$

every Δt_i for one discrete step as in, say, a continuous observer problem with discrete measurements. With the largest continuous eigenvalue $\bar{\lambda}$ of the symmetric part of $\mathbf{F}$ and the largest discrete eigenvalue $\bar{\lambda}_i$ of $\mathbf{F}_i^T\mathbf{F}_i$ in the *same coordinate system* $\mathbf{\Theta}$ the length dynamics over Δt_i and one discrete step i is bounded by

$$\delta\mathbf{z}_{i+1}^T\delta\mathbf{z}_{i+1} \leq \bar{\lambda}_i e^{\bar{\lambda}\Delta t_i}\delta\mathbf{z}_i^T\delta\mathbf{z}_i$$

This means that a hybrid system is contracting if $\exists\ \alpha < 1, \forall i, \bar{\lambda}_i e^{\bar{\lambda}\Delta t_i} < \alpha$. This result can be used to combine the continuous observer and controller designs of the previous chapter with the discrete observer and controller dynamics of the next chapter.

Example 10.2: Consider a hybrid observer

$$\dot{\hat{\mathbf{x}}} = \mathbf{f}(\hat{\mathbf{x}}, t)$$

that incorporates a discrete measurement every Δt_i with

$$\hat{\mathbf{x}}_{i+1} = \mathbf{f}_i(\hat{\mathbf{x}}_i, i)$$

and is contracting with $\bar{\lambda}_i e^{\bar{\lambda}\Delta t_i} < \alpha$. Assume now that there is a bounded model uncertainty $\mathbf{d}$ in the prediction part and a bounded measurement uncertainty $\mathbf{d}_i$. The observer error $R_i = \int_x^{\hat{x}} ||\delta\mathbf{z}_i||$ than verifies similar to remark 6 in Section 3.9.

$$R_{i+1} - \alpha R_i \leq ||\mathbf{d}\Delta t_i + \mathbf{d}_i||_M$$

Since initial conditions are exponentially forgotten we can state that any observer trajectory converges exponentially to a ball with radius R_i around the actual trajectory. □

Chapter 11

Discrete-time controller and observer designs

This Chapter uses the convergence results in section 10 to extend briefly the controller and observer designs in section 9 to the discrete case. Section 11.1 discusses a globally convergent discrete controller design, whereas Section 11.2 derives the corresponding observer design method. It turns out that the discrete controller and observer designs are considerably simpler than its continuous counterparts in Section 9. Since the proposed method also applies to time-varying systems it can be applied to sampled systems with changing sampling period.

11.1 Discrete-time controllers

Let us now generalize the discrete local controller designs around an equilibrium point in (Lee, Arapostathis and Marcus, 1987; Nijmeijer and Van der Schaft, 1990). Consider $\forall i \geq 0$ a continuously differentiable discrete system

$$\mathbf{x}_{i+1} = \mathbf{f}_i(\mathbf{x}_i, u_i, i) \tag{11.1}$$

with control input u_i. First we analyze the virtual dynamics around a general trajectory $\mathbf{x}_i$

$$\delta\mathbf{x}_{i+1} = \mathbf{A}_i\delta\mathbf{x}_i + \mathbf{b}_i\delta u_i$$

with $\mathbf{A}_i(\mathbf{x}_i, u_i, i) = \frac{\partial \mathbf{f}_i}{\partial \mathbf{x}_i}$, and $\mathbf{b}_i(\mathbf{x}_i, u_i, i) = \frac{\partial \mathbf{f}_i}{\partial u_i}$ and focus on choosing the gain $\mathbf{K}_i$ of the virtual control input

$$\delta u_i = \mathbf{K}_i\delta\mathbf{x}_i \tag{11.2}$$

so as to achieve contraction behavior around this general trajectory. Once $\mathbf{K}_i$ is found we perform a path integration between the actual trajectory $\mathbf{x}_i$ and the desired trajectory $\mathbf{x}_{di}$ leading to a finite control input u_i.

First, we need to find $\forall i \geq 0$ a coordinate transformation $\delta\mathbf{z}_i = \mathbf{\Theta}_i\delta\mathbf{x}_i$ and a

virtual control input δu_i that leads to the generalized Jacobian

$$\mathbf{F}_i = \mathbf{\Theta}_{i+1} \left(\mathbf{A}_i + \mathbf{b}_i \mathbf{K}_i \right) \mathbf{\Theta}_i^{-1} = \begin{pmatrix} 0 & 1 & 0 & \cdots & 0 \\ 0 & 0 & 1 & \cdots & 0 \\ \vdots & \vdots & \vdots & \ddots & \vdots \\ 0 & 0 & 0 & 0 & 1 \\ -a_0 & -a_1 & -a_2 & \cdots & -a_{n-1} \end{pmatrix}$$

with the desired stable characteristic coefficients a_i. The above equation can be rewritten in terms of the row vectors θ_i^j of $\mathbf{\Theta}_i$ as

$$\theta_{i+1}^j \left(\mathbf{A}_i + \mathbf{b}_i \mathbf{K}_i \right) = \theta_i^{j+1} \qquad j = 1, \cdots, n-2 \tag{11.3}$$

$$\theta_{i+1}^n \left(\mathbf{A}_i + \mathbf{b}_i \mathbf{K}_i \right) = -\mathbf{a} \begin{pmatrix} \theta_i^1 \\ \vdots \\ \theta_i^n \end{pmatrix} \tag{11.4}$$

with $\mathbf{a} = (a_1, ..., a_n)$. In order to make the coordinate transformation $\mathbf{\Theta}_i$ independent of the virtual control input gain δu_i, let us impose recursively, $\forall i \geq 0$, the following constraints on the θ_i^j

$$\begin{aligned} 0 &= \theta_i^1 \mathbf{b}_{i-1} = \theta_i^1 L_i^o \mathbf{b} \\ 0 &= \theta_{i-1}^2 \mathbf{b}_{i-2} = \theta_i^1 \mathbf{A}_{i-1} \mathbf{b}_{i-2} = \theta_i^1 L_i^1 \mathbf{b} \\ &\vdots \\ 1 &= \theta_{i-n+1}^n \mathbf{b}_{i-n} = \theta_i^1 L_i^{n-1} \mathbf{b} \end{aligned}$$

with the discrete Lie derivatives

$$L_i^j \mathbf{b} = \mathbf{A}_{i-1} ... \mathbf{A}_{i-j} \mathbf{b}_{i-j-1} \qquad j = 0, \cdots, n-1$$

For uniformly positive definite $\mathbb{C}_i \mathbb{C}_i^T$

$$\mathbb{C}_i(\mathbf{x}_{i-1}, ..., \mathbf{x}_{i-n}, u_{i-1}, ..., u_{i-n}, i) = \left(L_i^o \mathbf{b}, ..., L_i^{n-1} \mathbf{b} \right) \tag{11.5}$$

the above can be solved algebraically for θ_i^1. From (11.3) the remaining θ_i^j can be computed algebraically using the recursion

$$\theta_i^{j+1} = \theta_{i+1}^j \mathbf{A}_i \qquad j = 1, \cdots, n-1$$

Note that θ_{i+1}^n can be computed in a similar way. The feedback gain $\mathbf{K}_i$ can be computed from (11.4)

$$\mathbf{K}_i(\mathbf{x}_{i+n-1}, ..., \mathbf{x}_{i-n}, u_{i+n-1}, ..., u_{i-n}, i) = -\mathbf{a}\ \mathbf{\Theta}_i - \theta_{i+1}^n \mathbf{A}_i \tag{11.6}$$

Future states $\mathbf{x}_i$ and control inputs u_i in (11.6) can be computed with an open loop controller leading to a second order error in (11.2). Past states $\mathbf{x}_i$ and control inputs

u_i are available for $i \geq n$.

Let us now perform a path integration from $\mathbf{x}_i$ to $\mathbf{x}_{di}$ through a region of uniformly positive definite $\mathbb{C}_i\mathbb{C}_i^T$ leading to the control input $\forall i \geq n$

$$u_i = u_{di} + \int_{x_{di}}^{x_i} \mathbf{K}_i d\mathbf{x}_i$$

where u_{di} specifies the desired trajectory $\mathbf{x}_{di}$.

If the differential relation $\delta u_i = \mathbf{K}_i \delta \mathbf{x}_i$ in (11.2) is not exact then u_i not only depends on $\mathbf{x}_i$, $\mathbf{x}_{di}$ and i, but also on the chosen path from $\mathbf{x}_{di}$ to $\mathbf{x}_i$. However, if the path integral $\int_{x_{di}}^{x_i} \mathbf{K}_i d\mathbf{x}_i$ is computed along the forward image of an initial path from $\mathbf{x}_{di}$ to $\mathbf{x}_i$ then contraction behavior between neighboring trajectories on this path can still concluded, which implies exponential convergence of $\mathbf{x}_i$ to $\mathbf{x}_{di}$.

Note that a continuously differentiable system dynamics (11.1) implies bounded Lie derivatives $L_i^j \mathbf{b}$ that results with a uniformly positive definite $\mathbb{C}_i\mathbb{C}_i^T$ in bounded $\mathbf{\Theta}_i$ and $\mathbf{K}_i$. A similar argumentation to the continuous case in Section 9.1 shows that the metric is uniformly positive definite for uniformly positive definite $\mathbb{C}_i\mathbb{C}_i^T$. This leads with Theorem 8 to

Theorem 9 *Given the n-dimensional continuously differentiable system dynamics* $\forall i \geq 0$

$$\mathbf{x}_{i+1} = \mathbf{f}_i(\mathbf{x}_i, u_i, i)$$

in combination with the controller $\forall i \geq n$

$$u_i = u_{id} + \int_{x_{di}}^{x_i} \mathbf{K}_i d\mathbf{x}_i$$

where $\mathbf{K}_i$ *in (11.6) is defined for stable characteristic coefficients* $\mathbf{a}$ *and uniformly positive definite* $\mathbb{C}_i\mathbb{C}_i^T$ *in (11.5) and the path integral* $\int_{x_{di}}^{x_i} \mathbf{K}_i d\mathbf{x}_i$ *is computed along the forward image of an initial connecting path from* $\mathbf{x}_i$ *to the desired trajectory* $\mathbf{x}_{di}$.

As a result any trajectory $\mathbf{x}_i$ *which starts in a ball of constant radius, centered at a desired trajectory* $\mathbf{x}_{di}$, *and contained at all times in a region of uniformly positive definite* $\mathbb{C}_i\mathbb{C}_i^T$ *in (11.5), remains in that ball and converges exponentially to* $\mathbf{x}_{di}$.

Note that by letting the desired trajectory $\mathbf{x}_{di}$ start close enough to $\mathbf{x}_i$, the control input can be approximated as $u_i \approx u_{di} + \mathbf{K}_i(\mathbf{x}_{di+n-1}, ..., \mathbf{x}_{di-n}, u_{di+n-1}, ..., u_{di-n}, i)\Delta\mathbf{x}_i$. Since the only difference to pole-placement at LTI systems is that $\mathbf{\Theta}_i$, $\mathbf{A}_i$, and $\mathbf{b}_i$ are computed at different i the complexity of the feedback gain $\mathbf{K}_i$ is of the same order as that of the LTI case. It is also straightforward to extend the results from Section 9.1.1 to 9.1.4 to the discrete case.

11.2 Discrete-time observers

Let us now derive the corresponding locally convergent observer design. Consider $\forall i \geq 0$ the continuously differentiable open-loop plant dynamics and measurement

$$\mathbf{x}_{i+1} = \mathbf{f}_i(\mathbf{x}_i, i)$$

$$y_i = h_i(\mathbf{x}_i, i)$$

Consider now the virtual observer dynamics and measurement

$$\begin{aligned} \delta\dot{\hat{\mathbf{x}}}_i &= \mathbf{A}_i\delta\hat{\mathbf{x}}_i - \mathbf{E}_i\delta\hat{\mathbf{y}}_i \\ \delta\hat{y}_i &= \mathbf{c}_i\delta\hat{\mathbf{x}}_i \end{aligned} \tag{11.7}$$

with $\mathbf{A}_i = \frac{\partial \mathbf{f}_i}{\partial \mathbf{x}_i}(\hat{\mathbf{x}}_i, i)$, $\mathbf{c}_i = \frac{\partial h_i}{\partial \mathbf{x}_i}(\hat{\mathbf{x}}_i, i)$ and the feedback gain $\mathbf{E}_i$ to computed in the following

Similar to the controller design we need to find a coordinate transformation $\delta\hat{\mathbf{x}}_i = \mathbf{\Sigma}_i\delta\hat{\mathbf{z}}_i$ and an observer feedback gain $\mathbf{E}_i$ that leads to the generalized Jacobian

$$\mathbf{F}_i = \mathbf{\Sigma}_{i+1}^{-1}\left(\mathbf{A}_i - \mathbf{E}_i\mathbf{c}_i\right)\mathbf{\Sigma}_i = \begin{pmatrix} 0 & 0 & \cdots & 0 & -a_o \\ 1 & 0 & \cdots & 0 & -a_1 \\ 0 & 1 & \cdots & 0 & -a_2 \\ \vdots & \vdots & \ddots & 0 & \vdots \\ 0 & 0 & \cdots & 1 & -a_{n-1} \end{pmatrix}$$

with the desired stable characteristic coefficients a_i. The above equation can be rewritten in terms of the column vectors σ_i^j of $\mathbf{\Sigma}_i$ as

$$\left(\mathbf{A}_i - \mathbf{E}_i\mathbf{c}_i\right)\sigma_i^j = \sigma_{i+1}^{j+1} \qquad j = 1, \cdots, n-1 \tag{11.8}$$

$$\left(\mathbf{A}_i - \mathbf{E}_i\mathbf{c}_i\right)\sigma_i^n = -\begin{pmatrix} \sigma_{i+1}^1 & \cdots & \sigma_{i+1}^n \end{pmatrix}\mathbf{a} \tag{11.9}$$

with $\mathbf{a} = (a_1, ..., a_n)^T$. In order to make the coordinate transformation $\mathbf{\Sigma}_i$ independent of the virtual measurement $\delta\hat{y}_i$, let us impose recursively, $\forall i \geq 0$, the following constraints on the σ_i^j

$$\begin{aligned} 0 &= \mathbf{c}_i\sigma_i^1 = L_i^o\mathbf{c}\ \sigma_i^1 \\ 0 &= \mathbf{c}_{i+1}\sigma_{i+1}^2 = \mathbf{c}_{i+1}\mathbf{A}_i\sigma_i^1 = L_i^1\mathbf{c}\ \sigma_i^1 \\ &\vdots \\ 1 &= \mathbf{c}_{i+n-1}\sigma_{i+n-1}^n = L_i^{n-1}\mathbf{c}\ \sigma_i^1 \end{aligned}$$

with the Lie derivatives

$$L_i^j\mathbf{c} = \mathbf{c}_{i+j}\mathbf{A}_{i+j-1}...\mathbf{A}_i \qquad j = 0, ..., n-1$$

For uniformly positive definite $\mathbf{\Phi}_i^T\mathbf{\Phi}_i$ with

$$\mathbf{\Phi}_i(\hat{\mathbf{x}}_{i+n-1}, ..., \hat{\mathbf{x}}_i) = \begin{pmatrix} L_i^o\mathbf{c} \\ \vdots \\ L_i^{n-1}\mathbf{c} \end{pmatrix} \tag{11.10}$$

the above can be solved algebraically for σ_i^1. Equation (11.8) then allows to compute

the remaining σ_i^j recursively

$$\sigma_i^{j+1} = \mathbf{A}_{i-1}\sigma_{i-1}^j \qquad j = 1, \cdots, n-1$$

Note that $\mathbf{\Sigma}_{i+1}$ can be computed in a similar way. The feedback gain $\mathbf{E}_i$ can then be computed from equation (11.9)

$$\mathbf{E}_i(\hat{\mathbf{x}}_{i+n-1}, ..., \hat{\mathbf{x}}_{i-n+1}) = \mathbf{\Sigma}_{i+1}\mathbf{a} + \mathbf{A}_i\sigma_i^n \tag{11.11}$$

Future states $\hat{\mathbf{x}}_i$ in (11.11) can be computed with an identity observer leading to a second order error in (11.7). Past states are available for $i \geq n-1$. The resulting local observer dynamics

$$\hat{\mathbf{x}}_{i+1} = \mathbf{f}_i(\hat{\mathbf{x}}_i, i) - \mathbf{E}_i(\hat{\mathbf{x}}_i, i)\,(h_i(\hat{\mathbf{x}}_i, i) - y_i)$$

Note that we cannot perform a path integration $\int_{\hat{x}_i}^{x_i} \mathbf{E}_i d\hat{x}_i$ as in the controller case since one end $\mathbf{x}_i$ of the path is unknown.

Finally, the same reasoning as in the controller case shows that the metric of this observer dynamics is bounded and uniformly positive definite for uniformly positive definite $\mathbf{\Phi}_i^T\mathbf{\Phi}_i$. This leads with Theorem 8 to

Theorem 10 *Given the n-dimensional continuously differentiable system dynamics and measurement* $\forall i \geq 0$

$$\begin{aligned} \mathbf{x}_{i+1} &= \mathbf{f}_i(\mathbf{x}_i, i) \\ y_i &= h_i(\mathbf{x}_i, i) \end{aligned}$$

in combination with the observer $\forall i \geq n-1$

$$\hat{\mathbf{x}}_{i+1} = \mathbf{f}_i(\hat{\mathbf{x}}_i, i) - \mathbf{E}_i(h_i(\hat{\mathbf{x}}_i, i) - y_i)$$

where $\mathbf{E}_i$ *is defined in (11.11) for stable characteristic coefficients* $\mathbf{a}$, *any trajectory* $\hat{\mathbf{x}}_i$ *which starts in the neighborhood of* $\mathbf{x}_i$ *and contained at all times in a region of uniformly positive definite* $\mathbf{\Phi}_i^T\mathbf{\Phi}_i$ *in (11.10), converges exponentially to* $\mathbf{x}_i$.

Since in the discrete-time case the only difference to pole-placement in LTI systems is that $\mathbf{\Theta}_i$, $\mathbf{A}_i$, and $\mathbf{b}_i$ are computed at different i, the complexity of the feedback gain $\mathbf{E}_i$ is similar to that of the LTI case. Also, similarly to the continuous case, robustness and a separation principle can be shown.

Example 11.1: Consider the "lighthouse" problem in Figure 11-1 of navigating a boat using only measurements of the direction α_i to a fixed point in space.

The dynamic equations of the boat's motion are

$$\begin{pmatrix} x_{i+1} \\ y_{i+1} \end{pmatrix} = 0.8 \begin{pmatrix} x_i \\ y_i \end{pmatrix} + \begin{pmatrix} x_i y_i \\ -0.5x_i^2 \end{pmatrix} + 0.2 \begin{pmatrix} \cos 0.1i \\ \sin 0.1i \end{pmatrix}$$

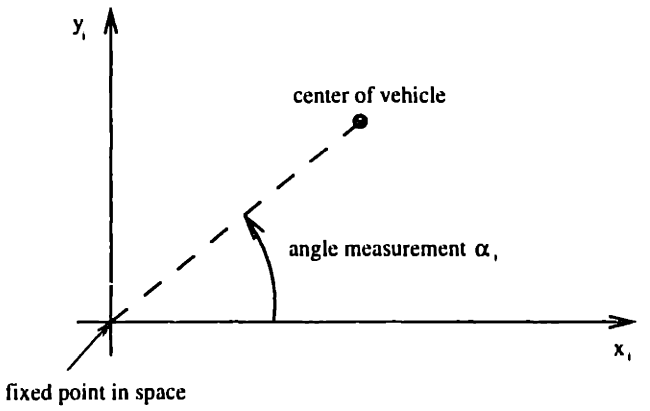

Figure 11-1: Direction navigation problem

The vehicle measures only the direction

$$\alpha_i = \arctan \frac{y_i}{x_i}$$

to the lighthouse. We can compute from equation (11.7)

$$\begin{aligned} \mathbf{A}_i &= \begin{pmatrix} 0.8 + \hat{y}_i & \hat{x}_i \\ -\hat{x}_i & 0.8 \end{pmatrix} \\ \mathbf{c}_i &= \begin{pmatrix} -\frac{\hat{y}_i}{\hat{x}_i^2+\hat{y}_i^2} & \frac{\hat{x}_i}{\hat{x}_i^2+\hat{y}_i^2} \end{pmatrix} \end{aligned}$$

that are both bounded for $\hat{x}_i, \hat{y}_i \neq 0$. This implies in equation (11.10)

$$\Phi_i = \begin{pmatrix} L_i^o \mathbf{c} \\ L_i^1 \mathbf{c} \end{pmatrix} = \begin{pmatrix} \mathbf{c}_i \\ \mathbf{c}_{i+1}\mathbf{A}_i \end{pmatrix}$$

so that $\Phi_i^T \Phi_i$ is uniformly positive definite for $\hat{x}_i, \hat{y}_i \neq 0$. As a result we can conclude on local exponential of the following observer design for $\hat{x}_i, \hat{y}_i \neq 0$. The coordinate transformation $\mathbf{\Sigma}_i = (\sigma_i^1 \ \sigma_i^2)$ is then

$$\begin{aligned} \sigma_i^1 &= \Phi_i^{-1} \begin{pmatrix} 0 \\ 1 \end{pmatrix} \\ \sigma_i^2 &= \mathbf{A}_{i-1}\sigma_{i-1}^1 \end{aligned}$$

Note that $\mathbf{\Sigma}_{i+1}$ can be computed in a similar way. The feedback gain $\mathbf{E}_i$ for the characteristic coefficients $\mathbf{a} = (0.16, -0.8)^T$ verifies

$$\mathbf{E}_i = \mathbf{\Sigma}_{i+1}\mathbf{a} + \mathbf{A}_i\sigma_i^2$$

Future state estimates in the computation of $\mathbf{E}_i$ are simply computed with an identity

observer. The final local exponential observer design is given by

$$\begin{pmatrix} \hat{x}_{i+1} \\ \hat{y}_{i+1} \end{pmatrix} = 0.8 \begin{pmatrix} \hat{x}_i \\ \hat{y}_i \end{pmatrix} + \begin{pmatrix} \hat{x}_i \hat{y}_i \\ -0.5\hat{x}_i^2 \end{pmatrix} + 0.2 \begin{pmatrix} \cos 0.1i \\ \sin 0.1i \end{pmatrix} - \mathbf{E}_i \left(\arctan \frac{\hat{y}_i}{\hat{x}_i} - \alpha_i \right)$$

Observer and plant responses with initial conditions $x_o = 0.9$, $y_o = 0.5$, $\hat{x}_o = 0.4$, $\hat{y}_o = 0.1$ are illustrated in Figure 11-2. The solid lines represent the real plant and the dashed lines the observer estimate. Note that a standard linearized design diverges in our simulations. □

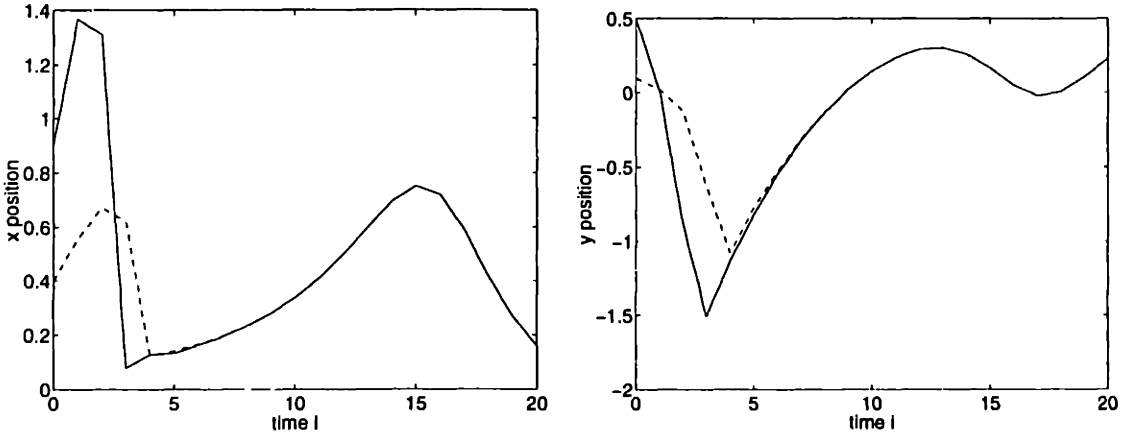

Figure 11-2: Vehicle position and observer dynamics

Chapter 12

Concluding remarks

With the use of a differential approach, convergence analysis and limit behavior are in a sense treated separately. Guaranteeing contraction means that after exponential transients the system's behavior will be independent of the initial conditions.

In an observer context, one then needs only verify that the observer equations contain the actual plant state as a particular solution to automatically guarantee convergence to that state. In a control context, once contraction is guaranteed through feedback, specifying the final behavior reduces to the problem of shaping one particular solution, i.e., specifying an adequate open-loop control input to be added to the feedback terms, a necessary step of any control method.

It turns out that contraction analysis leads for many mechanical and chemical systems to simple controller and observer designs. The relative simplicity of these designs stems from their effective exploitation of the systems' structural specificities.

Contraction analysis also allows to analyze and quantify the convergence rate of the reaction-diffusion equation. Because contraction implies exponential forgetting of initial conditions, the technique provides a new perspective on important classes of nonlinear physical laws, such as diffusion processes, heat transfer, Burgers equation and the Schroedinger equation. Its physical implications may be further explored, and it may be extended in a similar way to other practical classes of partial differential equations.

The thesis also proposes a generalization of linear eigenvalue analysis to nonlinear systems. The system decomposition and the singularities in Θ allow one to conclude to which submanifold the system converges. In contrast to Lyapunov exponents, by design the proposed method is coordinate invariant, and analyzes the whole state space instead of considering specific trajectories.

Finally, the thesis proposes an extension of feedback linearization to the case where the corresponding integrability conditions are violated. It turns out that the complexity of the resulting controller and observer designs in the discrete case are considerable simpler than its continuous counterparts.

Bibliography

Ackermann, J (1985). Sampled-Data Control Systems, *Springer-Verlag.*

Adebekun, D.K., and Schork, F.J. (1989). Continuous solution polymerization reactor control. 1. Nonlinear reference control of methyl methacrylate polymerization, *Industrial Engineering and Chemical Research, 28:1308 - 1324.*

Argyris, J., Faust, G., Haase, M. (1994) An Exploration of chaos. *Elsevier Science B.V..*

Aris, R. (1989). Vectors, Tensors, and the Basic Equations of Fluid Mechanics, *Dover Publications.*

Arnold, V.I. (1978). Mathematical Methods of Classical Mechanics, *Springer Verlag.*

Bar-Shalom Y., and Fortmann, T. (1988). Tracking and Data Association, *Academic Press.*

Berghuis, H., and Nijmeyer, H. (1993). A passivity-based approach to controller-observer design for robots, *I.E.E.E. Transactions on Robotics and Automation, 9(6), page 740 - 754.*

Berthoz, A., Ed. (1993). Multisensory Control of Movement, *Oxford University Press.*

Branicky, M.S. (1994). Stability of Switched and Hybrid Systems, *I.E.E.E. Conference on Decision and Control, Lake Buena Vista, Florida.*

Bizzi E., Giszter S.F., Loeb E., Mussa-Ivaldi F.A., Saltiel P (1995). Modular organization of motor behavior in the frog's spinal cord. *Trends in Neurosciences. Review 18:442-446*

Branicky, M.S. (1994). Stability of Switched and Hybrid Systems, *I.E.E.E. Conference on Decision and Control, Lake Buena Vista, Florida.*

Brockhaus, R. (1994). Flugregelung, *Springer Verlag.*

Cho, Y.M., and Gyugyi, P. (1997). Control of Rapid Thermal Processing: A System Theoretic Approach, *I.E.E.E. Transactions on control systems technology, volume 5, number 6.*

Dong,. G. (1991). Nonlinear Partial Differential Equations of Second Order, *American Mathematical Society.*

Dowling, J.E. (1992). Neurons and Networks, *Belknap.*

Droulez, J., et al. (1983). Motor Control, *7th International Symposium of the International Society of Posturography, Houston, Karger, 1985.*

Ezal, K., Pan, Z., and Kokotovic, P. (1997), Locally optimal backstepping design, *I.E.E.E. Conf. Decision and Control*, San Diego, CA.

Flash, T. (1995). Trajectory Learning and Control Models, *I.F.A.C. Man-Machine Systems Symposium, Cambridge, MA.*

Guckenheimer, J., and Holmes, P. (1983). Nonlinear Oscillations, Dynamical Systems, and Bifurcations of Vector Fields, *Springer Verlag.*

Groeber, Erk and Grigull (1988). Die Grundgesetze der Waermeuebertragung, *Springer Verlag.*

Hartmann, P. (1982). Ordinary differential equations, *Birkhauser.*

Hahn, W. (1967). Stability of motion, *Springer Verlag.*

Haykin, S. (1994). Neuronal Networks, *Macmillan College Publishing Company, Inc.*

Henson, M.A., and Seborg, D.E., Eds. (1997). Nonlinear Process Control, *Prentice-Hall.*

Isidori, A. (1995). Nonlinear Control Systems, 3rd Ed., *Springer Verlag.*

Jazwinski, A.H. (1970). Stochastic Processes and Filtering Theory, *Academic Press.*

Kalman, R.E. (1960). On the General Theory of Control Systems, *Proceedings on first International Congress on Automatic Control, Moscow.*

Kandel, E.R., Schwartz, J.H., and Jessel, T.M. (1991). Principles of Neural Science, *Appleton and Lange.*

Khalil, H. (1995). Nonlinear Systems, 2nd Ed., *Prentice-Hall.*

Krasovskii, N.N. (1959). Problems of the Theory of Stability of Motion, *Mir, Moscow.* English translation by Stanford University Press, 1963.

Kwakernaak, H., Sivan, R. (1972). Linear Optimal Control Systems, *Wiley-Interscience.*

Lawrence, D.A., and Rugh, W.J. (1995). Gain-scheduling dynamic linear controllers for a nonlinear plant, *Automatica, 31(3)*, page 381 - 390.

Lee, H.G., Arapostathis, A., Marcus, S.I. (1987). Linearization of discrete-time systems, *International Journal of Control, volume 45, number 5, 1803-1822.*

Lohmiller, W., and Slotine, J.J.E. (1996a). Metric Observers for Nonlinear Systems, *I.E.E.E. International Conference on Control Applications, Dearborn, Michigan.*

Lohmiller, W., and Slotine, J.J.E. (1996b). Applications of Metric Observers for Nonlinear Systems, *I.E.E.E. International Conference on Control Applications, Dearborn, Michigan.*

Lohmiller, W., and Slotine, J.J.E. (1996c). On Metric Controllers for Nonlinear Systems, *I.E.E.E. Conference on Decision and Control, Kobe, Japan.*

Lohmiller, W., and Slotine, J.J.E. (1996d). On Metric Observers for Nonlinear Systems, *Master Thesis at the Department of Aerospace Engineering, University of Stuttgart, Germany.*

Lohmiller, W., and Slotine, J.J.E. (1997a). Practical Observers for Hamiltonian Systems, *I.E.E.E. American Control Conference, Albuquerque, New Mexico.*

Lohmiller, W., and Slotine, J.J.E. (1997b). Applications of Contraction Analysis, *I.E.E.E. Conference on Control Applications, Hartford, Connecticut.*

Lohmiller, W., and Slotine, J.J.E. (1997c). Applications of Contraction Analysis, *I.E.E.E. Conference on Decision and Control, San Diego, California.*

Lohmiller, W., and Slotine, J.J.E. (1997d). Contraction Analysis: The Discrete-Time Case, *MIT-NSL Report 971101, November 1997.*
Lohmiller, W., and Slotine, J.J.E. (1998a). On Contraction Analysis for Nonlinear Systems, *Automatica (1998/6).*
Lohmiller, W., and Slotine, J.J.E. (1998b). Contraction Analysis: A Practical Approach to Nonlinear Control Applications , *I.E.E.E. Conference on Control Applications, Trieste, Italy.*
Lovelock, D., and Rund, H. (1989). Tensors, differential forms, and variational principles, *Dover.*
Luenberger, D. G. (1979). Introduction to Dynamic Systems, *John Wiley & Sons.*
Mracek, P., Cloutier, J., D'Souza C. (1996 A new Technique for Nonlinear Estimation, *I.E.E.E. International Conference on Control Applications, Dearborn, Michigan.*
Marino, R., and Tomei, T. (1995). Nonlinear Control, *Prentice-Hall.*
Moore, B.C. (1976). On the Flexibility Offered by State Feedback in Multi-variable Systems Beyond Closed Loop Eigenvalue Assignment *IEEE Transactions on Automatic Control 10 (1976) 689-692.*
Mussa-Ivaldi, F.A. (1997). Nonlinear Force Fields: a distributed system of control primitives for representing and learning movements, *1997 IEEE International Symposium on Computational Intelligence in Robotics and Automation, pp. 84-90.*
Mussa-Ivaldi, F.A., Giszter S.F., Bizzi E. (1994). Linear Superposition of primitives in motor control. *Proceedings and National Academy of Sciences. 91:7534-7538.*
Narendra, K.S., and Annaswamy, A.M. (1989). Stable Adpative Systems, *Prentice Hall.*
Niemeyer, G., and Slotine, J.J.E. (1991), Stable Adaptive Teleoperation, *I.E.E.E. J. of Oceanic Engineering, 16(1).*
Nijmeyer, H., and Van der Schaft, A. (1990). Nonlinear Dynamical Control Systems, *Springer Verlag.*
Popov, V.M. (1973). Hyperstability of Control Systems, *Springer-Verlag.*
Reboulet, C., and Champetier, C. (1984). A new method for linearizing nonlinear systems: the pseudo-linearization, *International Journal of Control, 40, page 631.*
Ruelle, D. (1989). Chaotic Evolution and Strange Attractors, *Cambridge University Press.*
Schwartz, L. (1993). Analyse, *Hermann, Paris.*
Shorten, R.N. and Narendra, K.S. (1998). On the Existence of a Common Lyapunov Function for Linear Stable Switching Systems, *Proceedings of the Tenth Yale Workshop on Adaptive and Learning Systems.*
Simon, H.A. (1981). The Sciences of the Artificial, 2nd edition, *MIT Press.*
Slotine, J.J.E., and Li, W. (1991). Applied Nonlinear Control, *Prentice-Hall.*
Strogatz, S. (1994). Nonlinear Dynamics and Chaos, *Addison Wesley.*
Takegaki, M., and Arimoto. S., 1981. A New Feedback Method for Dynamic Control of Manipulators, *Journal of Dynamic Systems, Measurement, Control, 102.*

Vidyasagar, M. (1992). Nonlinear Systems Analysis, 2nd Edition, *Prentice-Hall.*
Withcomb, L., Yoerger, D. (1998). Preliminary Experiments in the Dynamical Control of Marine Thrusters Part 1: Dynamical Modeling. *submitted to IEEE Journal of Oceanic Engineering.*
Wu, F., Packard, A., Bals G. (1995). LPV Control Design for Pitch-Axis Missile Autopilots. *I.E.E.E. International Conference on Decision and Control, New Orleans, Louisiana.*
Zeitz, M. (1987). The extended Luenberger observer for nonlinear systems *Systems and Control Letters 9 (1987) 149-156.*